Supplemental material for 'Global Contrast based Salient Region Detection'

Ming-Ming Cheng[1] Guo-Xin Zhang[1] Niloy J. Mitra[2] Xiaolei Huang[3] Shi-Min Hu[1]
[1] TNList, Tsinghua University [2] KAUST / IIT Delhi [3] Lehigh University
[cmm.thu]@qq.com

1. Database

We used the ground truth database shared by Achanta et al. [2]. This database contains 1000 images as well as manually segmented salient objects. In Section 4, we show this database, as well as saliency detection results using our methods and 8 other state-of-the-art algorithms on this database.

2. Demo Software

We share the demo software for our saliency detection methods and the saliency cut application. We provide an installation program 'Saliency.msi' [1] to set up our software as well as necessary dependencies and sample data. These dependencies include "OpenCV dlls" ('cv210.dll', 'cxcore210.dll' and 'highgui210.dll') and "Microsoft visual studio 2010 runtime" ('Microsoft_VC100CRT_x86.msm', 'Microsoft_VC100_OpenMP_x86.msm'). The installation program creates the following files in the user-specified path: [2]

- $InstallDir$/Bin/AttCut.exe
- $InstallDir$/Bin/cv210.dll
- $InstallDir$/Bin/cxcore210.dll
- $InstallDir$/Bin/highgui210.dll
- $InstallDir$/Bin/ImgSaliency.exe
- $InstallDir$/Data/Src/0_0_272.jpg
- $InstallDir$/AttCutDemo.bat
- $InstallDir$/SaliencyDetectionDemo.bat

Saliency detection software. In this software, we implemented the following methods: FT[2], LC[8], SR[5], LC[8], our HC and our RC. (The C++ source code will be introduced in Section 3.). After copying the original images (in *.jpg format) into the folder '$InstallDir$/Data/Src/', users can directly get saliency detection and evaluation results by running '$InstallDir$/SaliencyDetectionDemo.bat'. In order to avoid this program exiting without evaluating the different approaches, the manually labeled ground-truth binary masks (in *.bmp format, downloaded from the public database introduced in Section 1) should be placed into the folder '$InstallDir$/Data/Src/'.

After the program finishes running, it produces results in the folder '$InstallDir$/Data/Src/Saliency/'. The resulting saliency maps are stored in *.png format. Statistical information about precision, recall and related thresholds as well as comparison results as in our paper can be viewed by running the Matlab file '$InstallDir$/Data/ShowEvaluate.m'.

Saliency cut software. In this software, we use our RC saliency maps to initialize our saliency cut method. After copying the original images as above, users can directly run '$InstallDir$/AttCutDemo.bat' to get saliency cut results. The results will be saved in the folder '$InstallDir$/Data/AttCut/'.

Run time environment. We have tested our software programs in common Windows operating systems including Windows XP, Windows Vista and Windows 7.

3. Source Code

We share the source code for our saliency detection software in the 'Source code' subfolder of our supplemental material. The source code is provided in form of a Visual Studio (VS) 2008 solution[3]. Before compiling this solution, the user needs to put OpenCV libs and header files in the 'VC++ Directories' of visual studio. This solution also contains our C++ implementation of several other methods: FT[2], SR[5]and LC[8].

The source code for other saliency detection methods that we compared our methods to can be found at the following URLs:

[1] We created the installer in visual studio 2010 with Windows 7 OS.

[2] **Please do not use disk C as the installation path if your operating system is windows 7 or vista. Our software does not have permission to write files there.**

[3] We share a VS 2008 solution instead of our own IDE environment VS 2010 since we suspect VS 2010 is not yet popular.

- GB[4]: Matlab code or C++ link.
- CA[3]: Windows binary code
- AC[1]: Matlab code
- FT[2]: Matlab & C++ code
- IT[6]: Matlab code
- SR[5]: Matlab code

4. Comparison of Saliency Detection Results

In Figure 1-61, we show visual comparison between our saliency detection methods (HC and RC) and 8 other state-of-the-art methods: IT[6], MZ[7], GB[4], SR[5], AC[1], CA[3], FT[2], and LC[8]. We also show comparison between our saliency cut results and the manual ground truth in these figures.

References

[1] R. Achanta, F. Estrada, P. Wils, and S. Süsstrunk. Salient region detection and segmentation. In *ICVS*, pages 66–75. Springer, 2008. 2

[2] R. Achanta, S. Hemami, F. Estrada, and S. Süsstrunk. Frequency-tuned salient region detection. In *CVPR*, pages 1597–1604, 2009. 1, 2

[3] S. Goferman, L. Zelnik-Manor, and A. Tal. Context-aware saliency detection. In *CVPR*, 2010. 2

[4] J. Harel, C. Koch, and P. Perona. Graph-based visual saliency. *Advances in neural information processing systems*, 19:545, 2007. 2

[5] X. Hou and L. Zhang. Saliency detection: A spectral residual approach. In *CVPR*, pages 1–8, 2007. 1, 2

[6] L. Itti, C. Koch, and E. Niebur. A model of saliency-based visual attention for rapid scene analysis. *IEEE TPAMI*, 20(11):1254–1259, 1998. 2

[7] Y.-F. Ma and H.-J. Zhang. Contrast-based image attention analysis by using fuzzy growing. In *ACM Multimedia*, pages 374–381, 2003. 2

[8] Y. Zhai and M. Shah. Visual attention detection in video sequences using spatiotemporal cues. In *ACM Multimedia*, pages 815–824, 2006. 1, 2

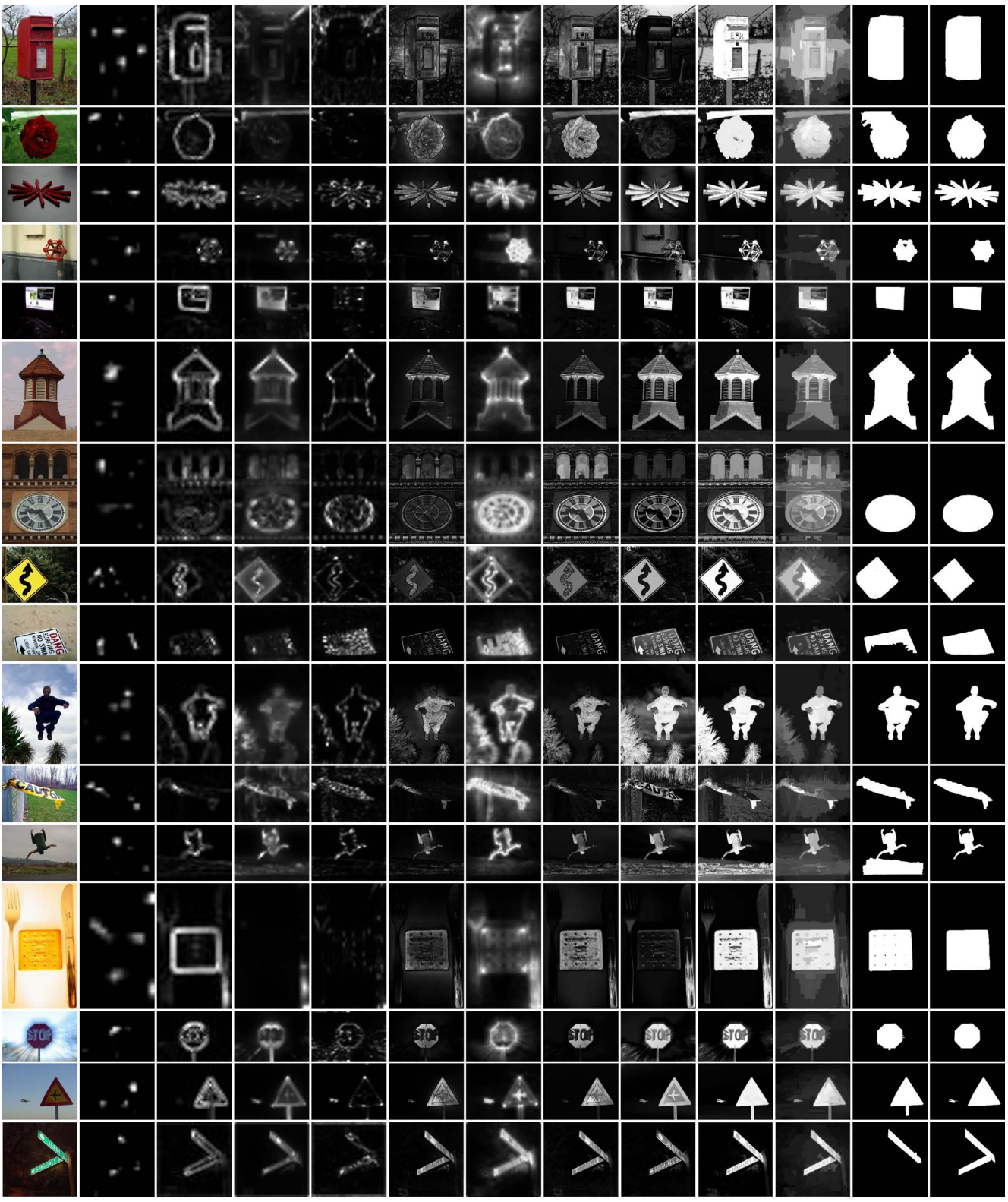

(a) (b) IT[6] (c) MZ[7] (d) GB[4] (e) SR[5] (f) AC[1] (g) CA[3] (h) FT[2] (i) LC[8] (j) HC (k) RC (l) RCC (m) g-tr

Figure 1. Typical saliency maps computed by different state-of-the-art methods (b-i) and by our proposed HC method (j) and RC method (k). Our saliency cut results (l) obtained using RC saliency maps are compared with ground truth (m).

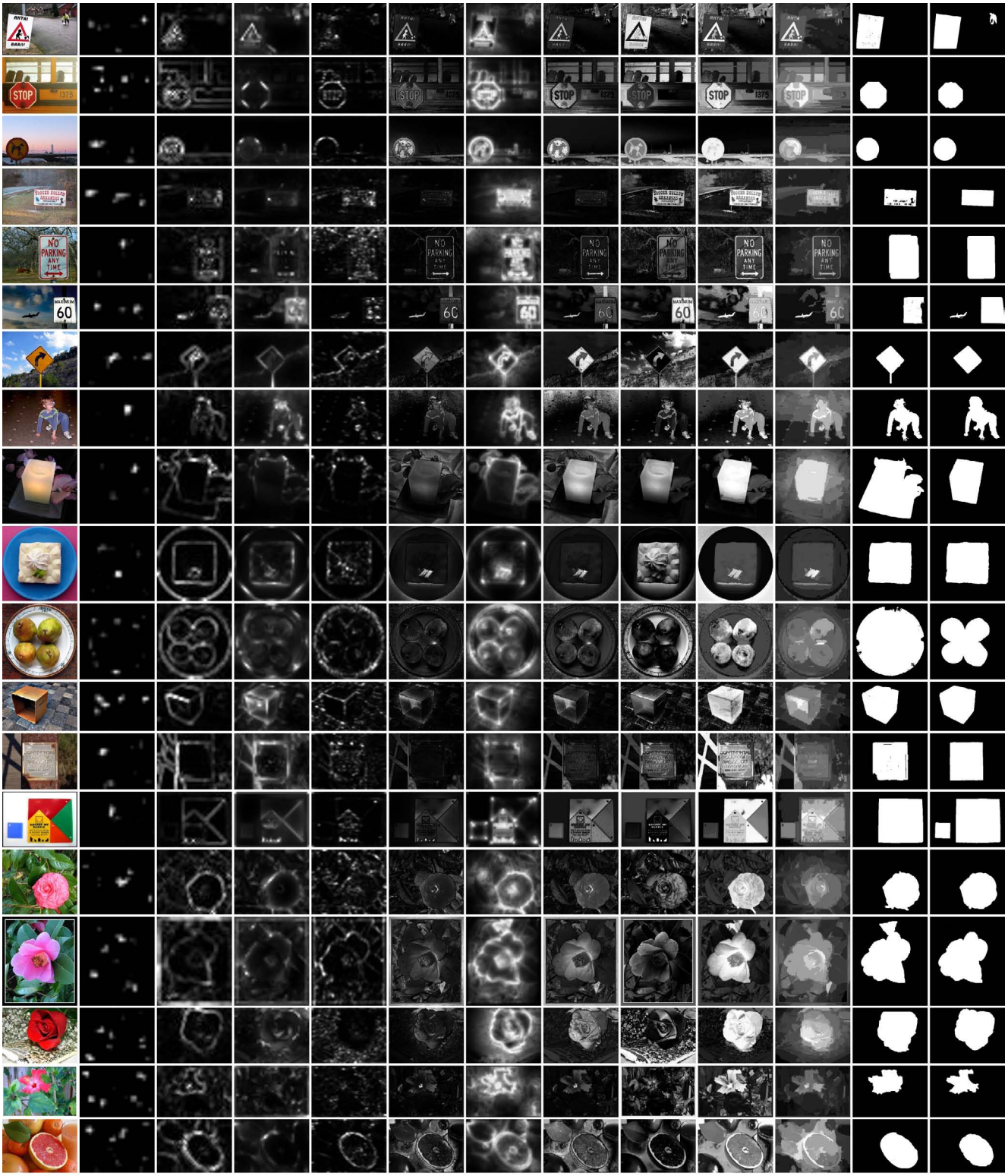

(a) (b) IT[6] (c) MZ[7] (d) GB[4] (e) SR[5] (f) AC[1] (g) CA[3] (h) FT[2] (i) LC[8] (j) HC (k) RC (l) RCC (m) g-tr

Figure 2. Typical saliency maps computed by different state-of-the-art methods (b-i) and by our proposed HC method (j) and RC method (k). Our saliency cut results (l) obtained using RC saliency maps are compared with ground truth (m).

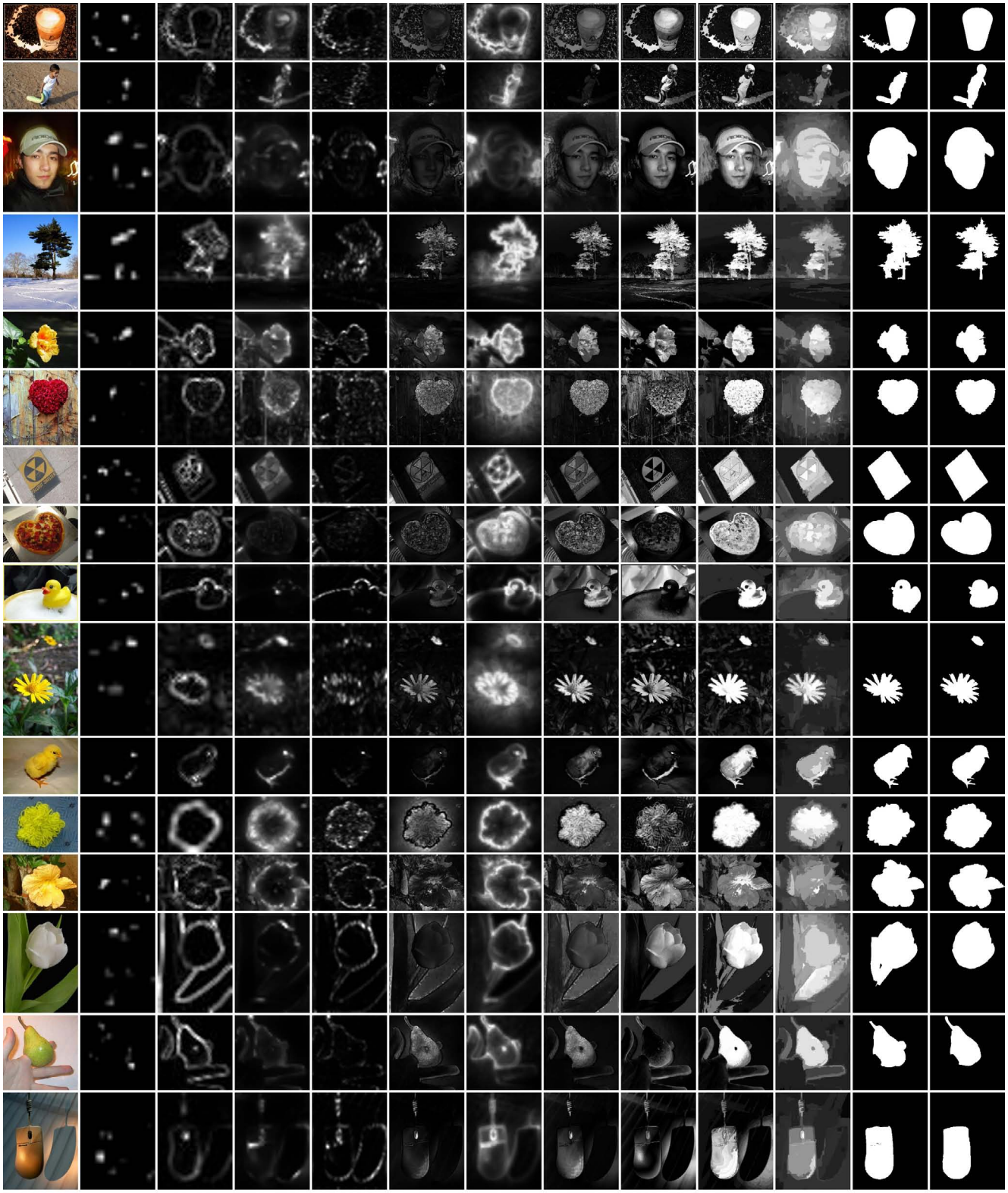

(a) (b) IT[6] (c) MZ[7] (d) GB[4] (e) SR[5] (f) AC[1] (g) CA[3] (h) FT[2] (i) LC[8] (j) HC (k) RC (l) RCC (m) g-tr

Figure 3. Typical saliency maps computed by different state-of-the-art methods (b-i) and by our proposed HC method (j) and RC method (k). Our saliency cut results (l) obtained using RC saliency maps are compared with ground truth (m).

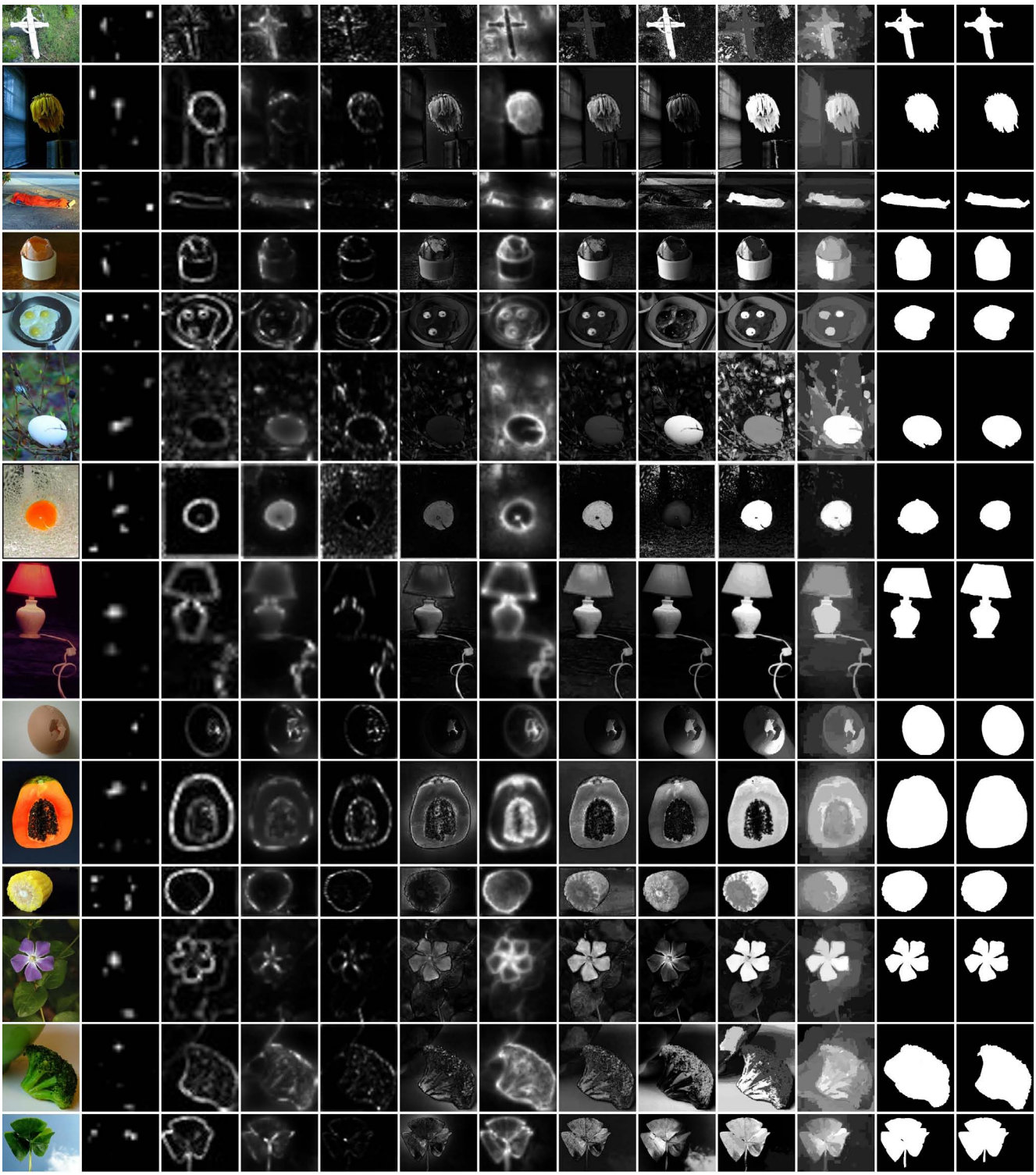

(a) (b) IT[6] (c) MZ[7] (d) GB[4] (e) SR[5] (f) AC[1] (g) CA[3] (h) FT[2] (i) LC[8] (j) HC (k) RC (l) RCC (m) g-tr

Figure 4. Typical saliency maps computed by different state-of-the-art methods (b-i) and by our proposed HC method (j) and RC method (k). Our saliency cut results (l) obtained using RC saliency maps are compared with ground truth (m).

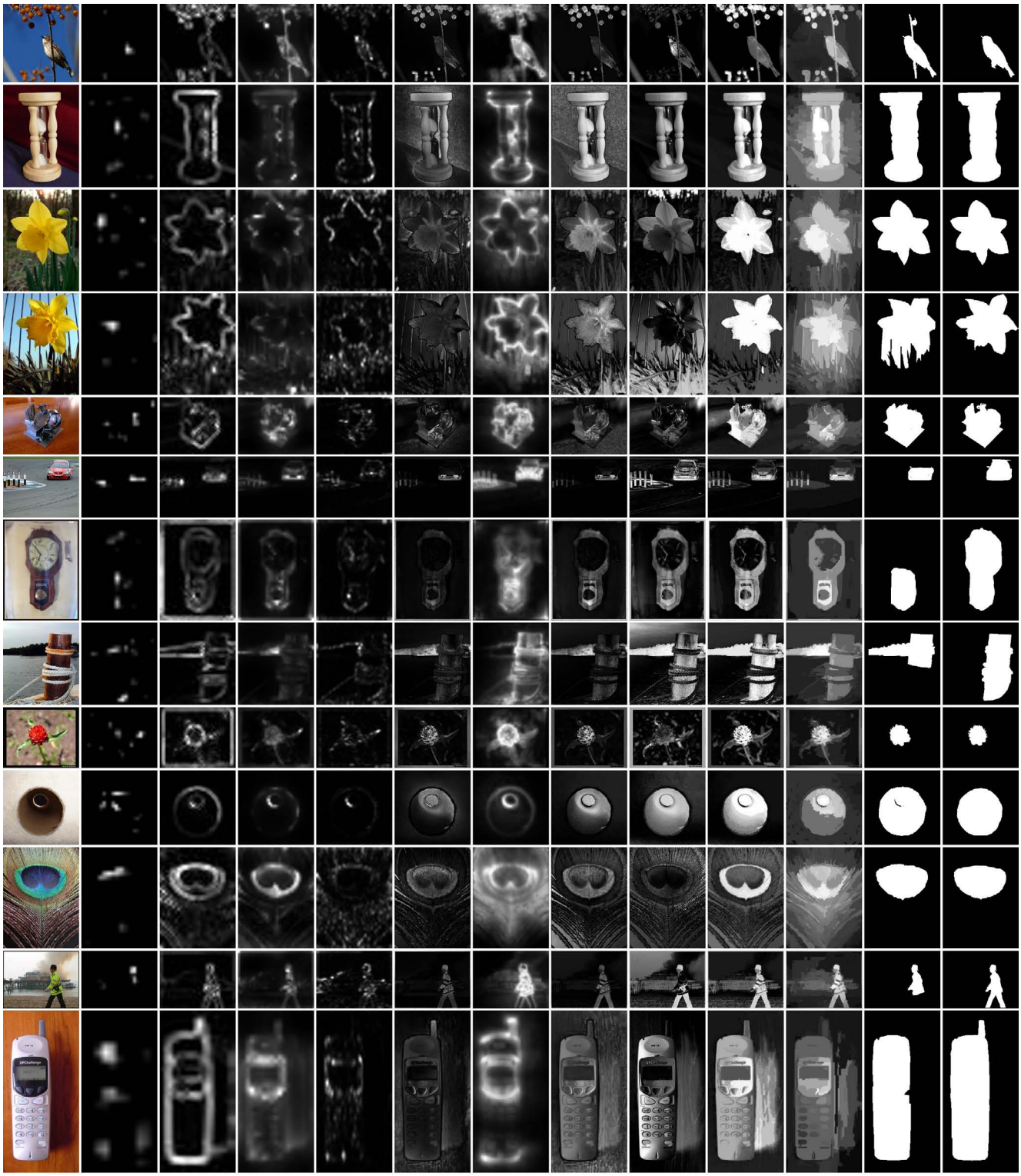

(a) (b) IT[6] (c) MZ[7] (d) GB[4] (e) SR[5] (f) AC[1] (g) CA[3] (h) FT[2] (i) LC[8] (j) HC (k) RC (l) RCC (m) g-tr

Figure 5. Typical saliency maps computed by different state-of-the-art methods (b-i) and by our proposed HC method (j) and RC method (k). Our saliency cut results (l) obtained using RC saliency maps are compared with ground truth (m).

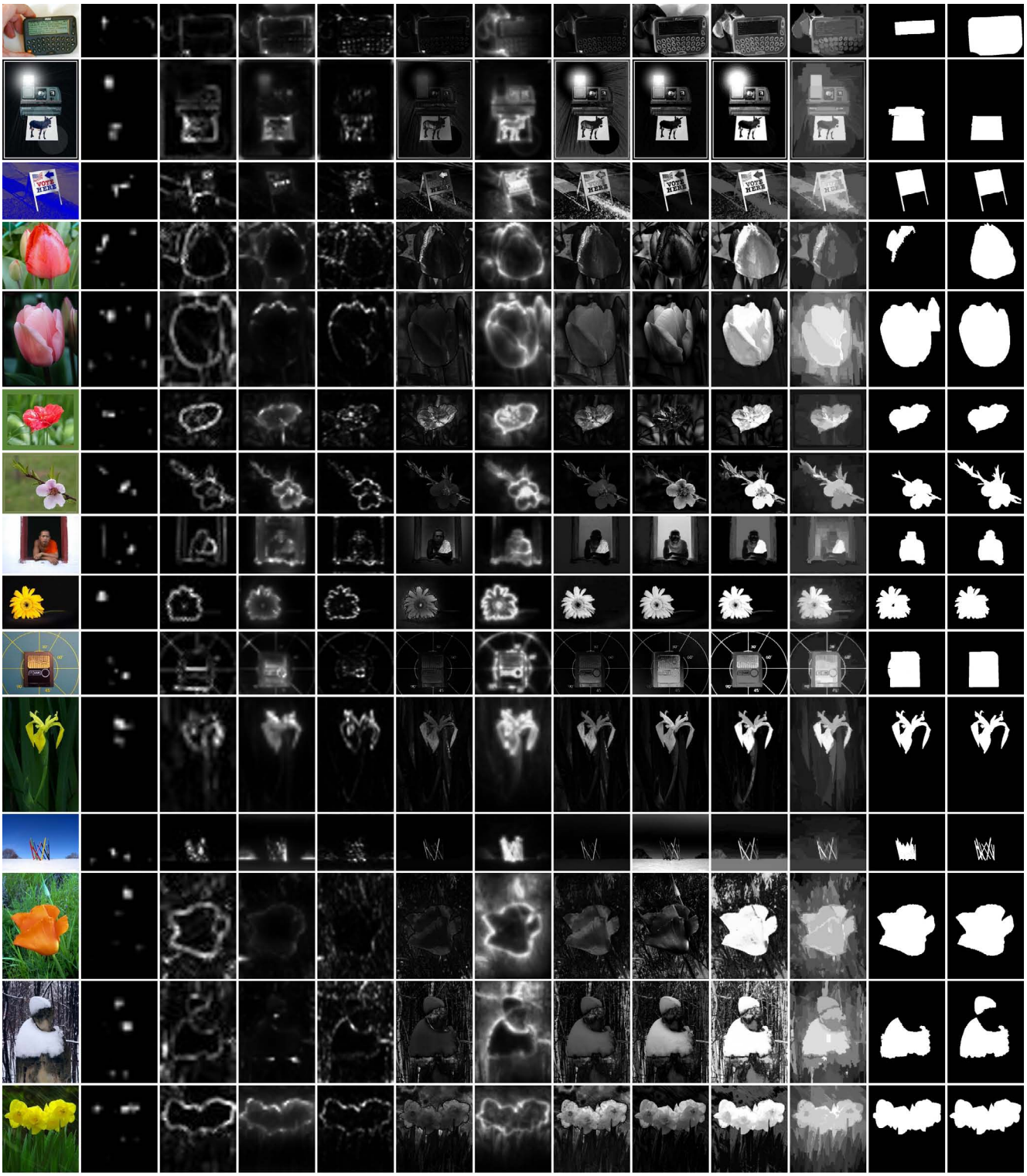

(a) (b) IT[6] (c) MZ[7] (d) GB[4] (e) SR[5] (f) AC[1] (g) CA[3] (h) FT[2] (i) LC[8] (j) HC (k) RC (l) RCC (m) g-tr

Figure 6. Typical saliency maps computed by different state-of-the-art methods (b-i) and by our proposed HC method (j) and RC method (k). Our saliency cut results (l) obtained using RC saliency maps are compared with ground truth (m).

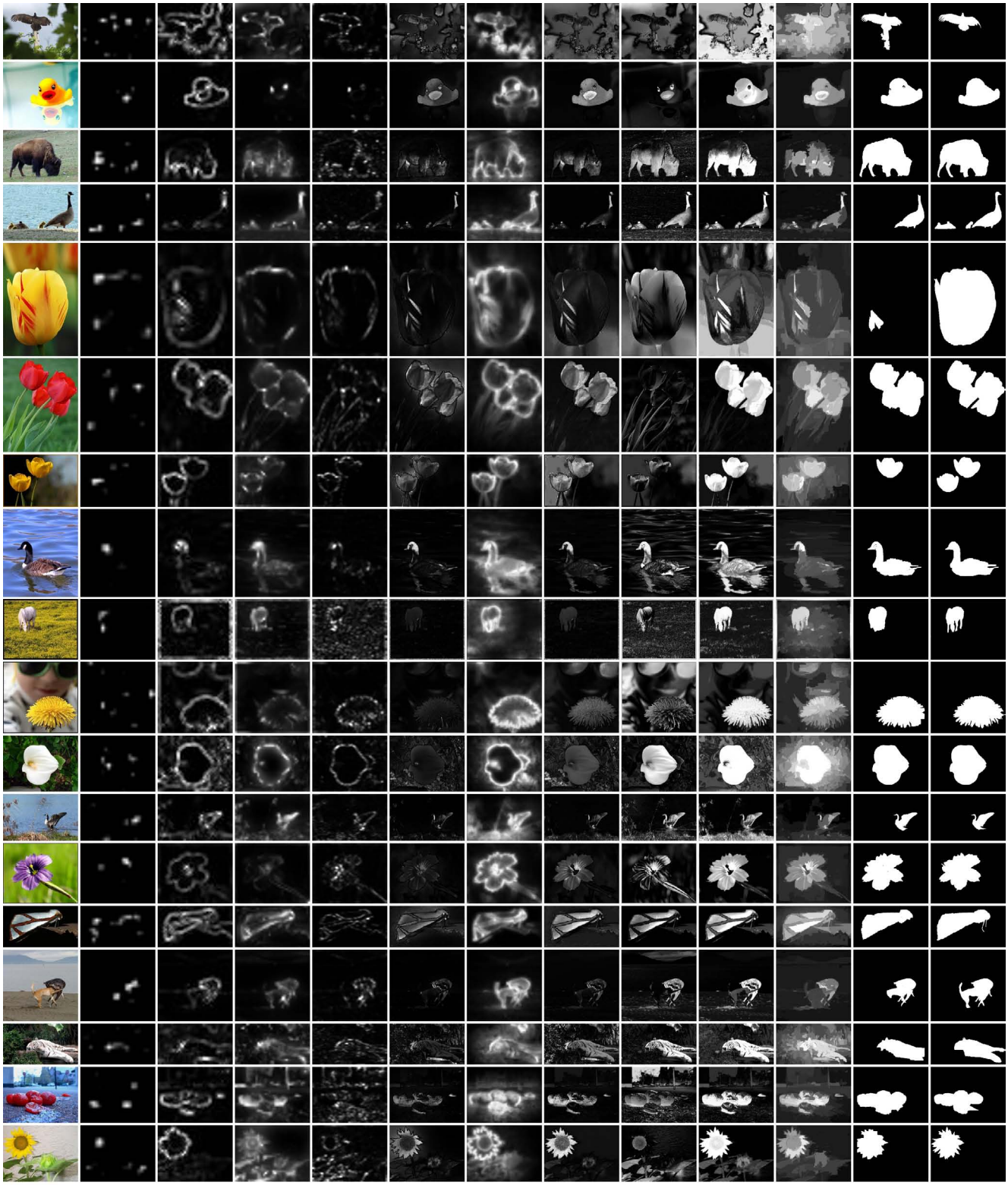

(a) (b) IT[6] (c) MZ[7] (d) GB[4] (e) SR[5] (f) AC[1] (g) CA[3] (h) FT[2] (i) LC[8] (j) HC (k) RC (l) RCC (m) g-tr

Figure 7. Typical saliency maps computed by different state-of-the-art methods (b-i) and by our proposed HC method (j) and RC method (k). Our saliency cut results (l) obtained using RC saliency maps are compared with ground truth (m).

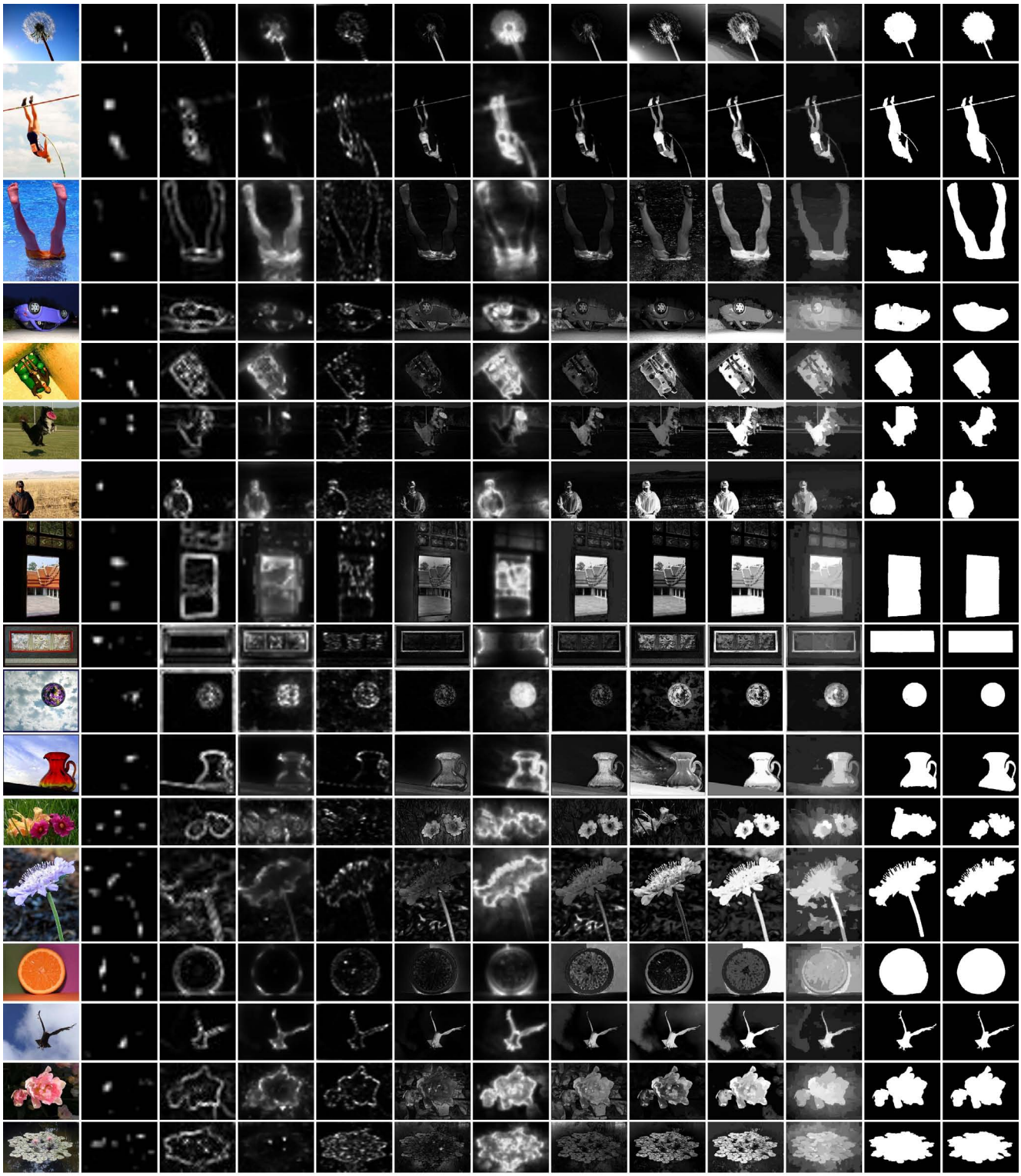

(a) (b) IT[6] (c) MZ[7] (d) GB[4] (e) SR[5] (f) AC[1] (g) CA[3] (h) FT[2] (i) LC[8] (j) HC (k) RC (l) RCC (m) g-tr

Figure 8. Typical saliency maps computed by different state-of-the-art methods (b-i) and by our proposed HC method (j) and RC method (k). Our saliency cut results (l) obtained using RC saliency maps are compared with ground truth (m).

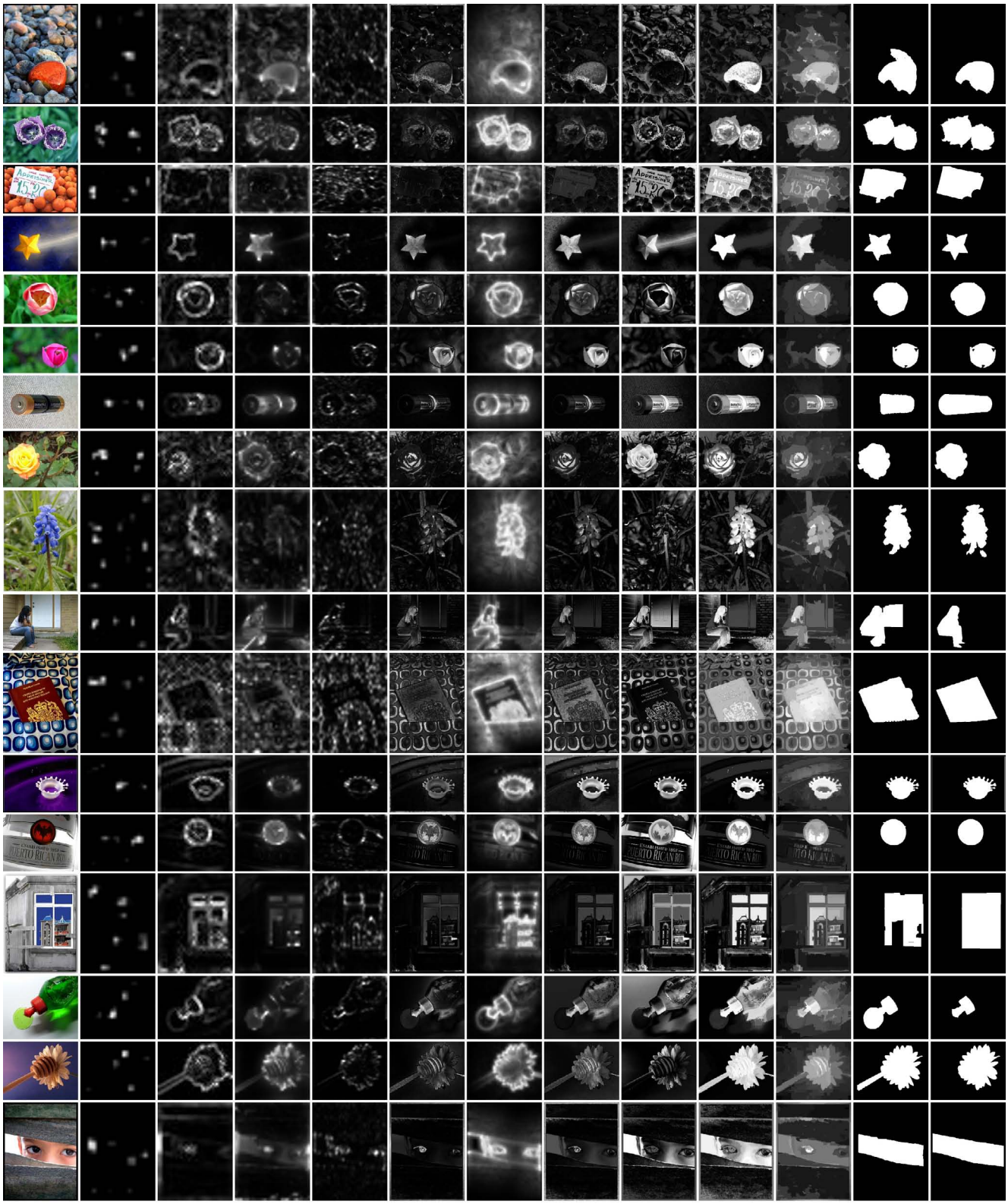

(a) (b) IT[6] (c) MZ[7] (d) GB[4] (e) SR[5] (f) AC[1] (g) CA[3] (h) FT[2] (i) LC[8] (j) HC (k) RC (l) RCC (m) g-tr

Figure 9. Typical saliency maps computed by different state-of-the-art methods (b-i) and by our proposed HC method (j) and RC method (k). Our saliency cut results (l) obtained using RC saliency maps are compared with ground truth (m).

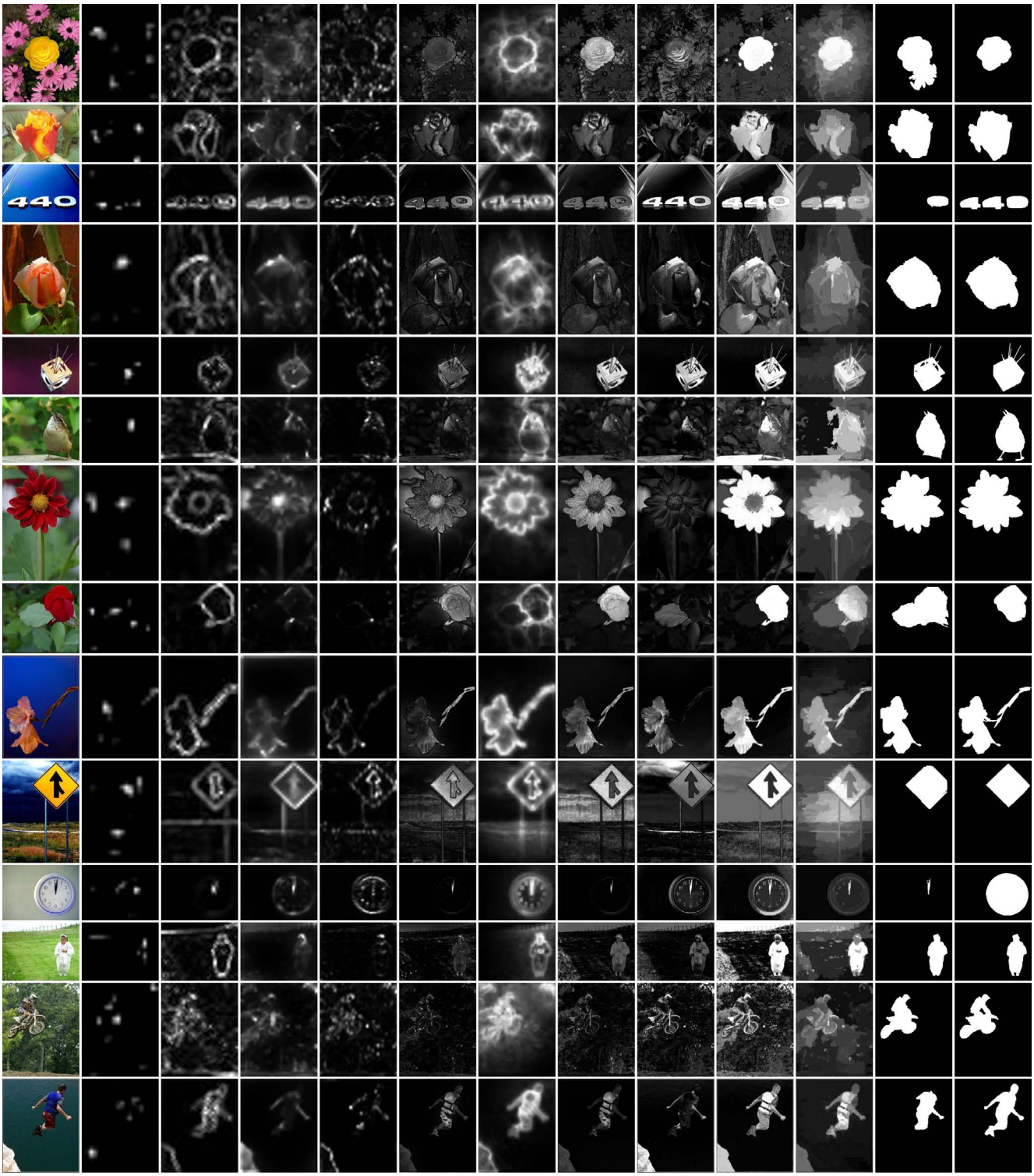

(a) (b) IT[6] (c) MZ[7] (d) GB[4] (e) SR[5] (f) AC[1] (g) CA[3] (h) FT[2] (i) LC[8] (j) HC (k) RC (l) RCC (m) g-tr

Figure 10. Typical saliency maps computed by different state-of-the-art methods (b-i) and by our proposed HC method (j) and RC method (k). Our saliency cut results (l) obtained using RC saliency maps are compared with ground truth (m).

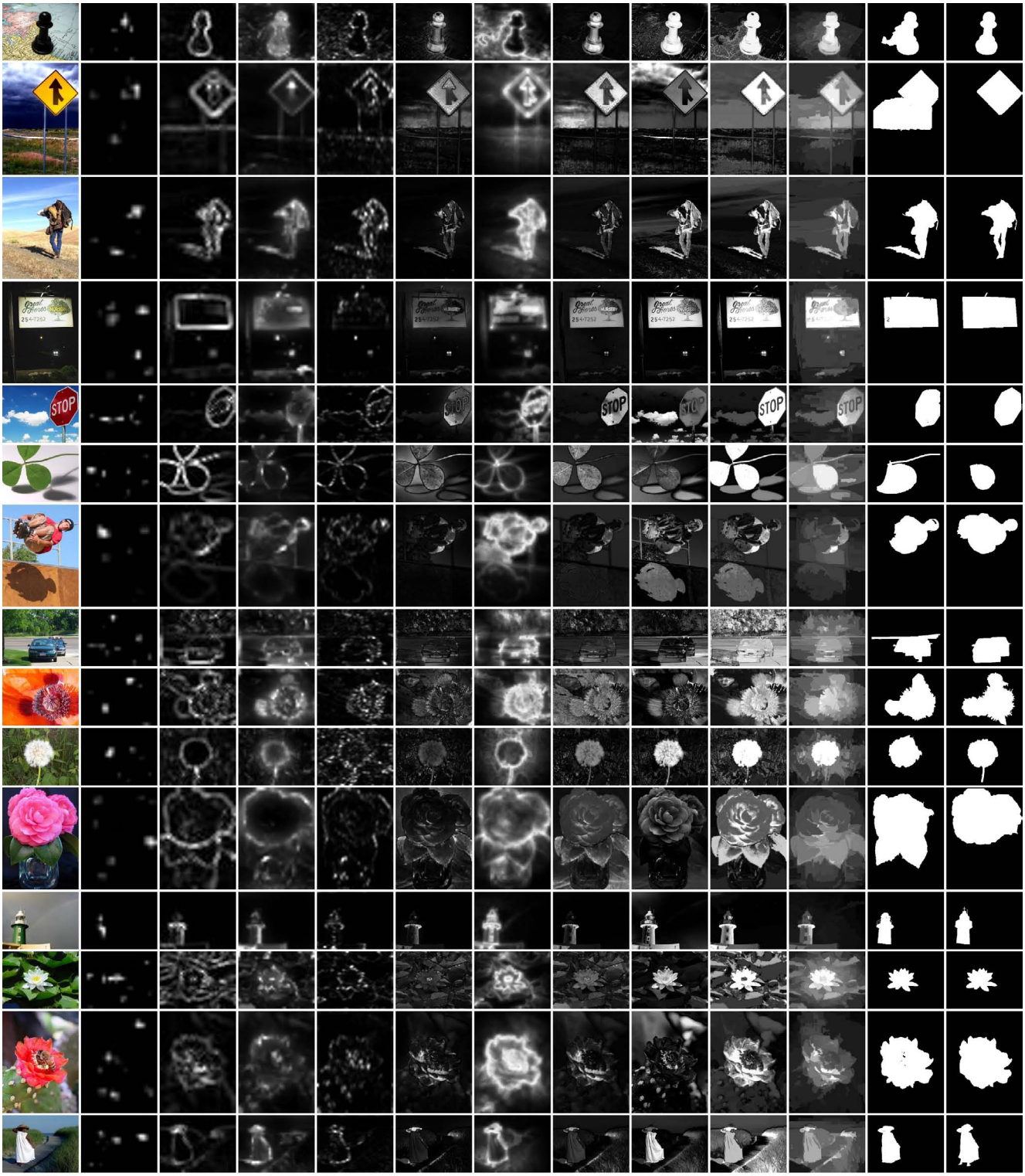

(a) (b) IT[6] (c) MZ[7] (d) GB[4] (e) SR[5] (f) AC[1] (g) CA[3] (h) FT[2] (i) LC[8] (j) HC (k) RC (l) RCC (m) g-tr

Figure 11. Typical saliency maps computed by different state-of-the-art methods (b-i) and by our proposed HC method (j) and RC method (k). Our saliency cut results (l) obtained using RC saliency maps are compared with ground truth (m).

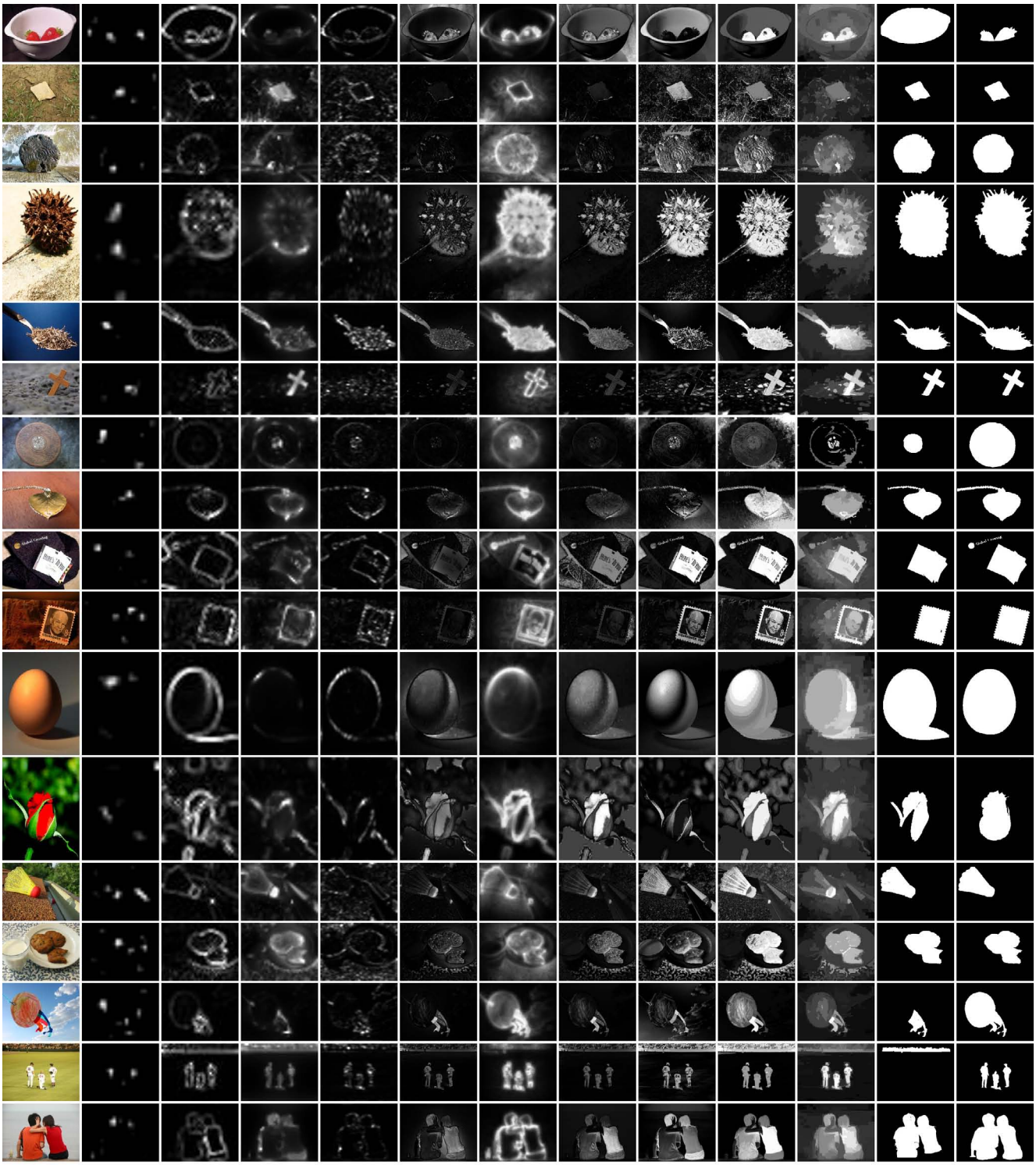

(a) (b) IT[6] (c) MZ[7] (d) GB[4] (e) SR[5] (f) AC[1] (g) CA[3] (h) FT[2] (i) LC[8] (j) HC (k) RC (l) RCC (m) g-tr

Figure 12. Typical saliency maps computed by different state-of-the-art methods (b-i) and by our proposed HC method (j) and RC method (k). Our saliency cut results (l) obtained using RC saliency maps are compared with ground truth (m).

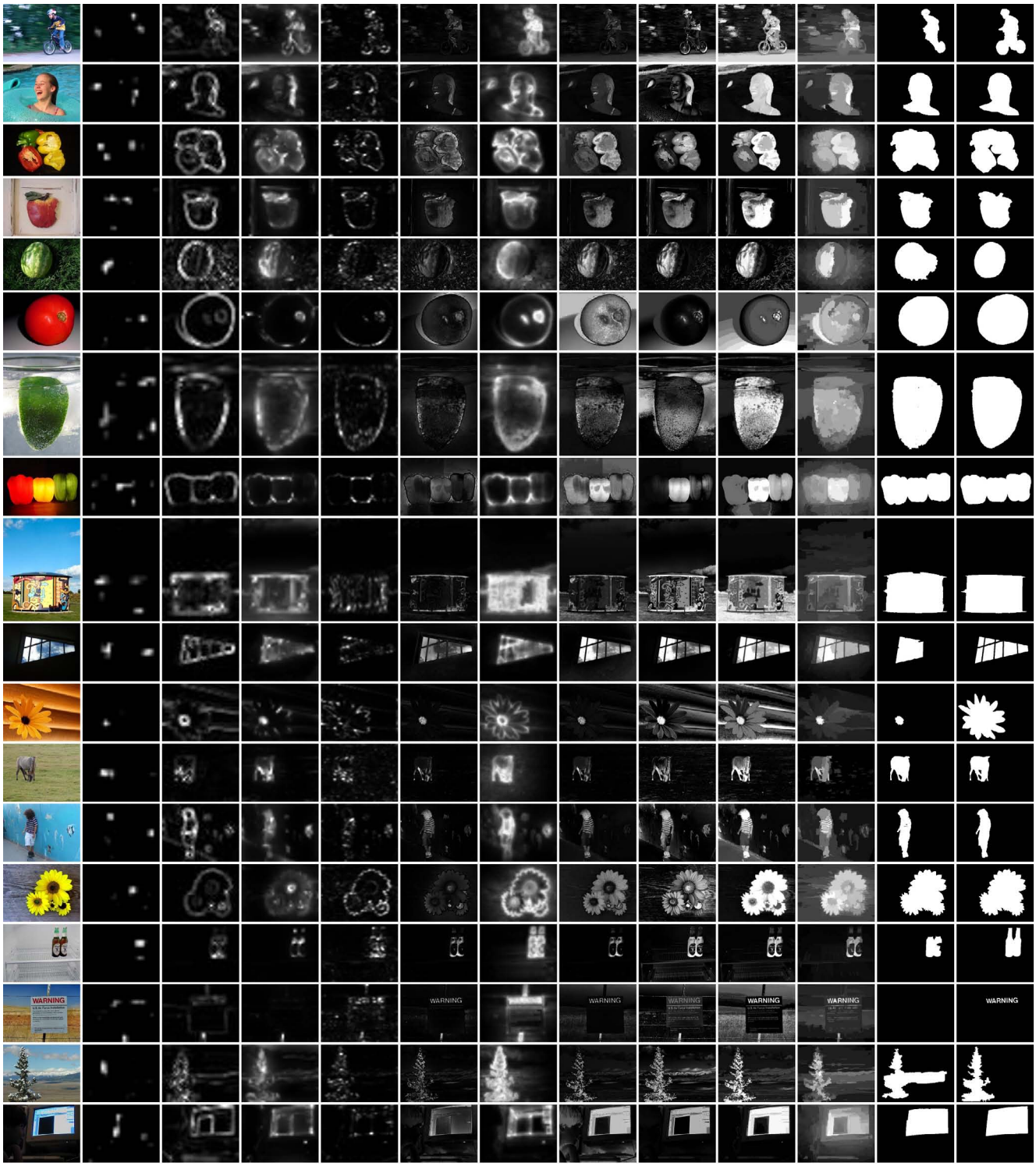

(a) (b) IT[6] (c) MZ[7] (d) GB[4] (e) SR[5] (f) AC[1] (g) CA[3] (h) FT[2] (i) LC[8] (j) HC (k) RC (l) RCC (m) g-tr

Figure 13. Typical saliency maps computed by different state-of-the-art methods (b-i) and by our proposed HC method (j) and RC method (k). Our saliency cut results (l) obtained using RC saliency maps are compared with ground truth (m).

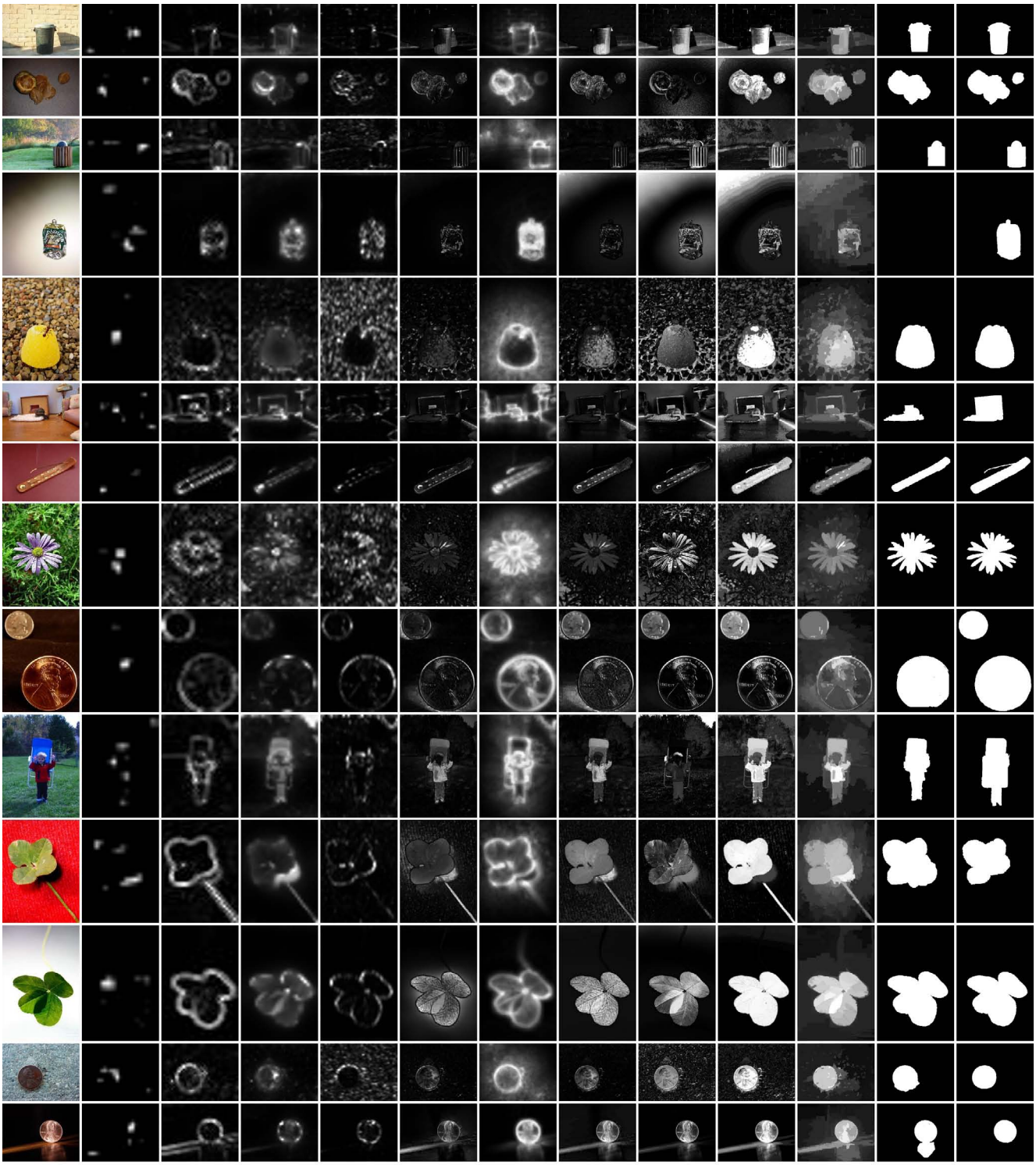

(a) (b) IT[6] (c) MZ[7] (d) GB[4] (e) SR[5] (f) AC[1] (g) CA[3] (h) FT[2] (i) LC[8] (j) HC (k) RC (l) RCC (m) g-tr

Figure 14. Typical saliency maps computed by different state-of-the-art methods (b-i) and by our proposed HC method (j) and RC method (k). Our saliency cut results (l) obtained using RC saliency maps are compared with ground truth (m).

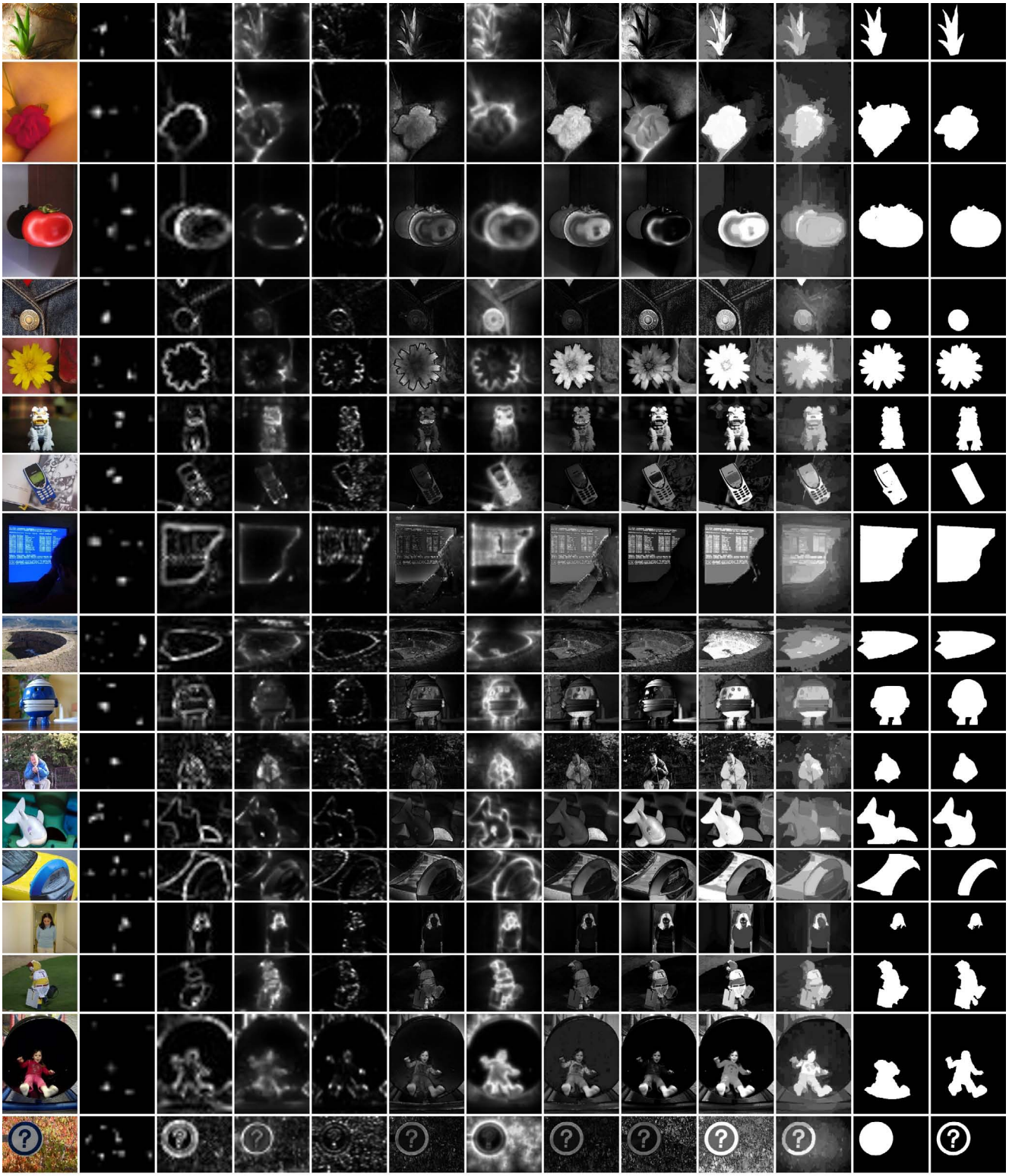

(a) (b) IT[6] (c) MZ[7] (d) GB[4] (e) SR[5] (f) AC[1] (g) CA[3] (h) FT[2] (i) LC[8] (j) HC (k) RC (l) RCC (m) g-tr

Figure 15. Typical saliency maps computed by different state-of-the-art methods (b-i) and by our proposed HC method (j) and RC method (k). Our saliency cut results (l) obtained using RC saliency maps are compared with ground truth (m).

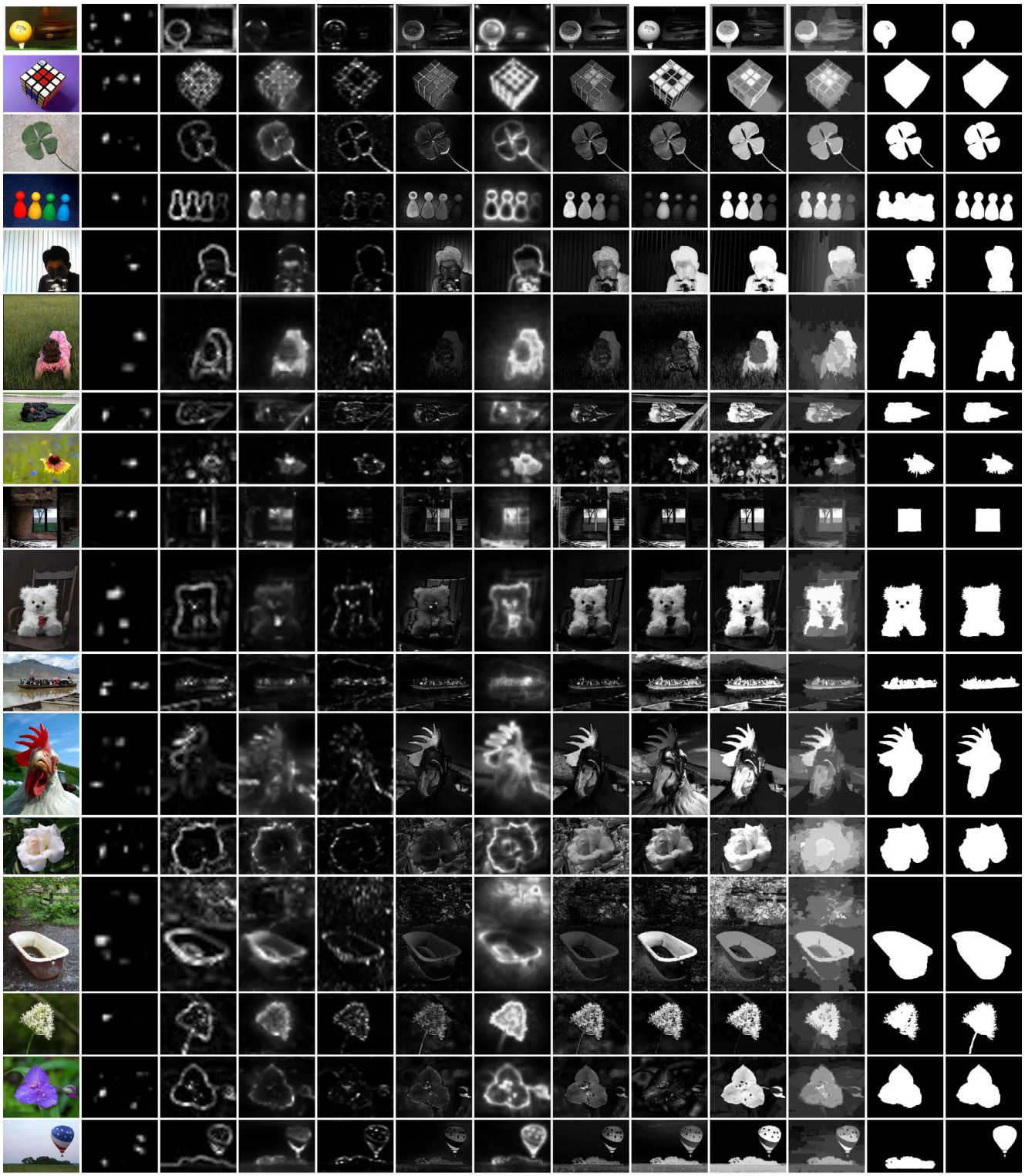

(a) (b) IT[6] (c) MZ[7] (d) GB[4] (e) SR[5] (f) AC[1] (g) CA[3] (h) FT[2] (i) LC[8] (j) HC (k) RC (l) RCC (m) g-tr

Figure 16. Typical saliency maps computed by different state-of-the-art methods (b-i) and by our proposed HC method (j) and RC method (k). Our saliency cut results (l) obtained using RC saliency maps are compared with ground truth (m).

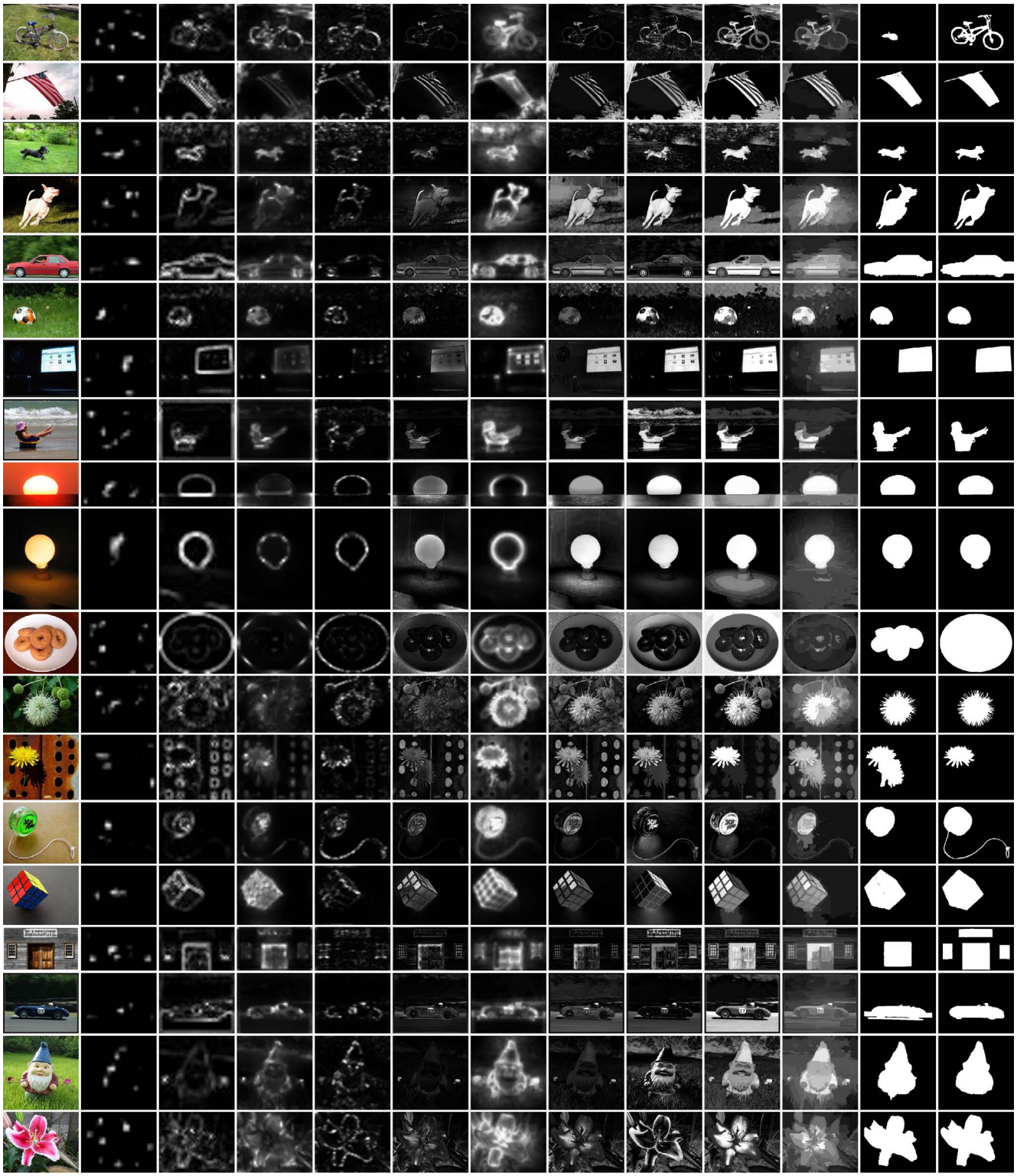

(a) (b) IT[6] (c) MZ[7] (d) GB[4] (e) SR[5] (f) AC[1] (g) CA[3] (h) FT[2] (i) LC[8] (j) HC (k) RC (l) RCC (m) g-tr

Figure 17. Typical saliency maps computed by different state-of-the-art methods (b-i) and by our proposed HC method (j) and RC method (k). Our saliency cut results (l) obtained using RC saliency maps are compared with ground truth (m).

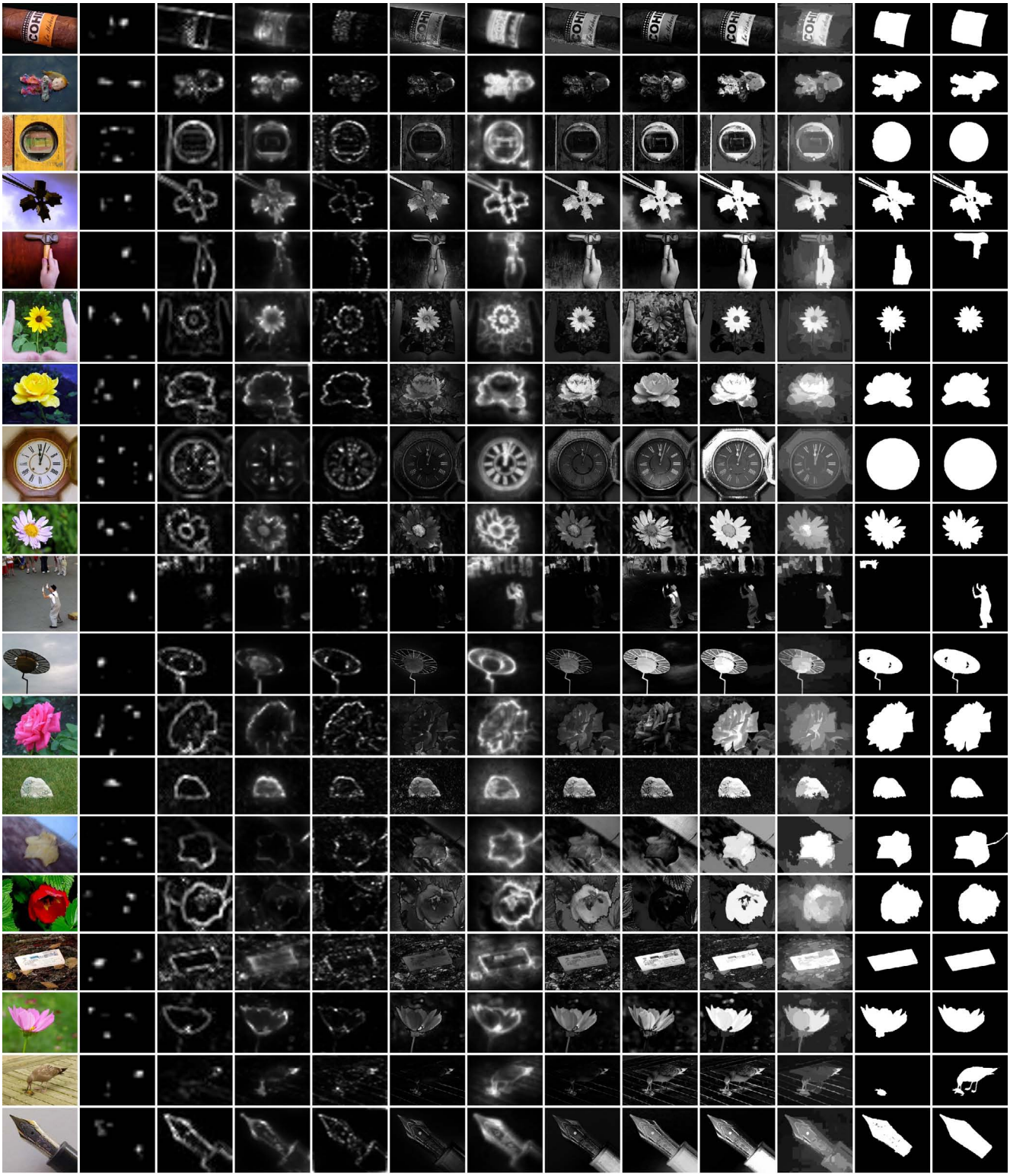

(a) (b) IT[6] (c) MZ[7] (d) GB[4] (e) SR[5] (f) AC[1] (g) CA[3] (h) FT[2] (i) LC[8] (j) HC (k) RC (l) RCC (m) g-tr

Figure 18. Typical saliency maps computed by different state-of-the-art methods (b-i) and by our proposed HC method (j) and RC method (k). Our saliency cut results (l) obtained using RC saliency maps are compared with ground truth (m).

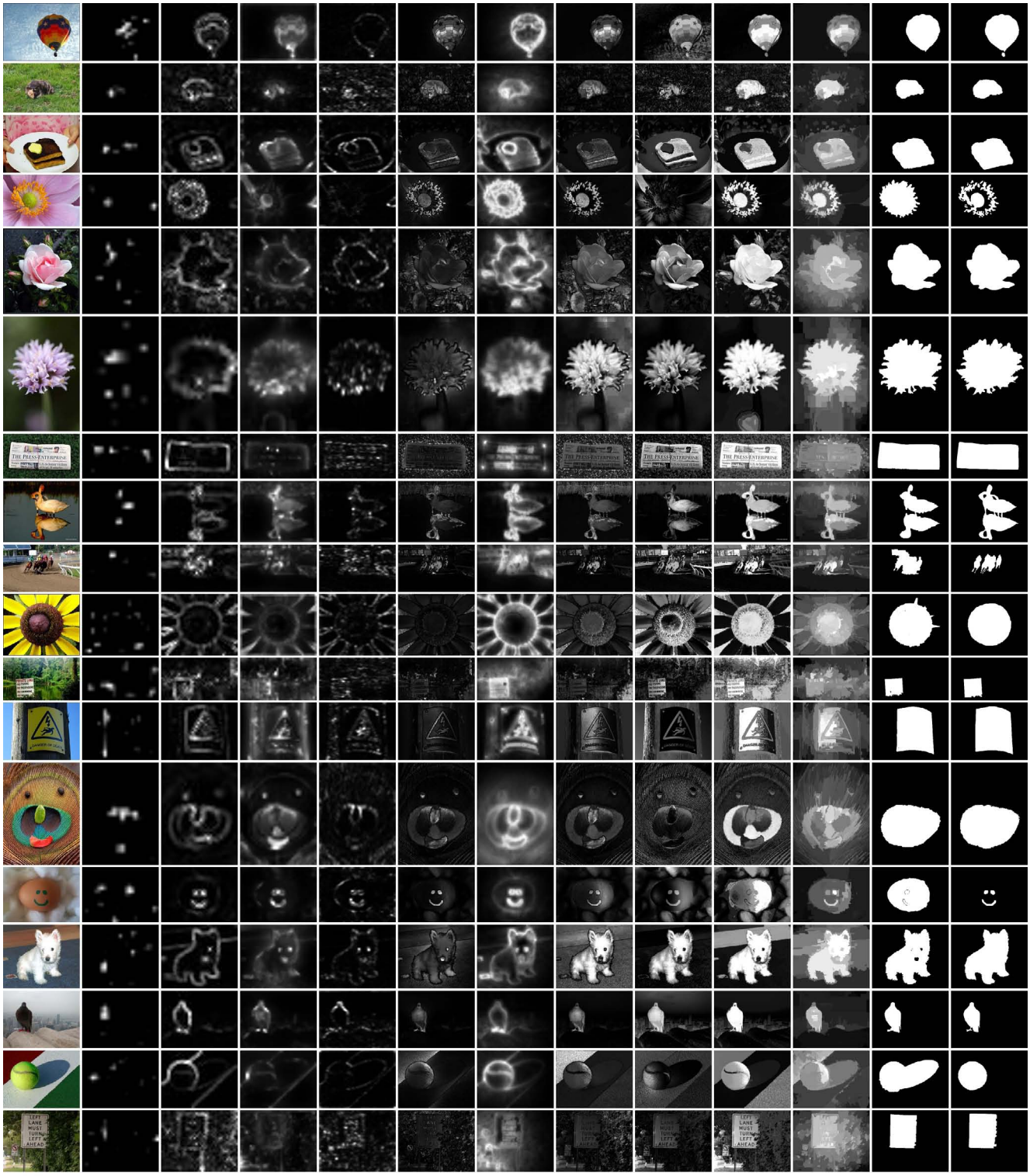

(a) (b) IT[6] (c) MZ[7] (d) GB[4] (e) SR[5] (f) AC[1] (g) CA[3] (h) FT[2] (i) LC[8] (j) HC (k) RC (l) RCC (m) g-tr

Figure 19. Typical saliency maps computed by different state-of-the-art methods (b-i) and by our proposed HC method (j) and RC method (k). Our saliency cut results (l) obtained using RC saliency maps are compared with ground truth (m).

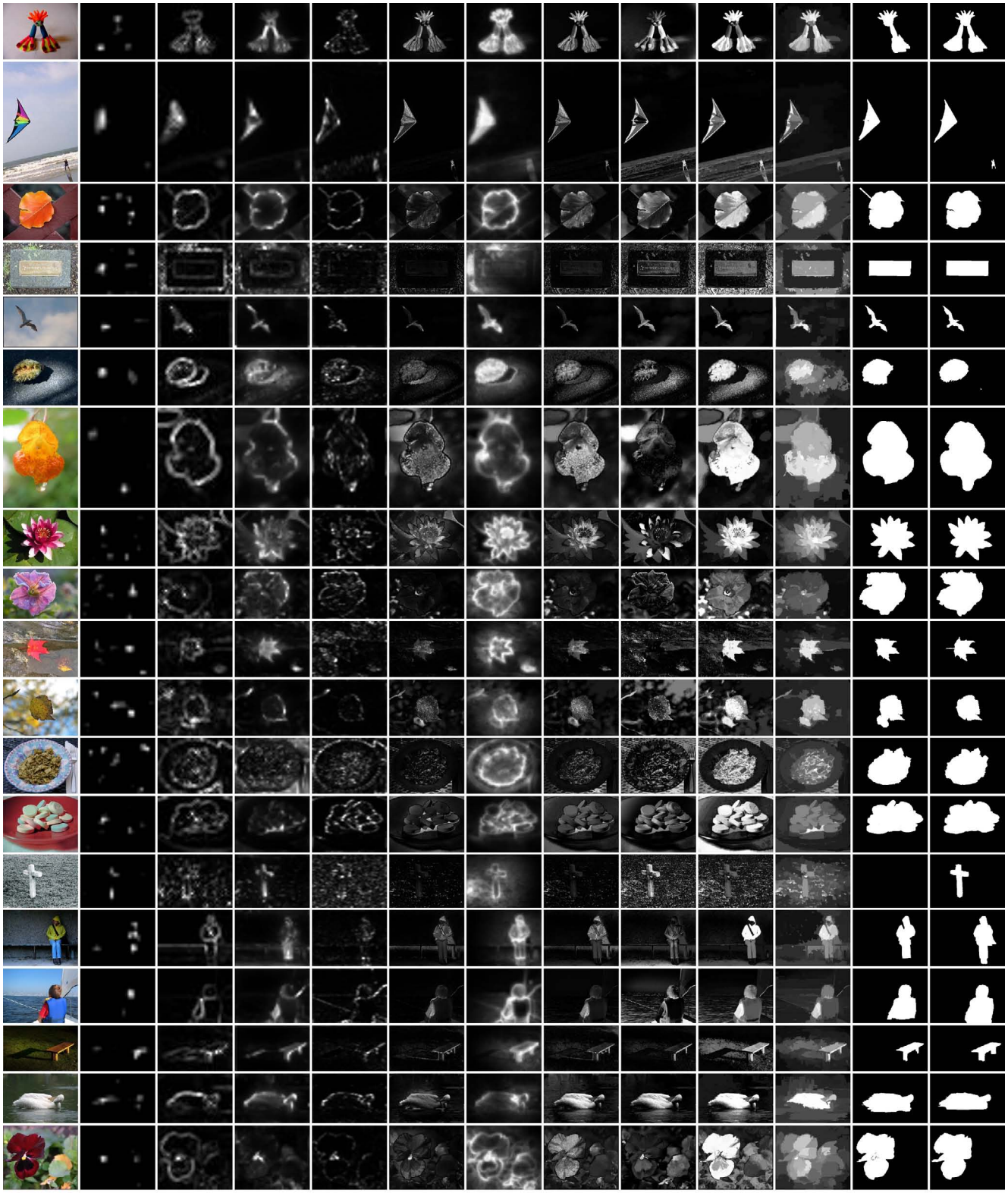

(a) (b) IT[6] (c) MZ[7] (d) GB[4] (e) SR[5] (f) AC[1] (g) CA[3] (h) FT[2] (i) LC[8] (j) HC (k) RC (l) RCC (m) g-tr

Figure 20. Typical saliency maps computed by different state-of-the-art methods (b-i) and by our proposed HC method (j) and RC method (k). Our saliency cut results (l) obtained using RC saliency maps are compared with ground truth (m).

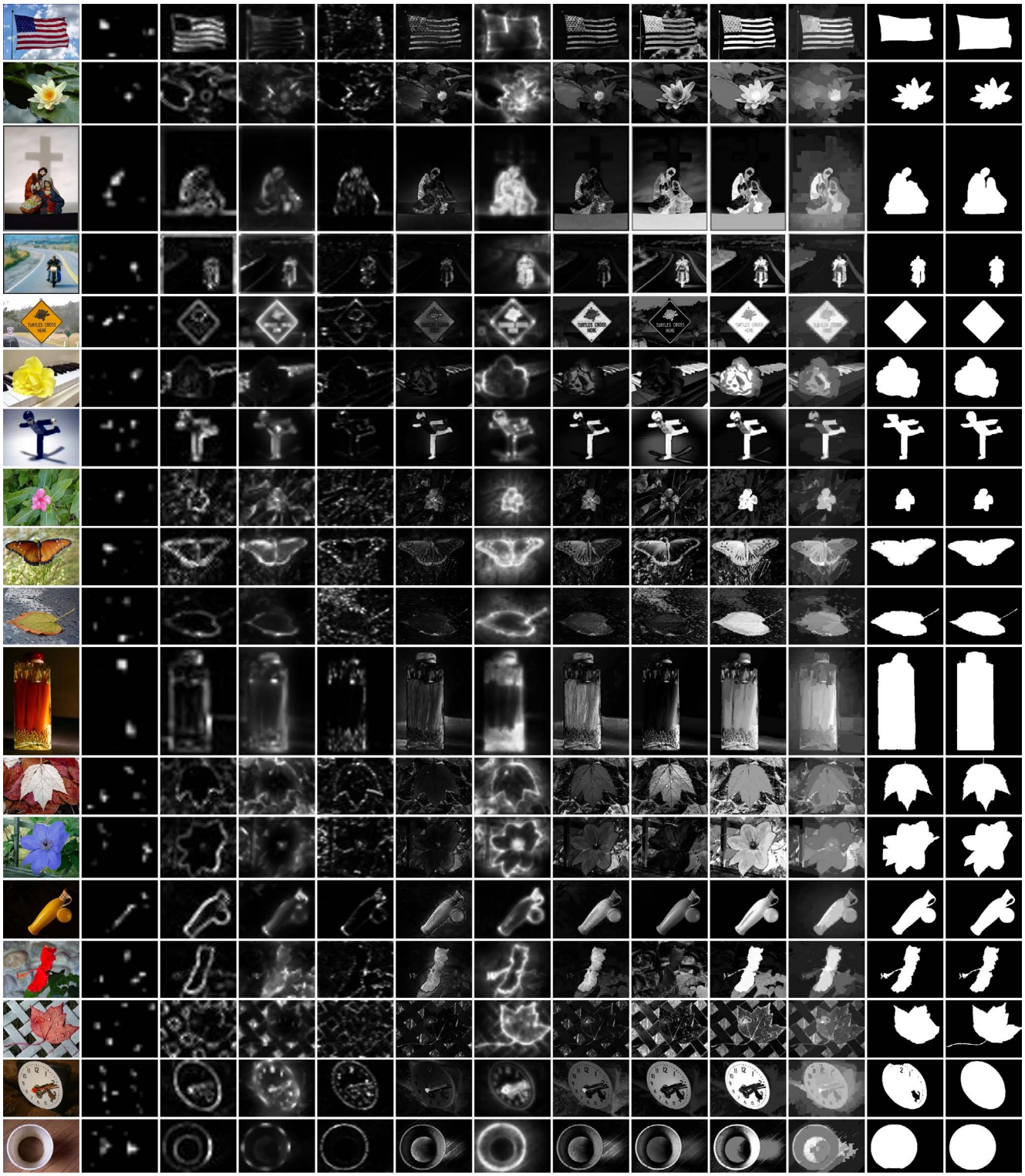

(a) (b) IT[6] (c) MZ[7] (d) GB[4] (e) SR[5] (f) AC[1] (g) CA[3] (h) FT[2] (i) LC[8] (j) HC (k) RC (l) RCC (m) g-tr

Figure 21. Typical saliency maps computed by different state-of-the-art methods (b-i) and by our proposed HC method (j) and RC method (k). Our saliency cut results (l) obtained using RC saliency maps are compared with ground truth (m).

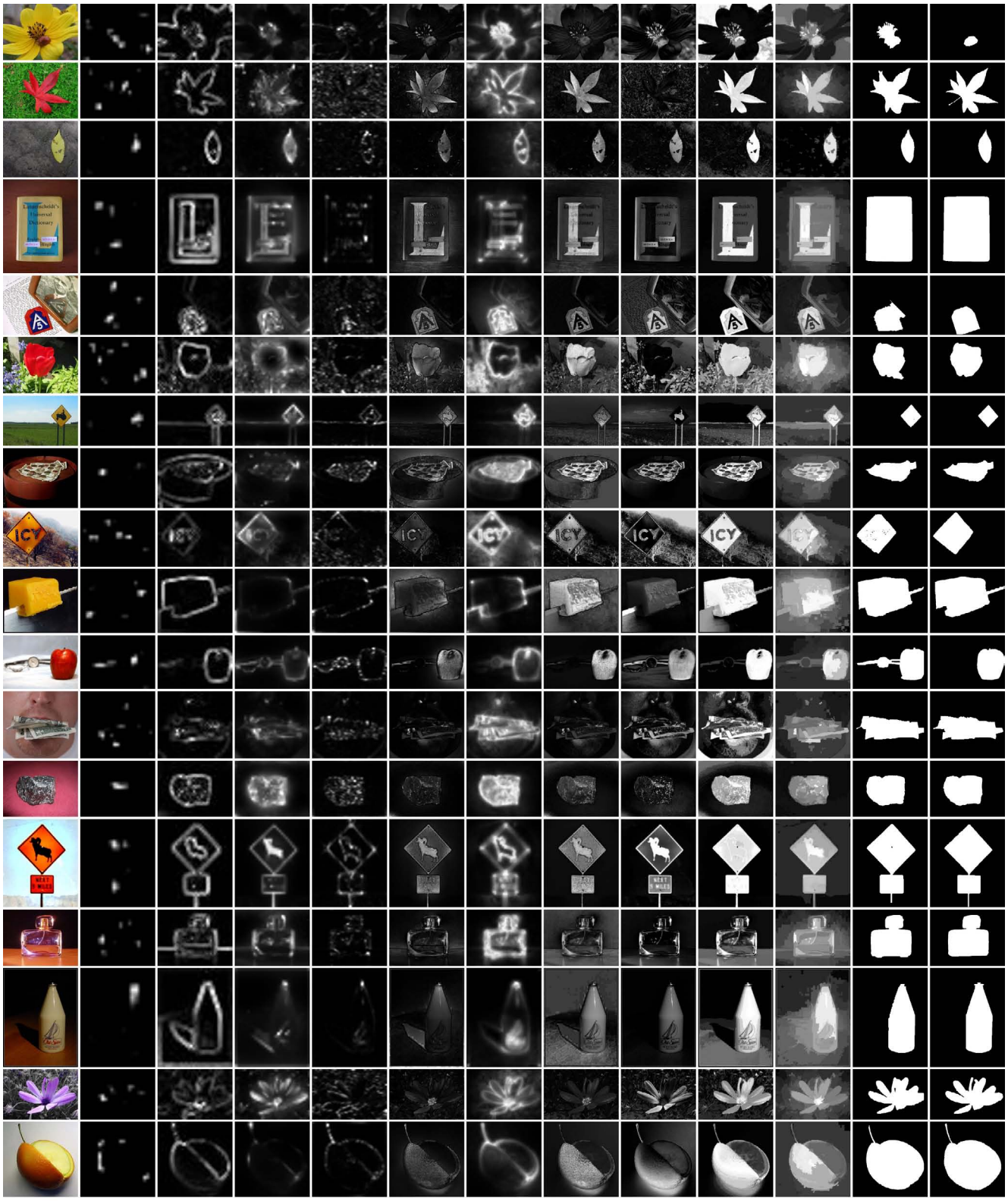

(a) (b) IT[6] (c) MZ[7] (d) GB[4] (e) SR[5] (f) AC[1] (g) CA[3] (h) FT[2] (i) LC[8] (j) HC (k) RC (l) RCC (m) g-tr

Figure 22. Typical saliency maps computed by different state-of-the-art methods (b-i) and by our proposed HC method (j) and RC method (k). Our saliency cut results (l) obtained using RC saliency maps are compared with ground truth (m).

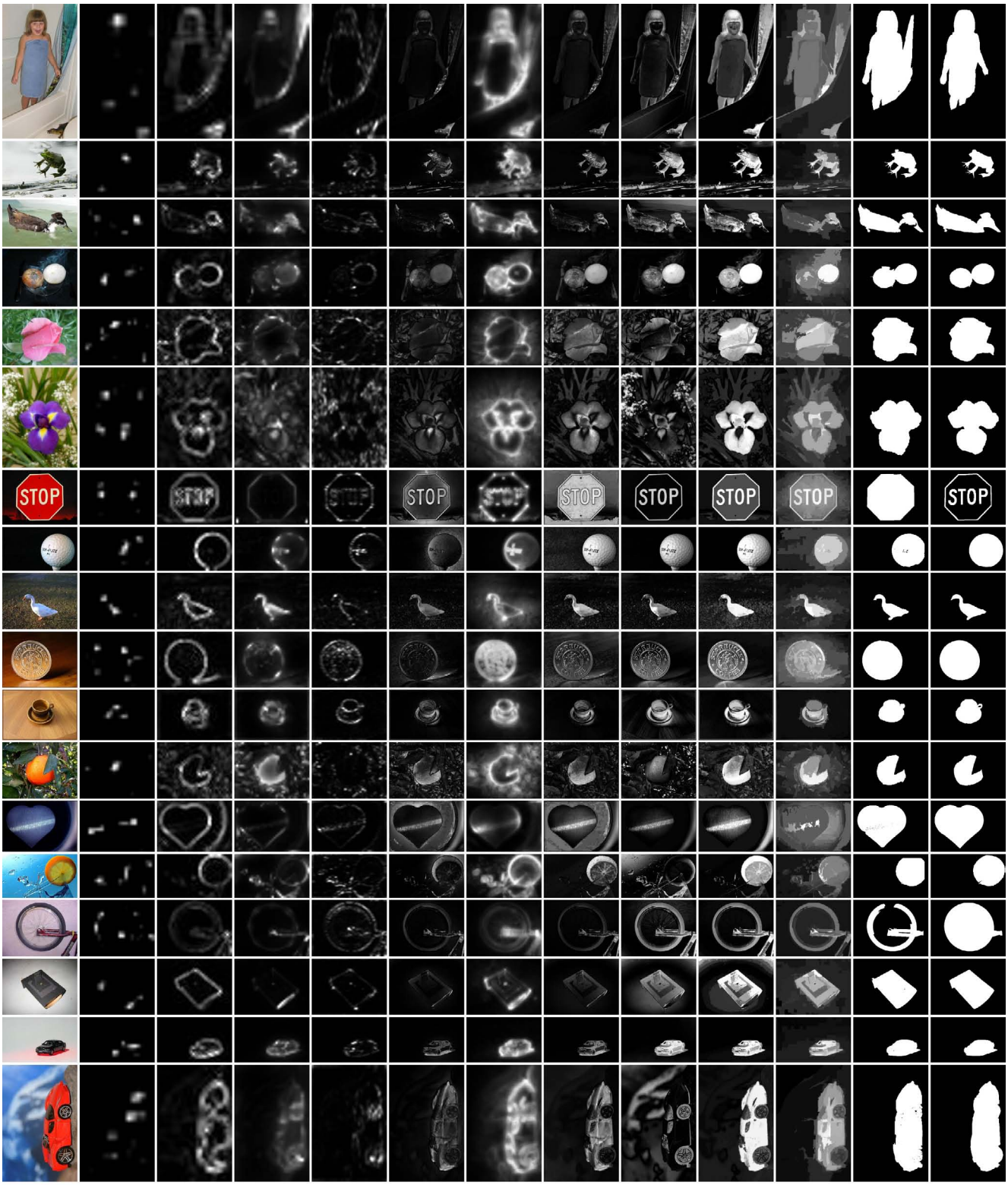

(a) (b) IT[6] (c) MZ[7] (d) GB[4] (e) SR[5] (f) AC[1] (g) CA[3] (h) FT[2] (i) LC[8] (j) HC (k) RC (l) RCC (m) g-tr

Figure 23. Typical saliency maps computed by different state-of-the-art methods (b-i) and by our proposed HC method (j) and RC method (k). Our saliency cut results (l) obtained using RC saliency maps are compared with ground truth (m).

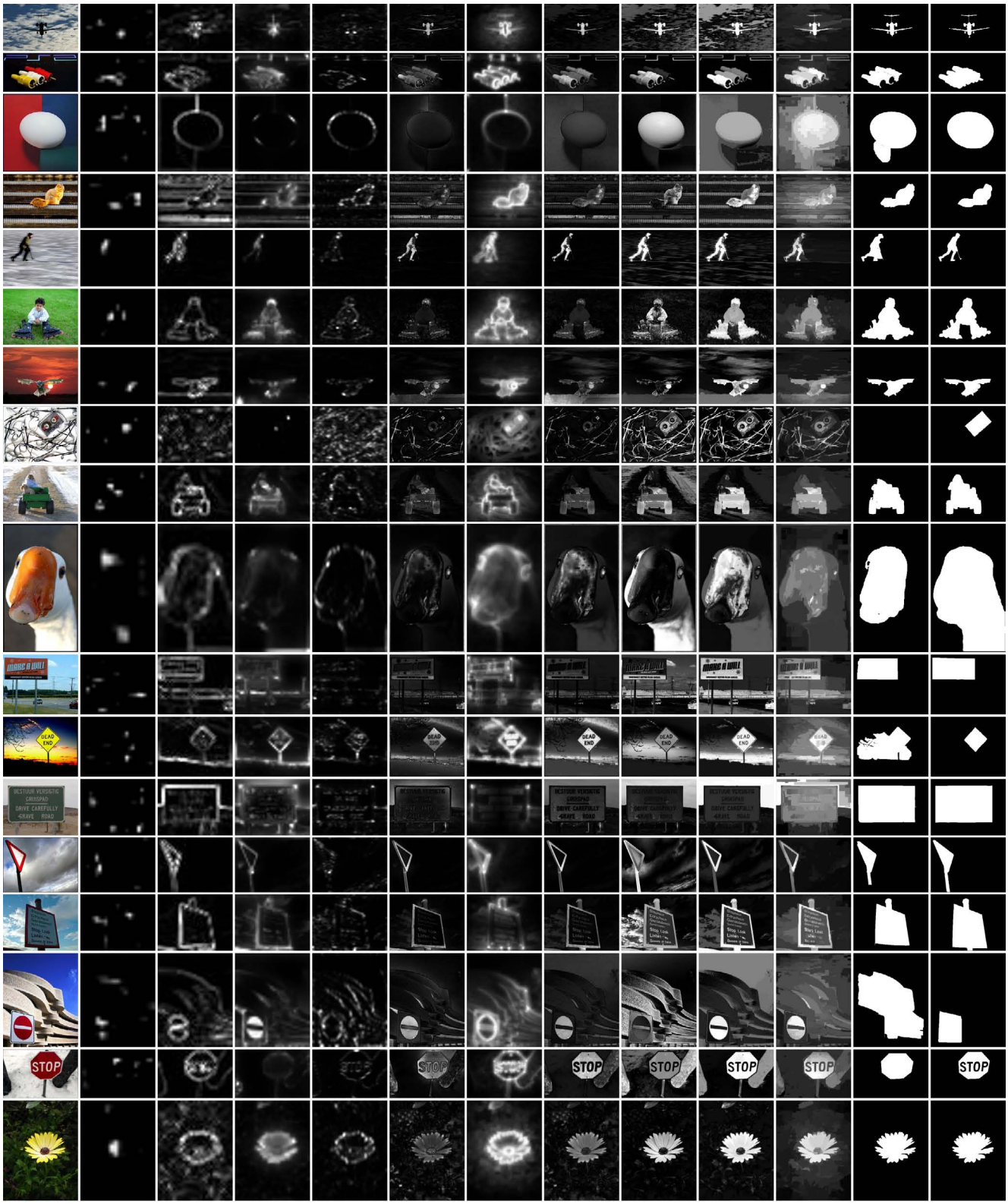

(a) (b) IT[6] (c) MZ[7] (d) GB[4] (e) SR[5] (f) AC[1] (g) CA[3] (h) FT[2] (i) LC[8] (j) HC (k) RC (l) RCC (m) g-tr

Figure 24. Typical saliency maps computed by different state-of-the-art methods (b-i) and by our proposed HC method (j) and RC method (k). Our saliency cut results (l) obtained using RC saliency maps are compared with ground truth (m).

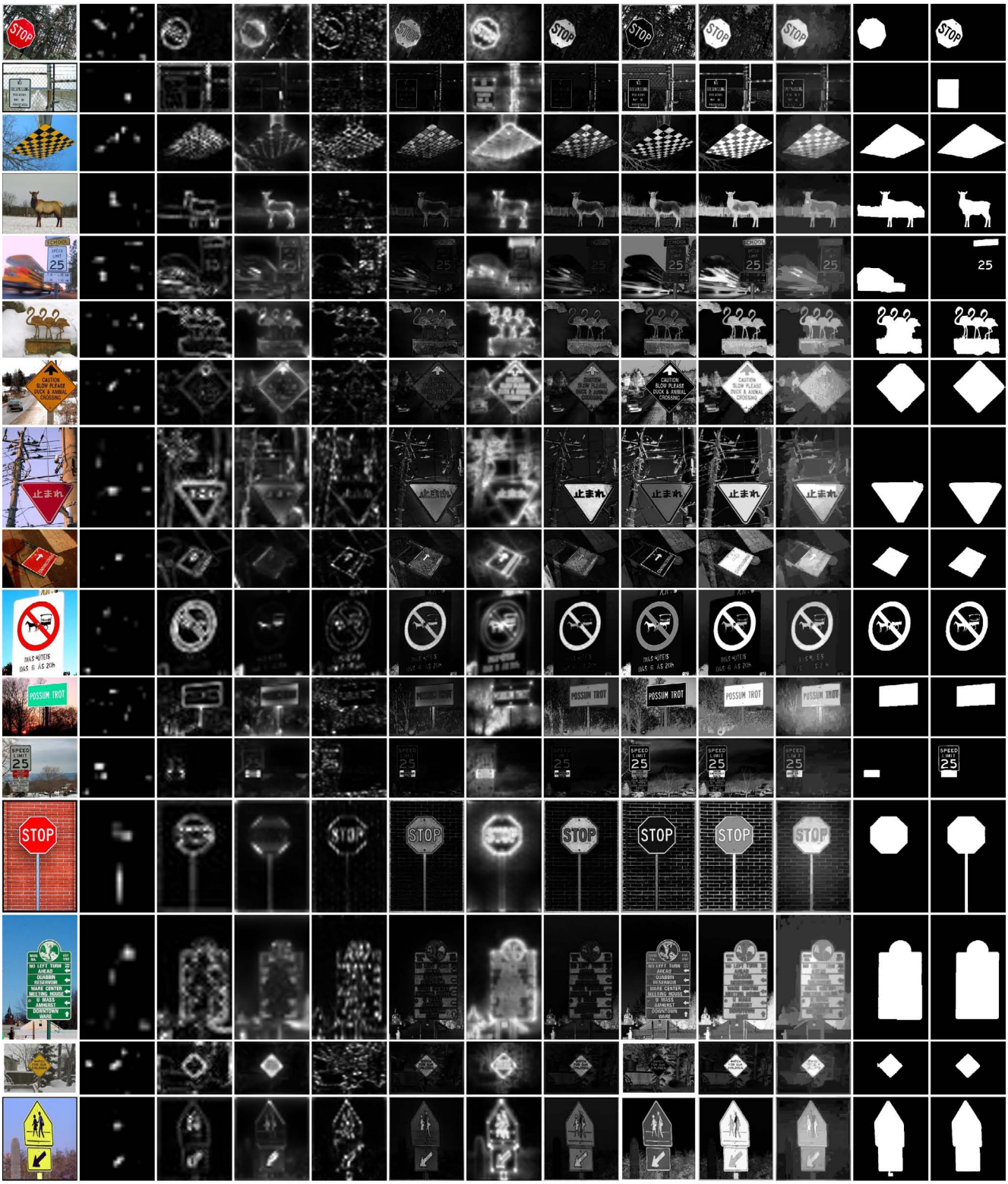

(a) (b) IT[6] (c) MZ[7] (d) GB[4] (e) SR[5] (f) AC[1] (g) CA[3] (h) FT[2] (i) LC[8] (j) HC (k) RC (l) RCC (m) g-tr

Figure 25. Typical saliency maps computed by different state-of-the-art methods (b-i) and by our proposed HC method (j) and RC method (k). Our saliency cut results (l) obtained using RC saliency maps are compared with ground truth (m).

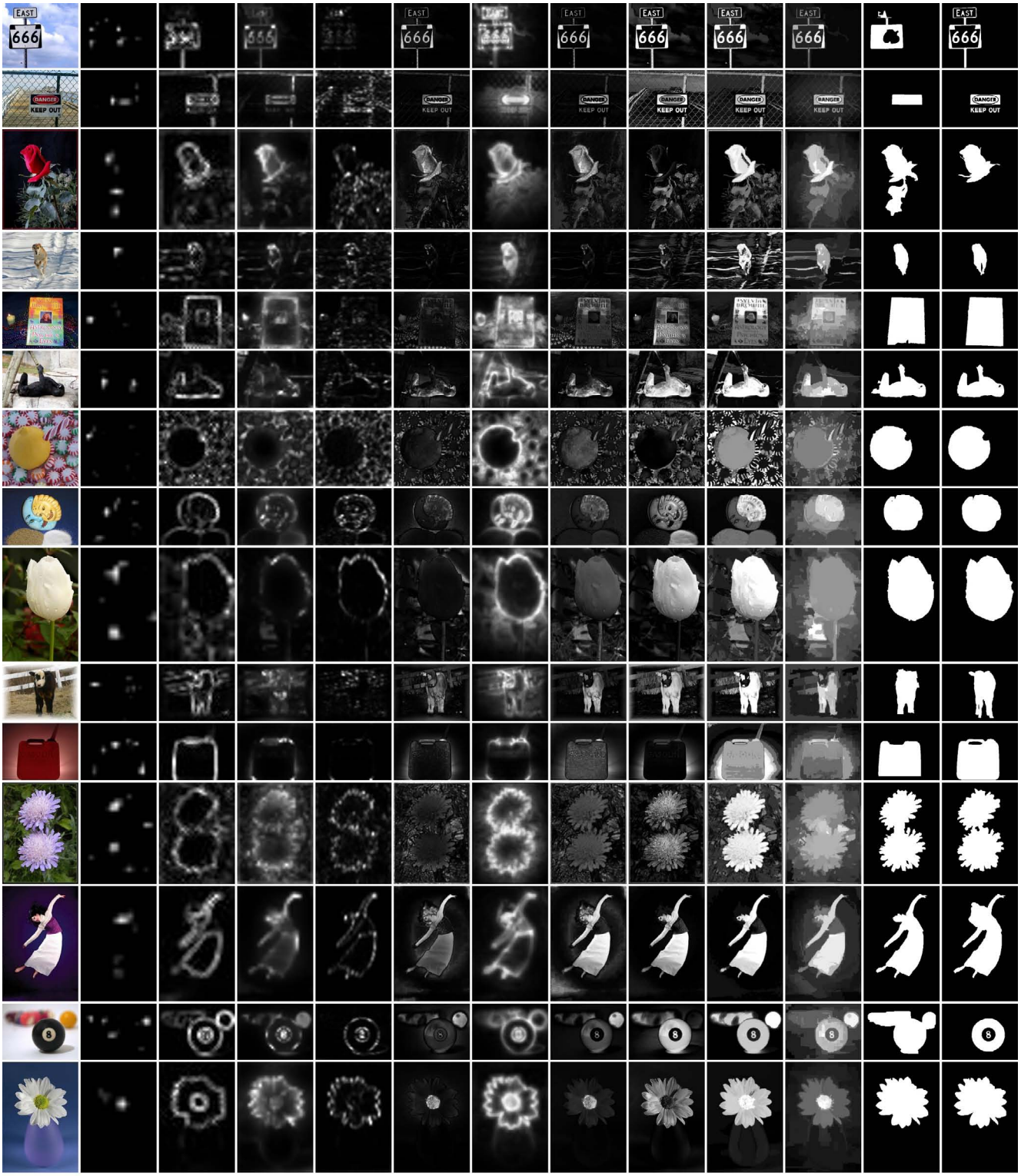

(a) (b) IT[6] (c) MZ[7] (d) GB[4] (e) SR[5] (f) AC[1] (g) CA[3] (h) FT[2] (i) LC[8] (j) HC (k) RC (l) RCC (m) g-tr

Figure 26. Typical saliency maps computed by different state-of-the-art methods (b-i) and by our proposed HC method (j) and RC method (k). Our saliency cut results (l) obtained using RC saliency maps are compared with ground truth (m).

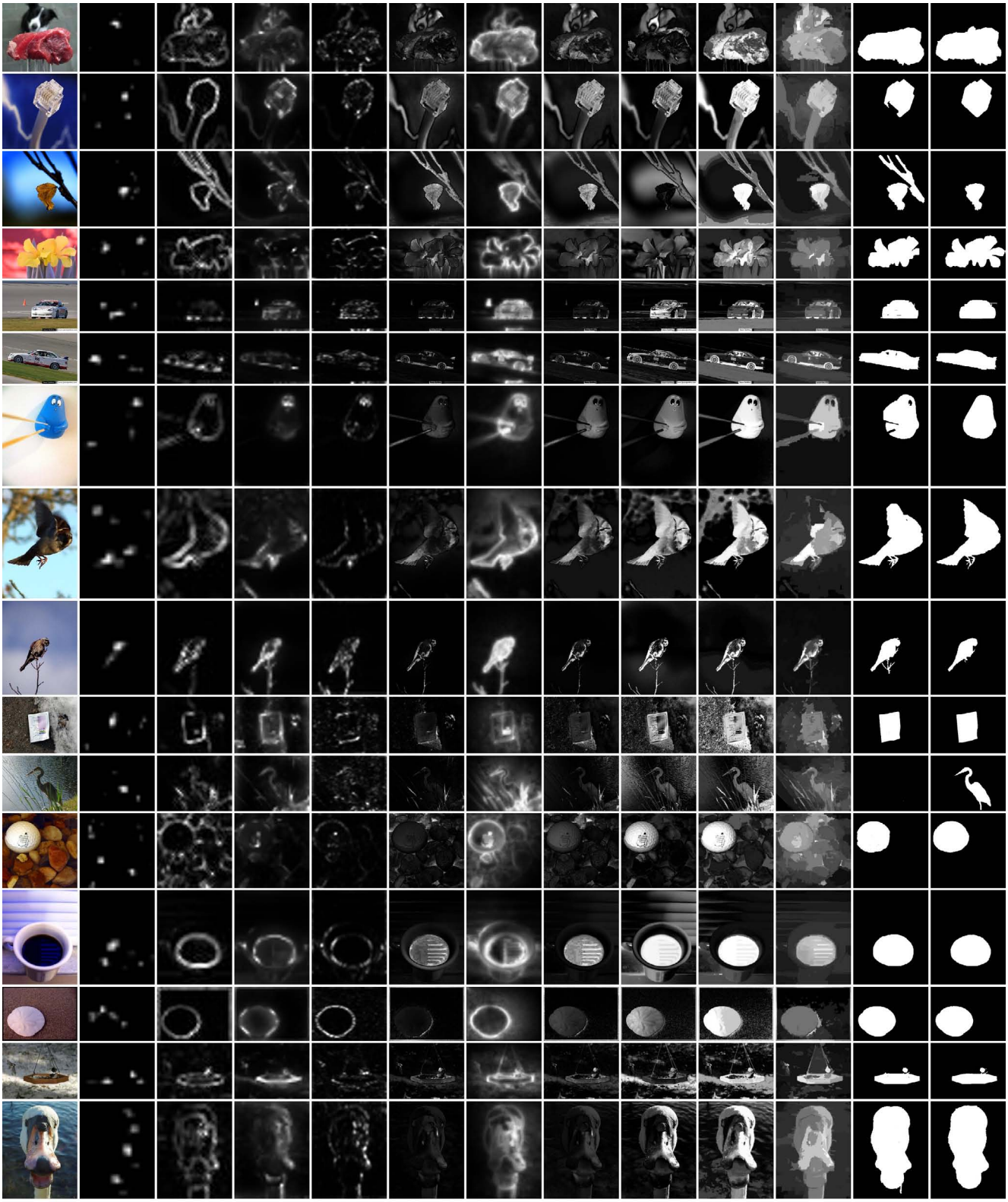

(a) (b) IT[6] (c) MZ[7] (d) GB[4] (e) SR[5] (f) AC[1] (g) CA[3] (h) FT[2] (i) LC[8] (j) HC (k) RC (l) RCC (m) g-tr

Figure 27. Typical saliency maps computed by different state-of-the-art methods (b-i) and by our proposed HC method (j) and RC method (k). Our saliency cut results (l) obtained using RC saliency maps are compared with ground truth (m).

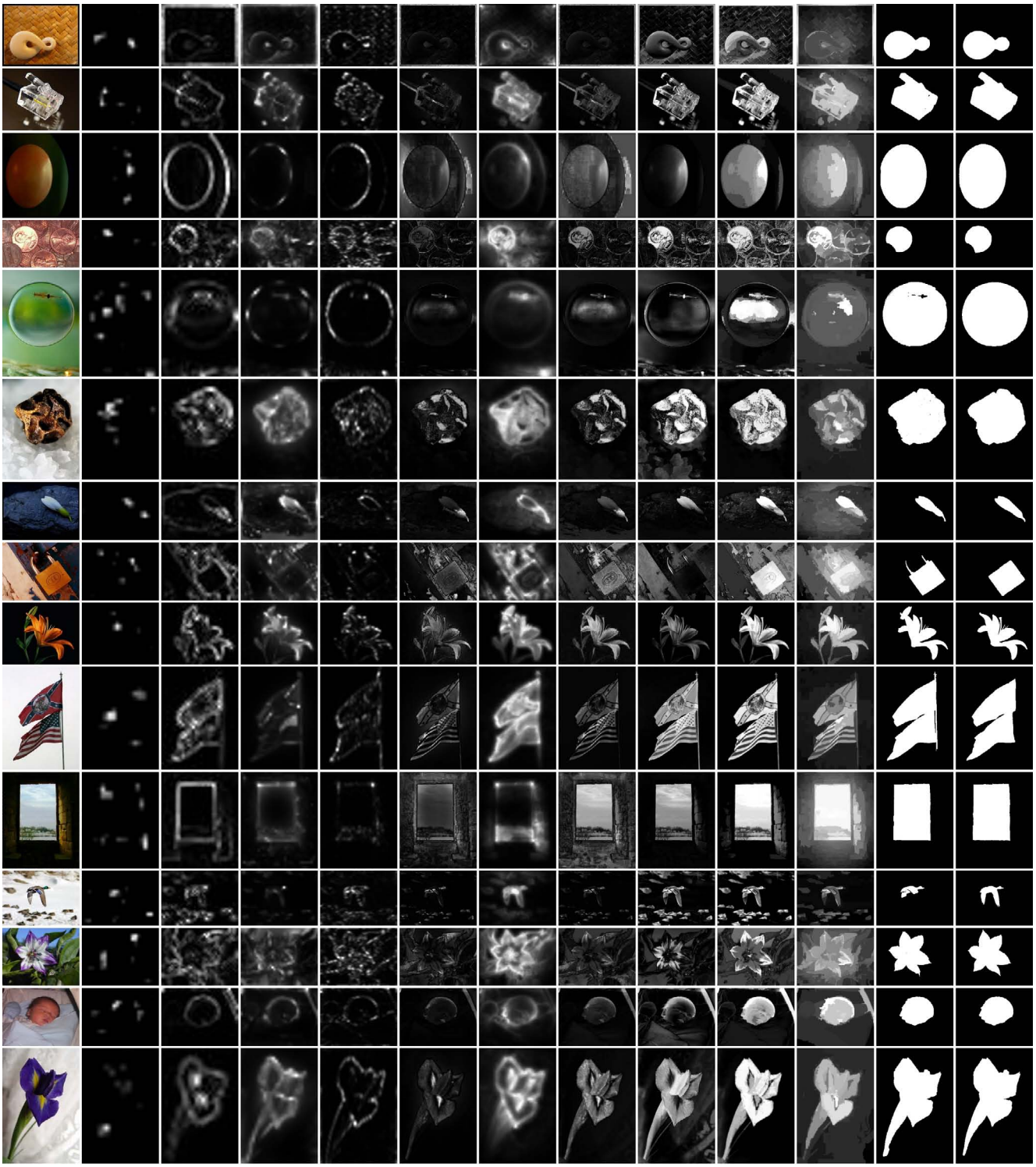

(a) (b) IT[6] (c) MZ[7] (d) GB[4] (e) SR[5] (f) AC[1] (g) CA[3] (h) FT[2] (i) LC[8] (j) HC (k) RC (l) RCC (m) g-tr

Figure 28. Typical saliency maps computed by different state-of-the-art methods (b-i) and by our proposed HC method (j) and RC method (k). Our saliency cut results (l) obtained using RC saliency maps are compared with ground truth (m).

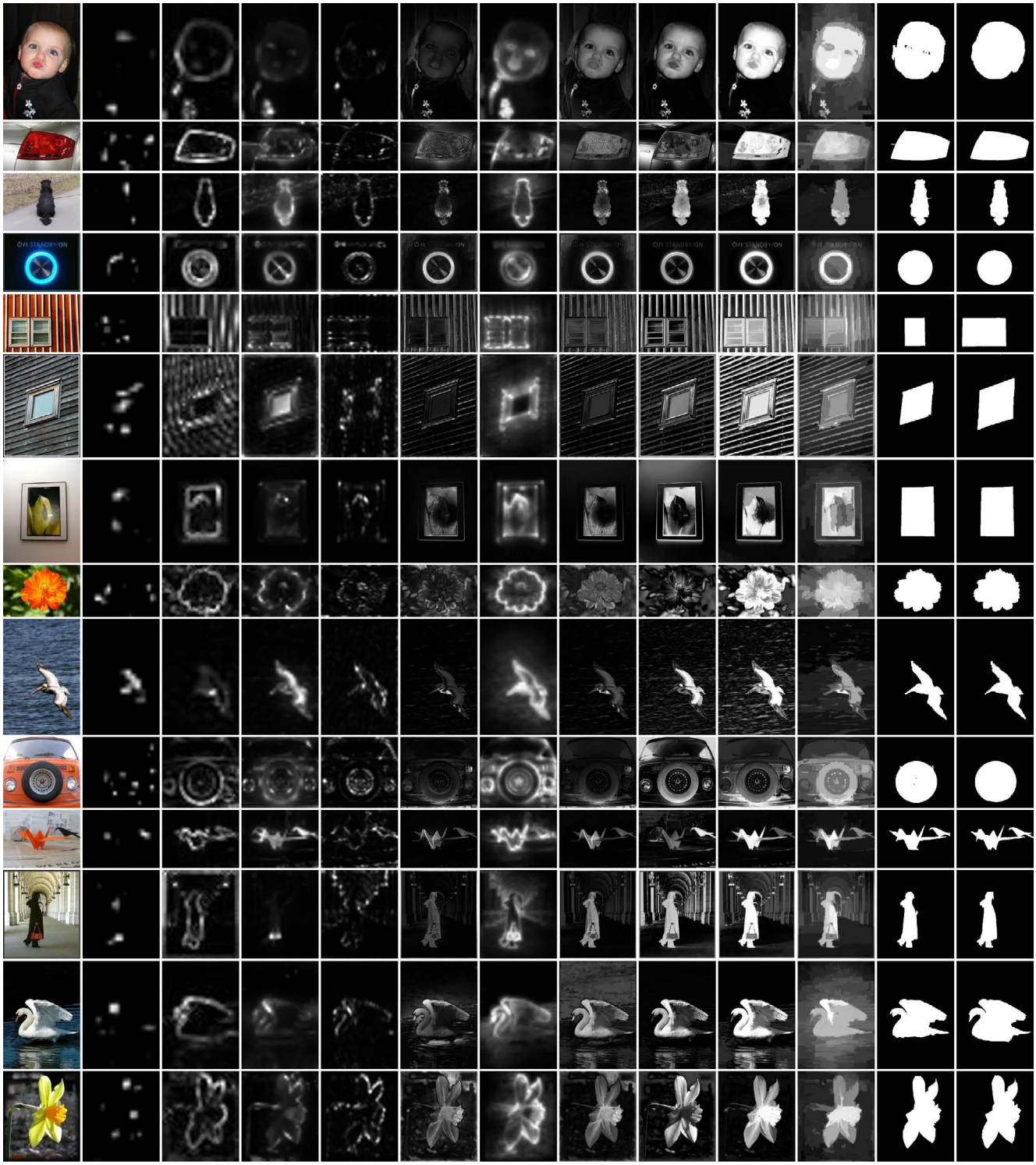

(a) (b) IT[6] (c) MZ[7] (d) GB[4] (e) SR[5] (f) AC[1] (g) CA[3] (h) FT[2] (i) LC[8] (j) HC (k) RC (l) RCC (m) g-tr

Figure 29. Typical saliency maps computed by different state-of-the-art methods (b-i) and by our proposed HC method (j) and RC method (k). Our saliency cut results (l) obtained using RC saliency maps are compared with ground truth (m).

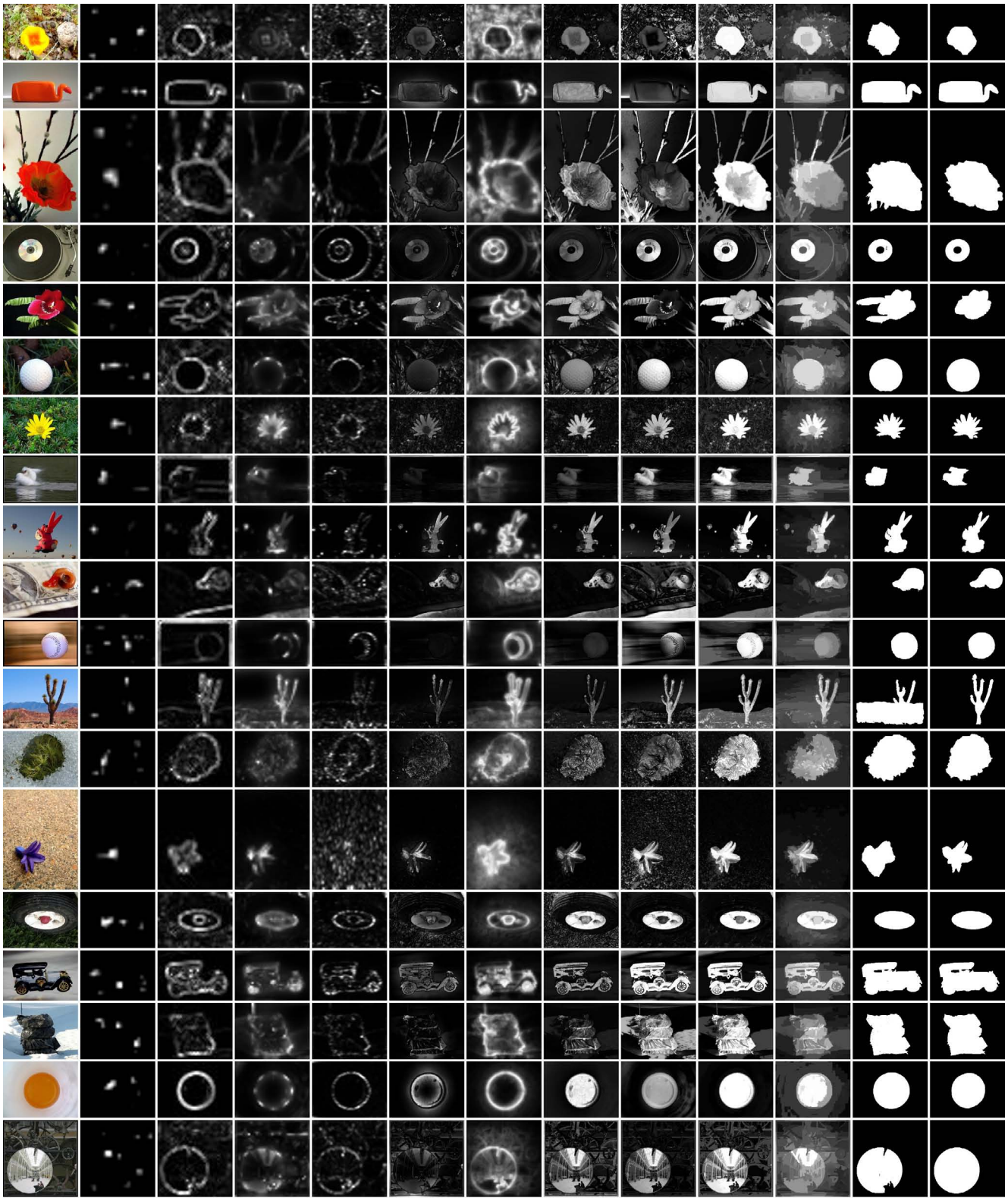

(a) (b) IT[6] (c) MZ[7] (d) GB[4] (e) SR[5] (f) AC[1] (g) CA[3] (h) FT[2] (i) LC[8] (j) HC (k) RC (l) RCC (m) g-tr

Figure 30. Typical saliency maps computed by different state-of-the-art methods (b-i) and by our proposed HC method (j) and RC method (k). Our saliency cut results (l) obtained using RC saliency maps are compared with ground truth (m).

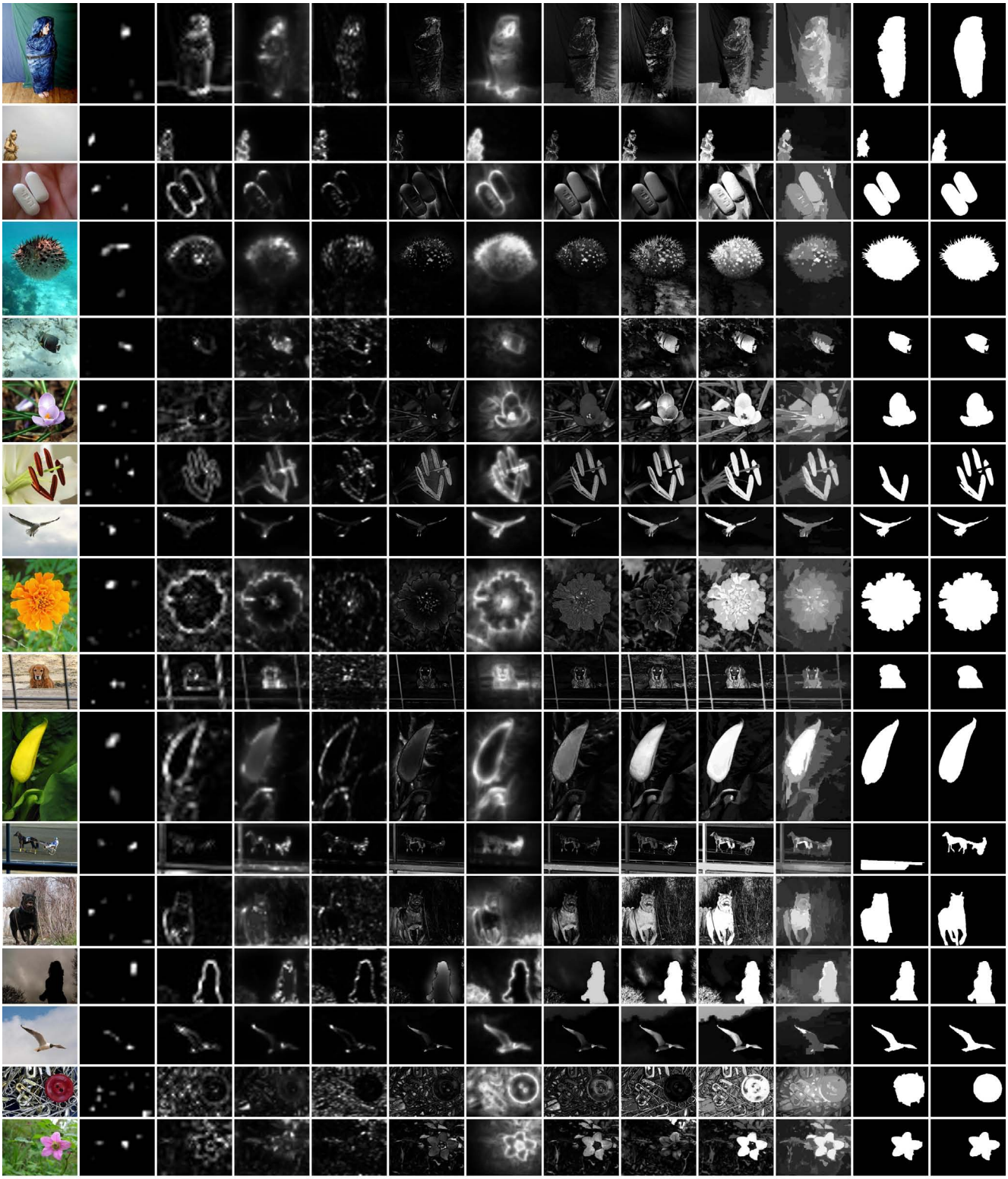

(a) (b) IT[6] (c) MZ[7] (d) GB[4] (e) SR[5] (f) AC[1] (g) CA[3] (h) FT[2] (i) LC[8] (j) HC (k) RC (l) RCC (m) g-tr

Figure 31. Typical saliency maps computed by different state-of-the-art methods (b-i) and by our proposed HC method (j) and RC method (k). Our saliency cut results (l) obtained using RC saliency maps are compared with ground truth (m).

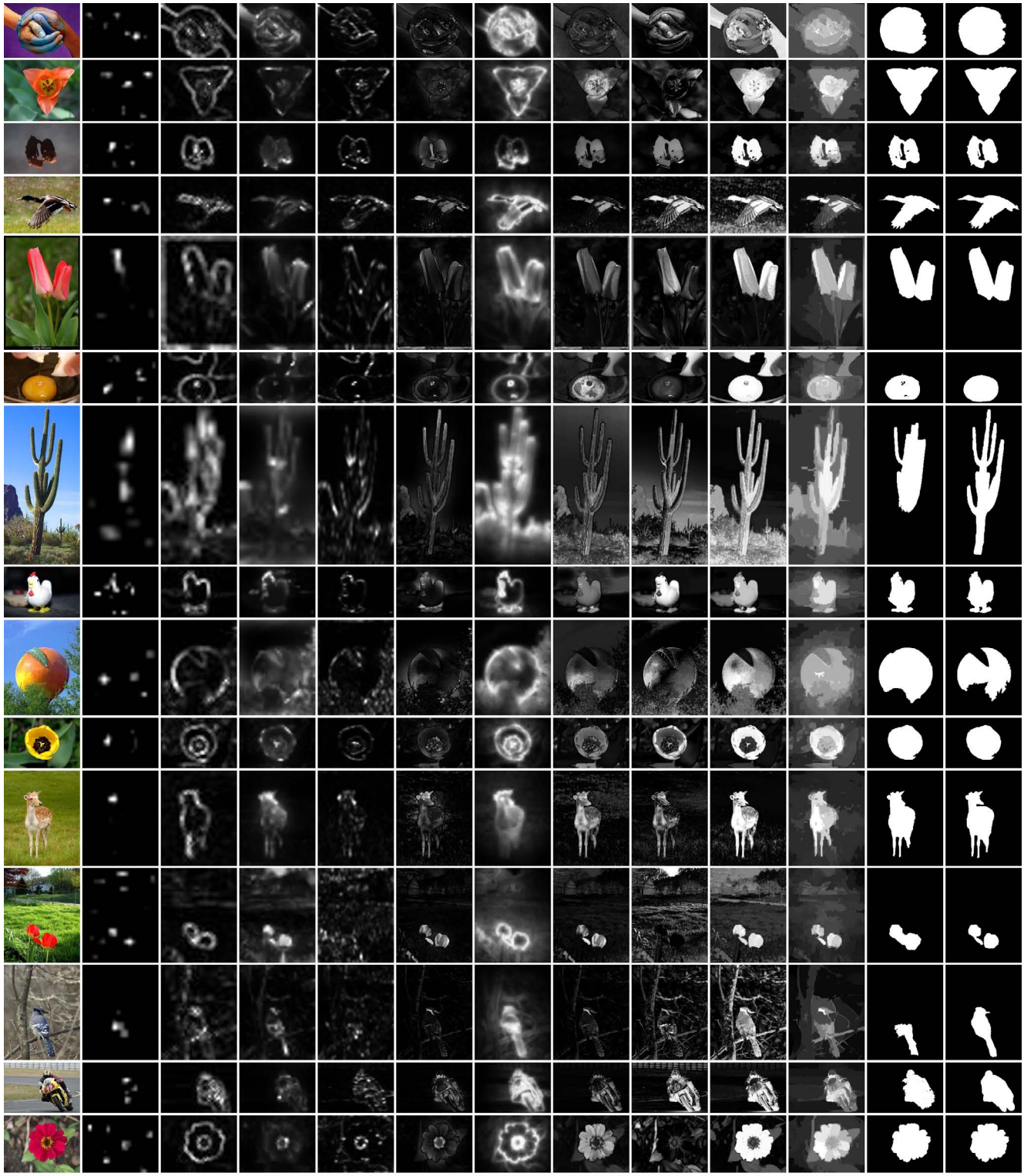

(a) (b) IT[6] (c) MZ[7] (d) GB[4] (e) SR[5] (f) AC[1] (g) CA[3] (h) FT[2] (i) LC[8] (j) HC (k) RC (l) RCC (m) g-tr

Figure 32. Typical saliency maps computed by different state-of-the-art methods (b-i) and by our proposed HC method (j) and RC method (k). Our saliency cut results (l) obtained using RC saliency maps are compared with ground truth (m).

(a) (b) IT[6] (c) MZ[7] (d) GB[4] (e) SR[5] (f) AC[1] (g) CA[3] (h) FT[2] (i) LC[8] (j) HC (k) RC (l) RCC (m) g-tr

Figure 33. Typical saliency maps computed by different state-of-the-art methods (b-i) and by our proposed HC method (j) and RC method (k). Our saliency cut results (l) obtained using RC saliency maps are compared with ground truth (m).

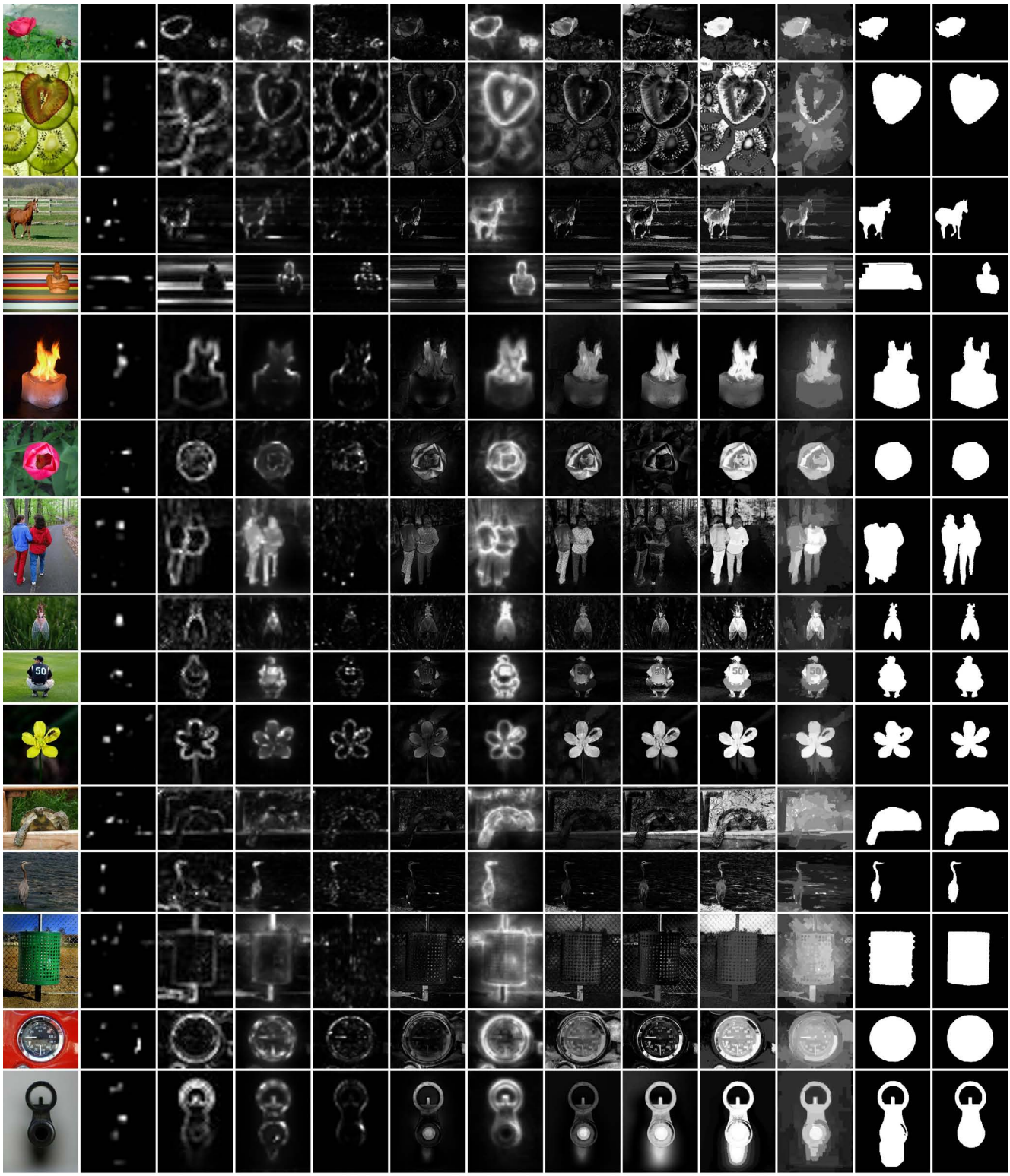

(a) (b) IT[6] (c) MZ[7] (d) GB[4] (e) SR[5] (f) AC[1] (g) CA[3] (h) FT[2] (i) LC[8] (j) HC (k) RC (l) RCC (m) g-tr

Figure 34. Typical saliency maps computed by different state-of-the-art methods (b-i) and by our proposed HC method (j) and RC method (k). Our saliency cut results (l) obtained using RC saliency maps are compared with ground truth (m).

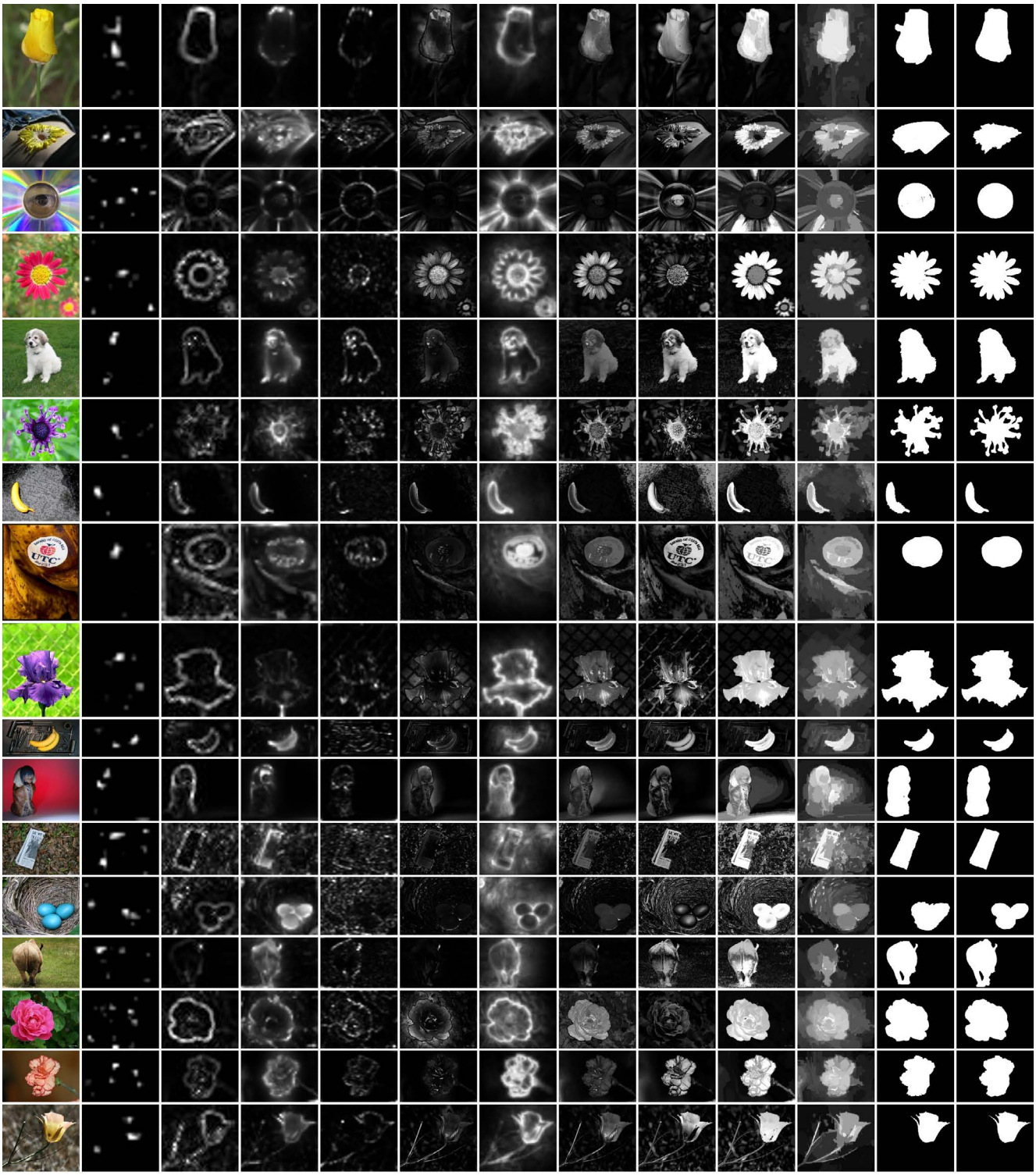

(a) (b) IT[6] (c) MZ[7] (d) GB[4] (e) SR[5] (f) AC[1] (g) CA[3] (h) FT[2] (i) LC[8] (j) HC (k) RC (l) RCC (m) g-tr

Figure 35. Typical saliency maps computed by different state-of-the-art methods (b-i) and by our proposed HC method (j) and RC method (k). Our saliency cut results (l) obtained using RC saliency maps are compared with ground truth (m).

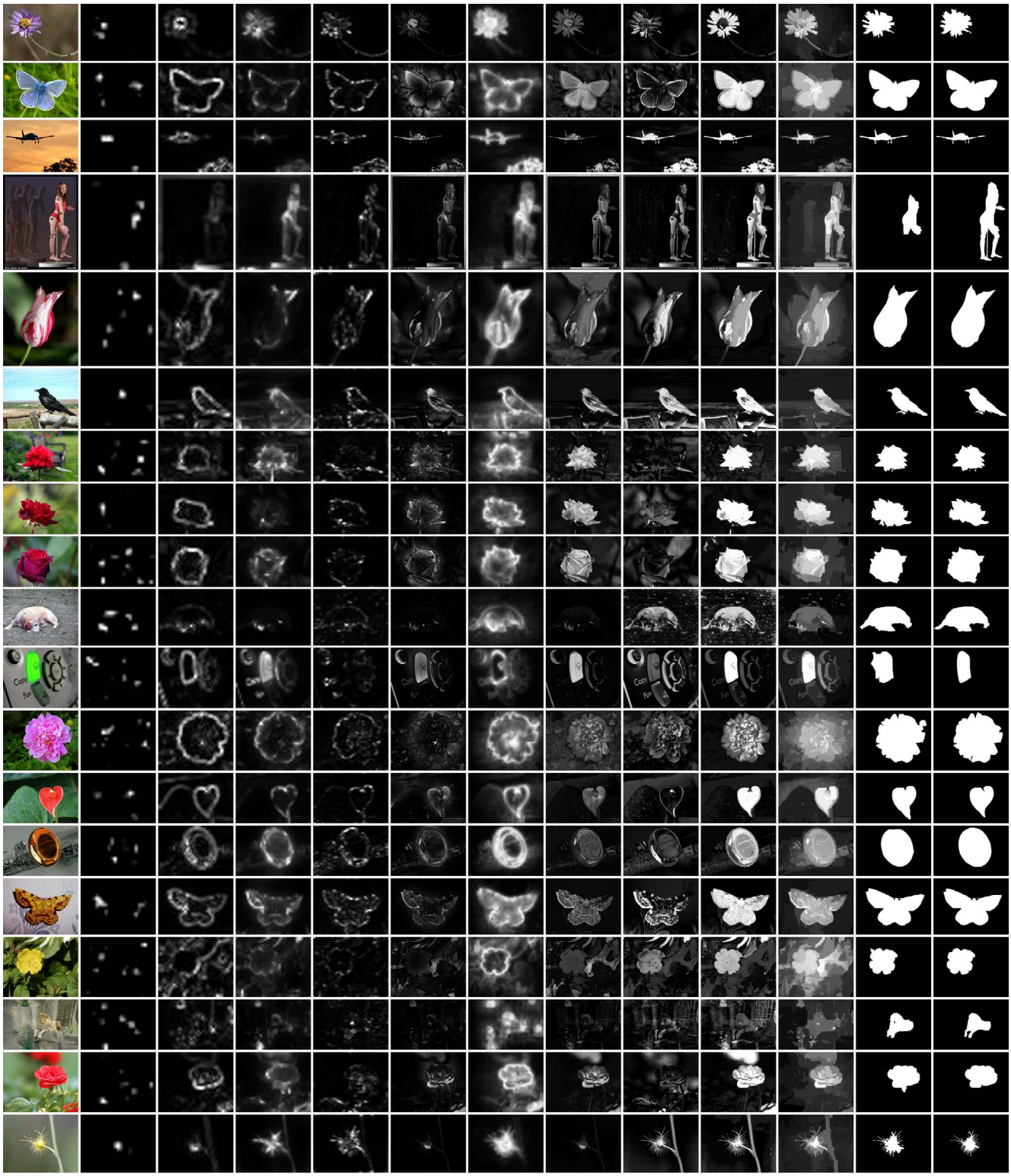

(a) (b) IT[6] (c) MZ[7] (d) GB[4] (e) SR[5] (f) AC[1] (g) CA[3] (h) FT[2] (i) LC[8] (j) HC (k) RC (l) RCC (m) g-tr

Figure 36. Typical saliency maps computed by different state-of-the-art methods (b-i) and by our proposed HC method (j) and RC method (k). Our saliency cut results (l) obtained using RC saliency maps are compared with ground truth (m).

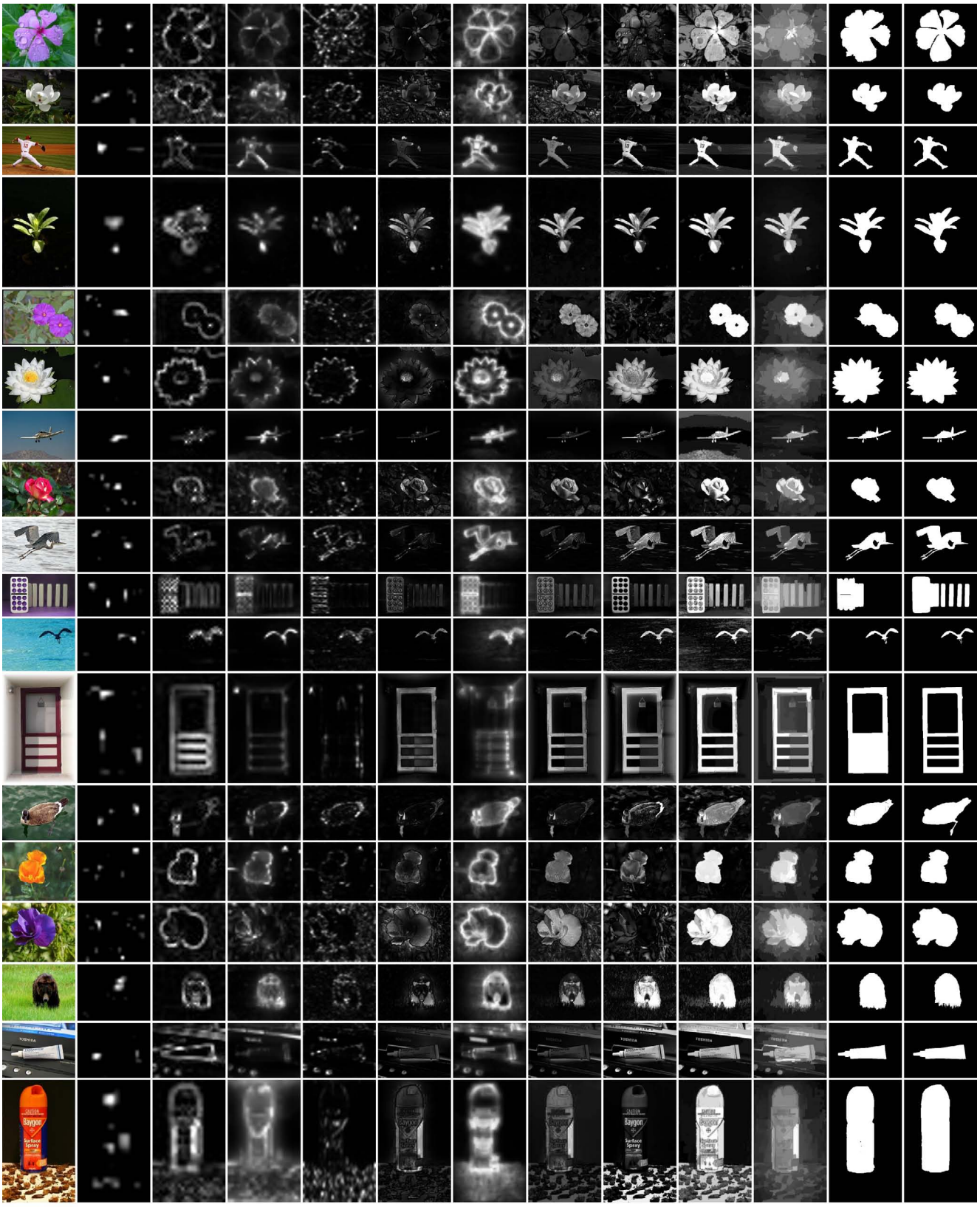

(a) (b) IT[6] (c) MZ[7] (d) GB[4] (e) SR[5] (f) AC[1] (g) CA[3] (h) FT[2] (i) LC[8] (j) HC (k) RC (l) RCC (m) g-tr

Figure 37. Typical saliency maps computed by different state-of-the-art methods (b-i) and by our proposed HC method (j) and RC method (k). Our saliency cut results (l) obtained using RC saliency maps are compared with ground truth (m).

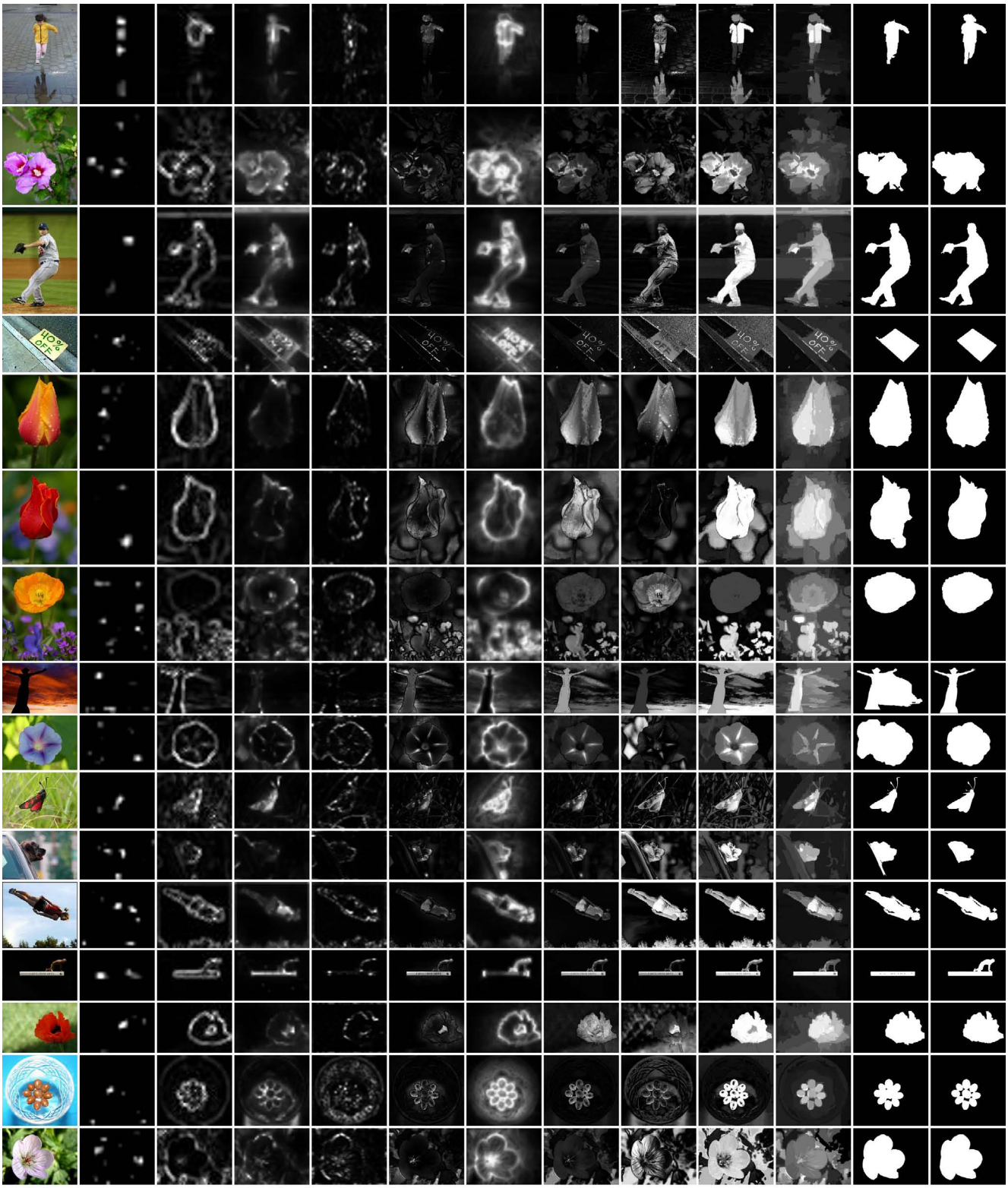

(a) (b) IT[6] (c) MZ[7] (d) GB[4] (e) SR[5] (f) AC[1] (g) CA[3] (h) FT[2] (i) LC[8] (j) HC (k) RC (l) RCC (m) g-tr

Figure 38. Typical saliency maps computed by different state-of-the-art methods (b-i) and by our proposed HC method (j) and RC method (k). Our saliency cut results (l) obtained using RC saliency maps are compared with ground truth (m).

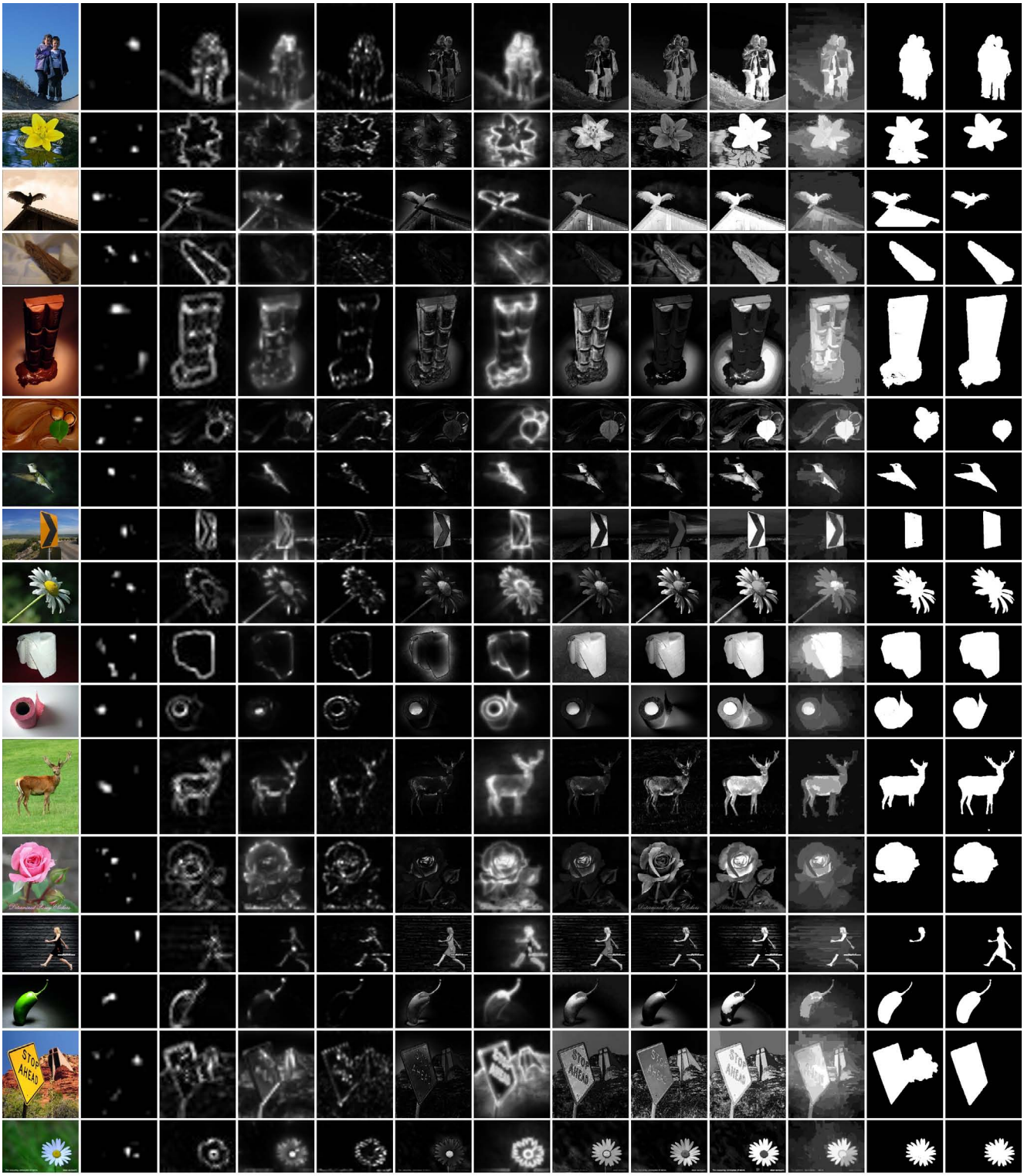

(a) (b) IT[6] (c) MZ[7] (d) GB[4] (e) SR[5] (f) AC[1] (g) CA[3] (h) FT[2] (i) LC[8] (j) HC (k) RC (l) RCC (m) g-tr

Figure 39. Typical saliency maps computed by different state-of-the-art methods (b-i) and by our proposed HC method (j) and RC method (k). Our saliency cut results (l) obtained using RC saliency maps are compared with ground truth (m).

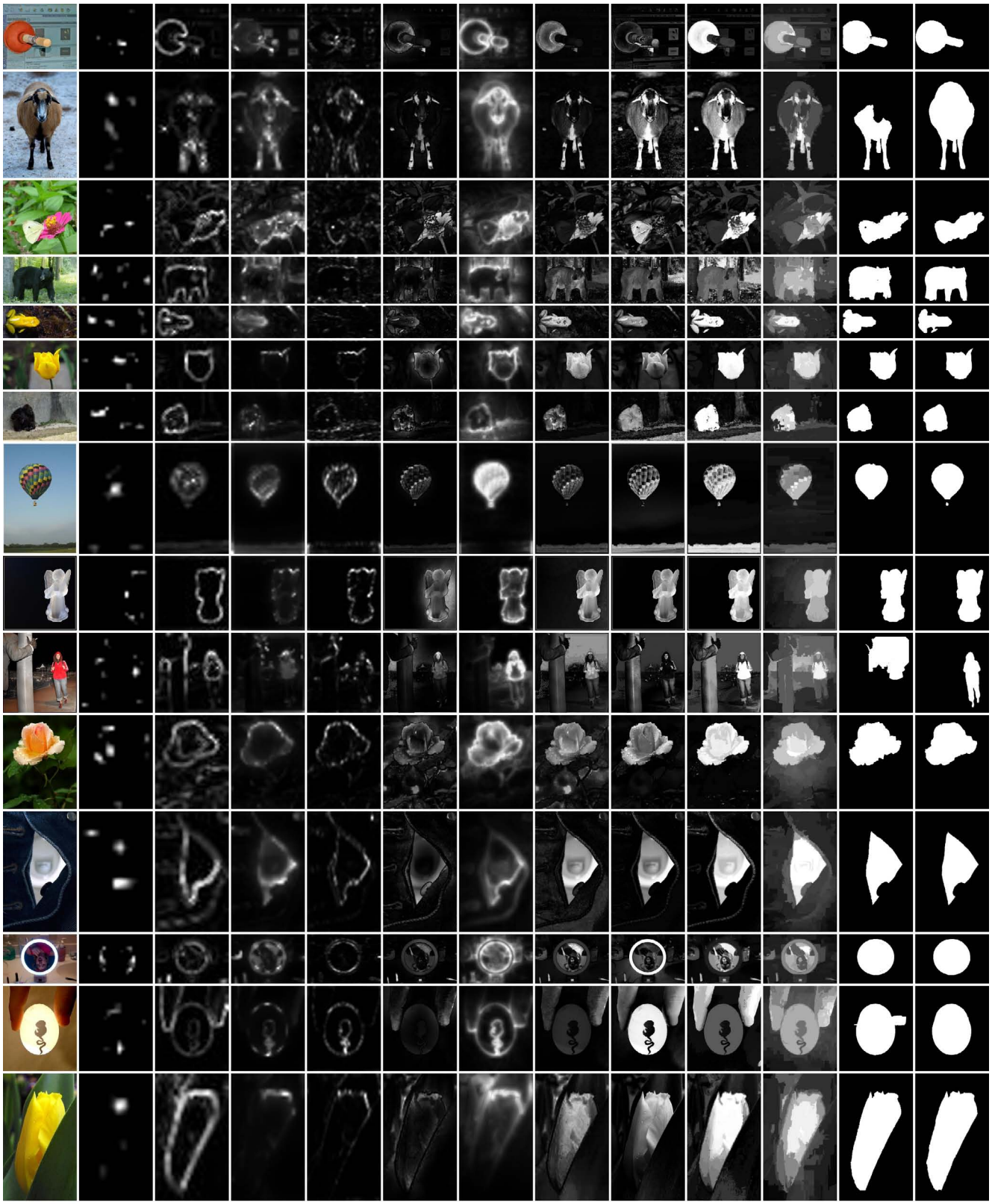

(a) (b) IT[6] (c) MZ[7] (d) GB[4] (e) SR[5] (f) AC[1] (g) CA[3] (h) FT[2] (i) LC[8] (j) HC (k) RC (l) RCC (m) g-tr

Figure 40. Typical saliency maps computed by different state-of-the-art methods (b-i) and by our proposed HC method (j) and RC method (k). Our saliency cut results (l) obtained using RC saliency maps are compared with ground truth (m).

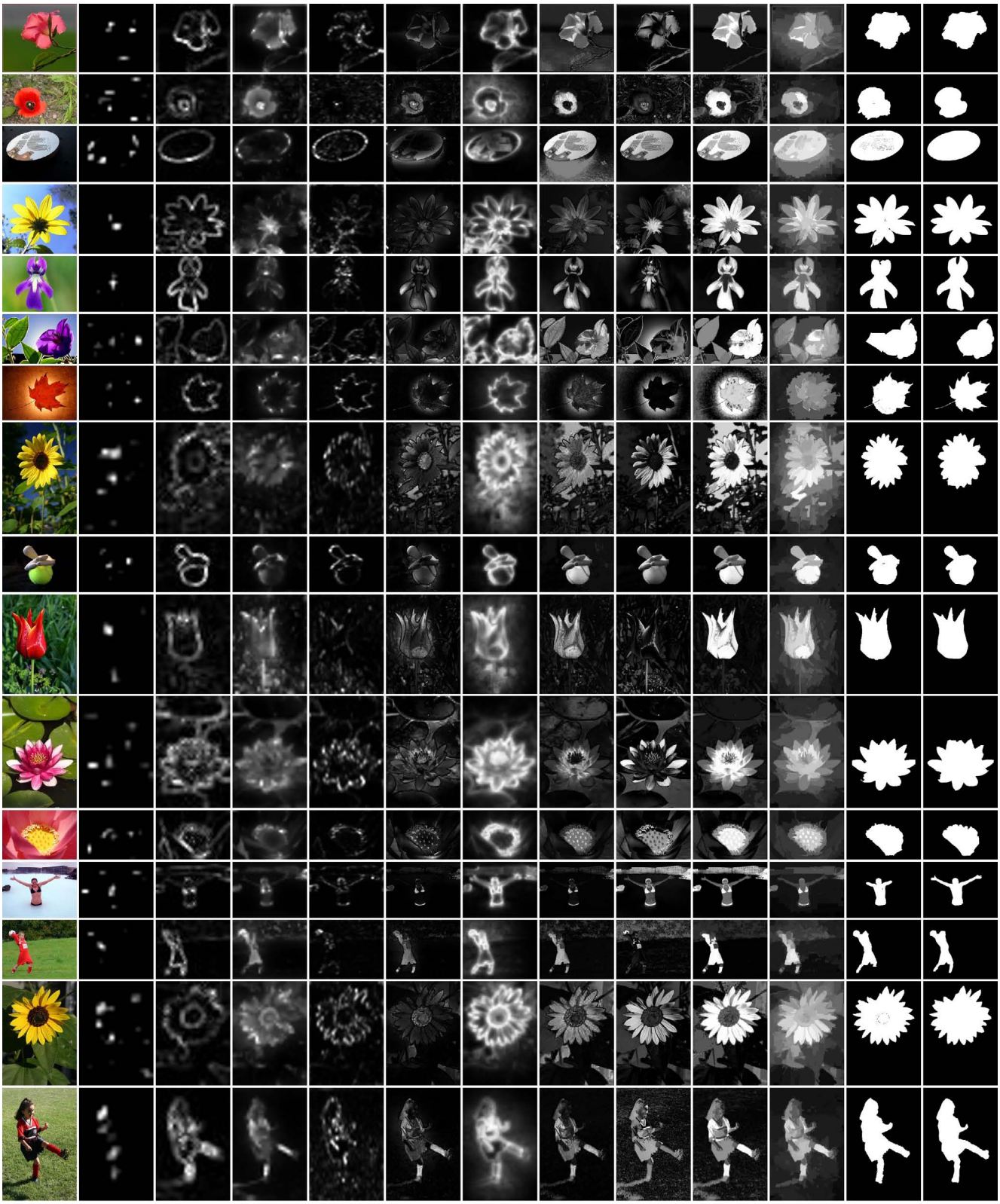

(a) (b) IT[6] (c) MZ[7] (d) GB[4] (e) SR[5] (f) AC[1] (g) CA[3] (h) FT[2] (i) LC[8] (j) HC (k) RC (l) RCC (m) g-tr

Figure 41. Typical saliency maps computed by different state-of-the-art methods (b-i) and by our proposed HC method (j) and RC method (k). Our saliency cut results (l) obtained using RC saliency maps are compared with ground truth (m).

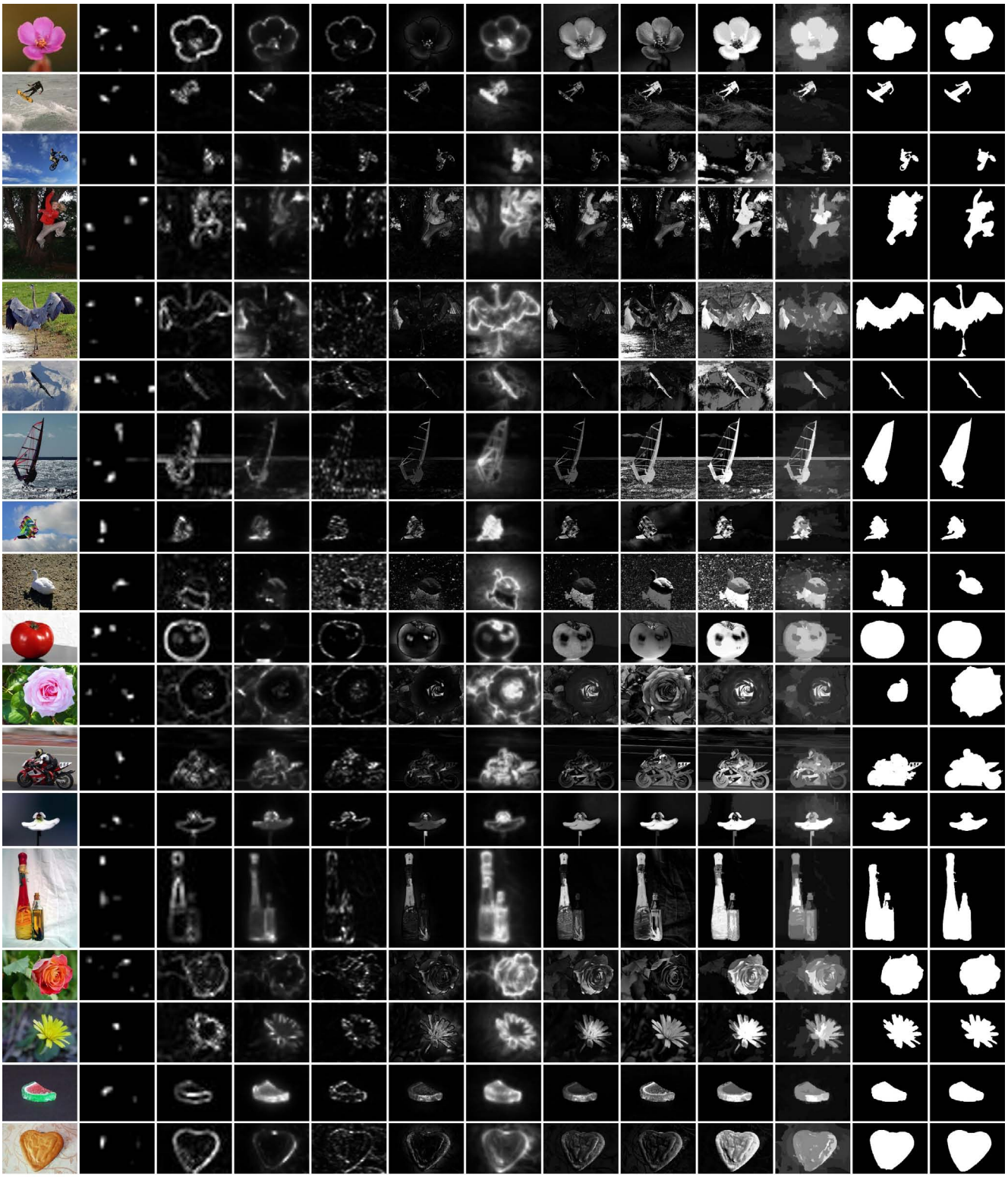

(a) (b) IT[6] (c) MZ[7] (d) GB[4] (e) SR[5] (f) AC[1] (g) CA[3] (h) FT[2] (i) LC[8] (j) HC (k) RC (l) RCC (m) g-tr

Figure 42. Typical saliency maps computed by different state-of-the-art methods (b-i) and by our proposed HC method (j) and RC method (k). Our saliency cut results (l) obtained using RC saliency maps are compared with ground truth (m).

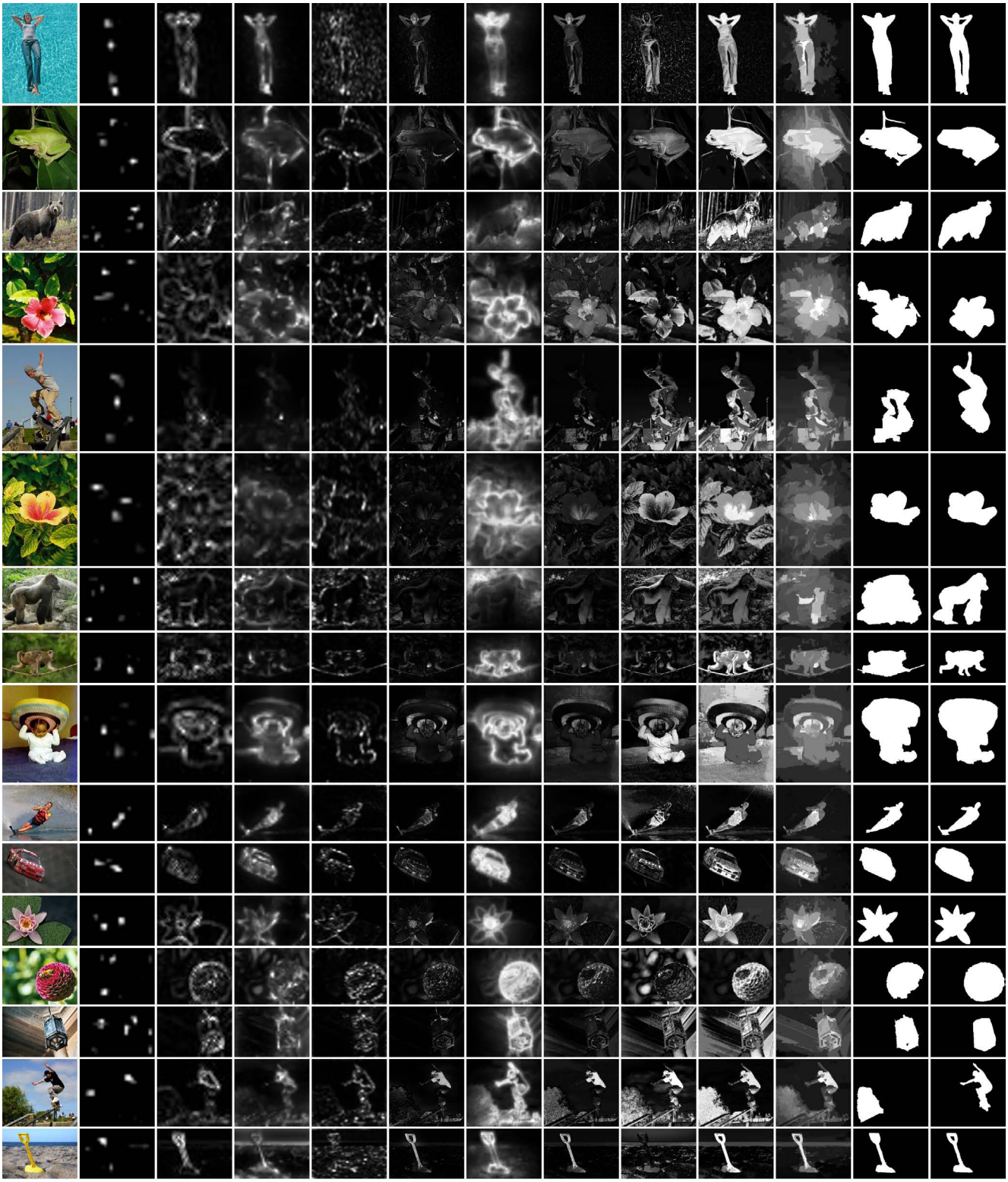

(a) (b) IT[6] (c) MZ[7] (d) GB[4] (e) SR[5] (f) AC[1] (g) CA[3] (h) FT[2] (i) LC[8] (j) HC (k) RC (l) RCC (m) g-tr

Figure 43. Typical saliency maps computed by different state-of-the-art methods (b-i) and by our proposed HC method (j) and RC method (k). Our saliency cut results (l) obtained using RC saliency maps are compared with ground truth (m).

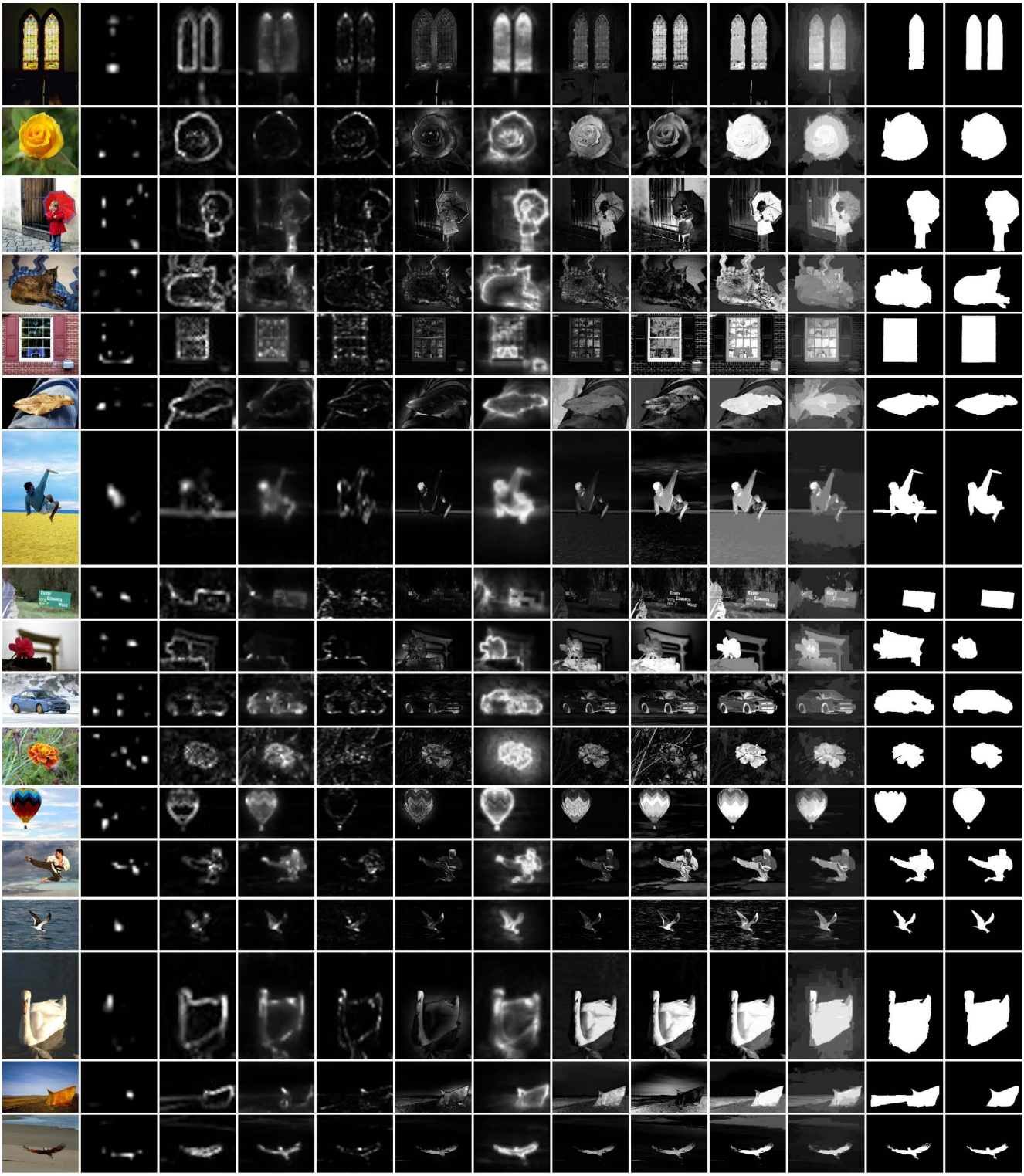

(a) (b) IT[6] (c) MZ[7] (d) GB[4] (e) SR[5] (f) AC[1] (g) CA[3] (h) FT[2] (i) LC[8] (j) HC (k) RC (l) RCC (m) g-tr

Figure 44. Typical saliency maps computed by different state-of-the-art methods (b-i) and by our proposed HC method (j) and RC method (k). Our saliency cut results (l) obtained using RC saliency maps are compared with ground truth (m).

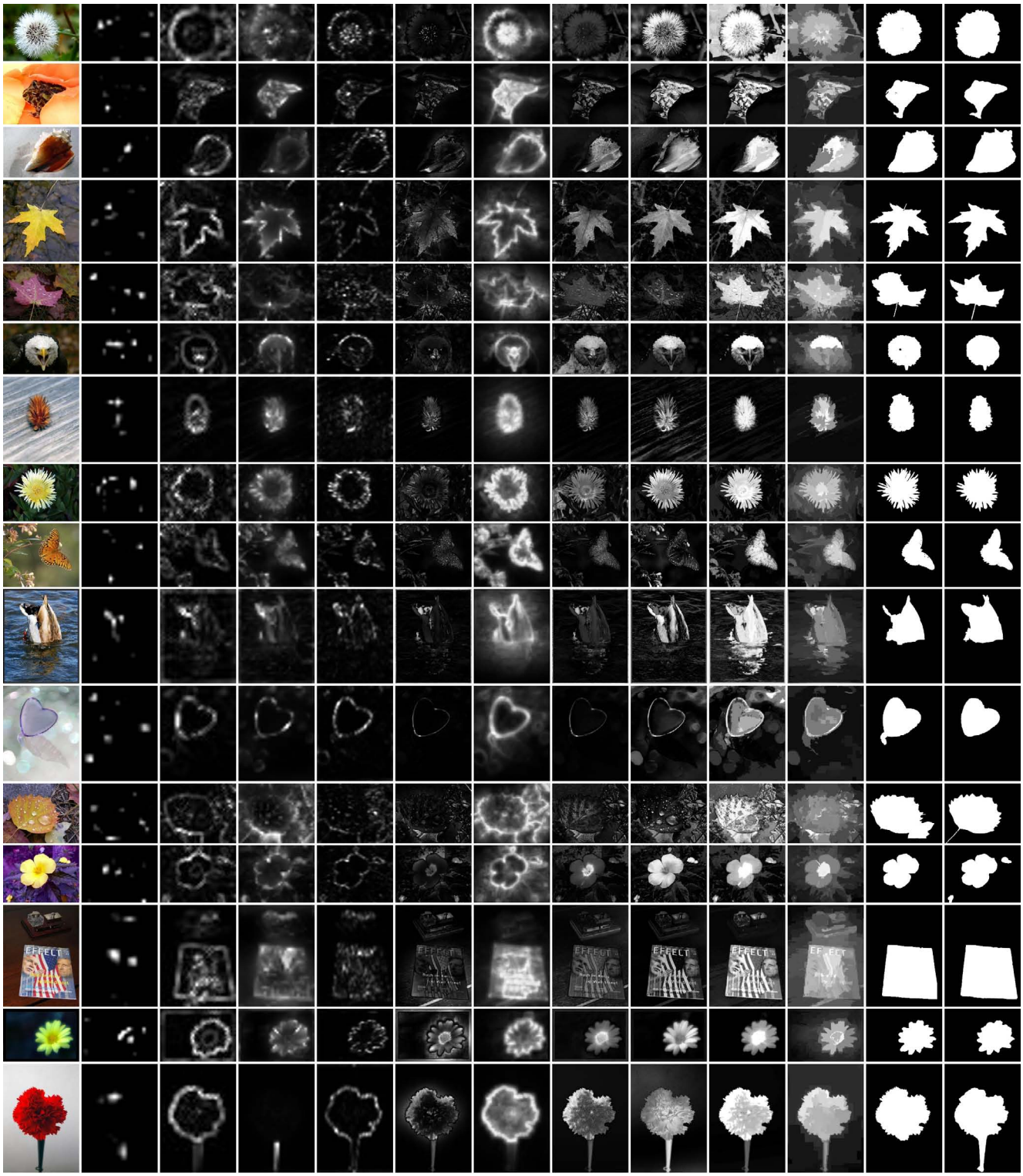

(a) (b) IT[6] (c) MZ[7] (d) GB[4] (e) SR[5] (f) AC[1] (g) CA[3] (h) FT[2] (i) LC[8] (j) HC (k) RC (l) RCC (m) g-tr

Figure 45. Typical saliency maps computed by different state-of-the-art methods (b-i) and by our proposed HC method (j) and RC method (k). Our saliency cut results (l) obtained using RC saliency maps are compared with ground truth (m).

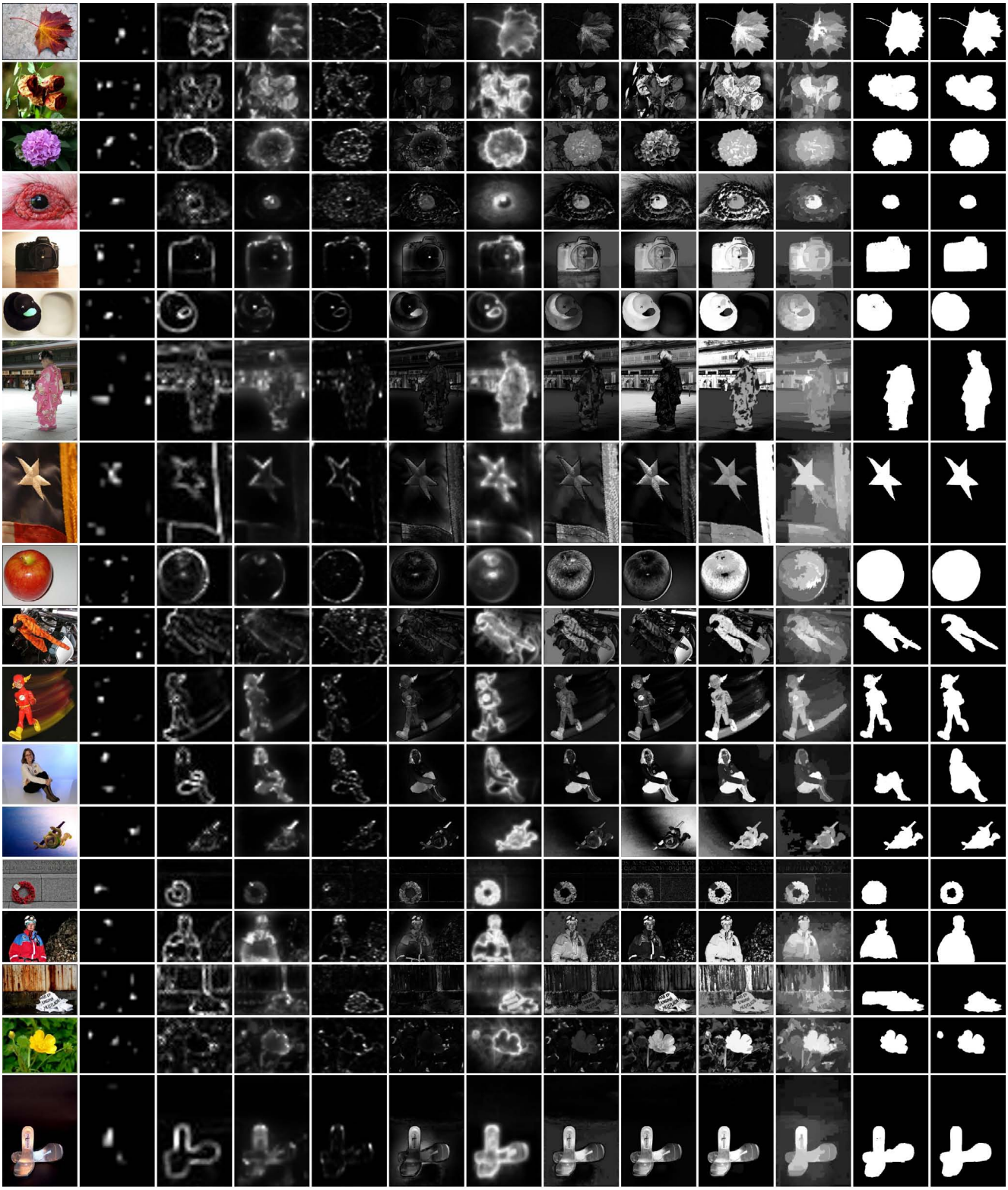

(a) (b) IT[6] (c) MZ[7] (d) GB[4] (e) SR[5] (f) AC[1] (g) CA[3] (h) FT[2] (i) LC[8] (j) HC (k) RC (l) RCC (m) g-tr

Figure 46. Typical saliency maps computed by different state-of-the-art methods (b-i) and by our proposed HC method (j) and RC method (k). Our saliency cut results (l) obtained using RC saliency maps are compared with ground truth (m).

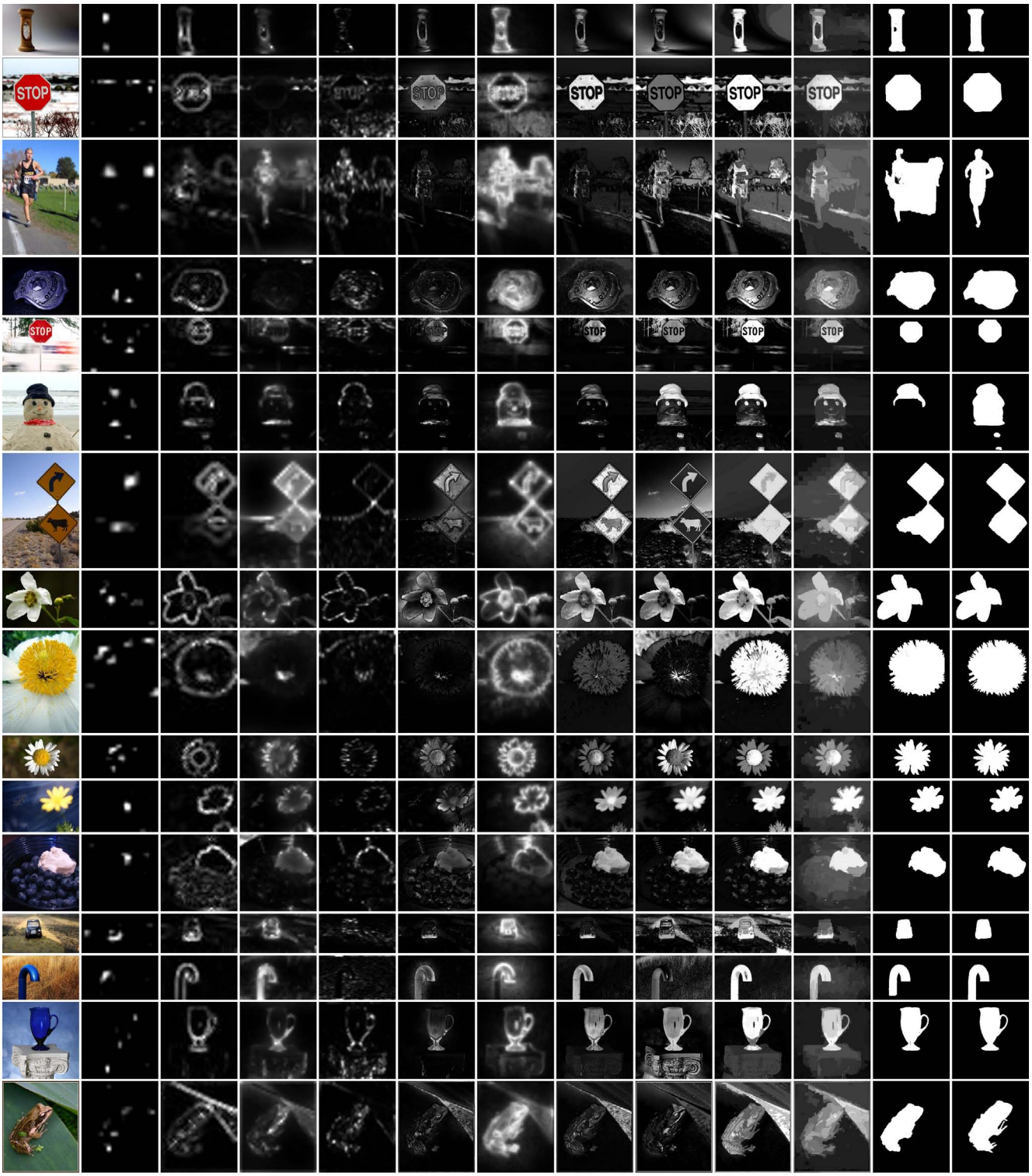

(a) (b) IT[6] (c) MZ[7] (d) GB[4] (e) SR[5] (f) AC[1] (g) CA[3] (h) FT[2] (i) LC[8] (j) HC (k) RC (l) RCC (m) g-tr

Figure 47. Typical saliency maps computed by different state-of-the-art methods (b-i) and by our proposed HC method (j) and RC method (k). Our saliency cut results (l) obtained using RC saliency maps are compared with ground truth (m).

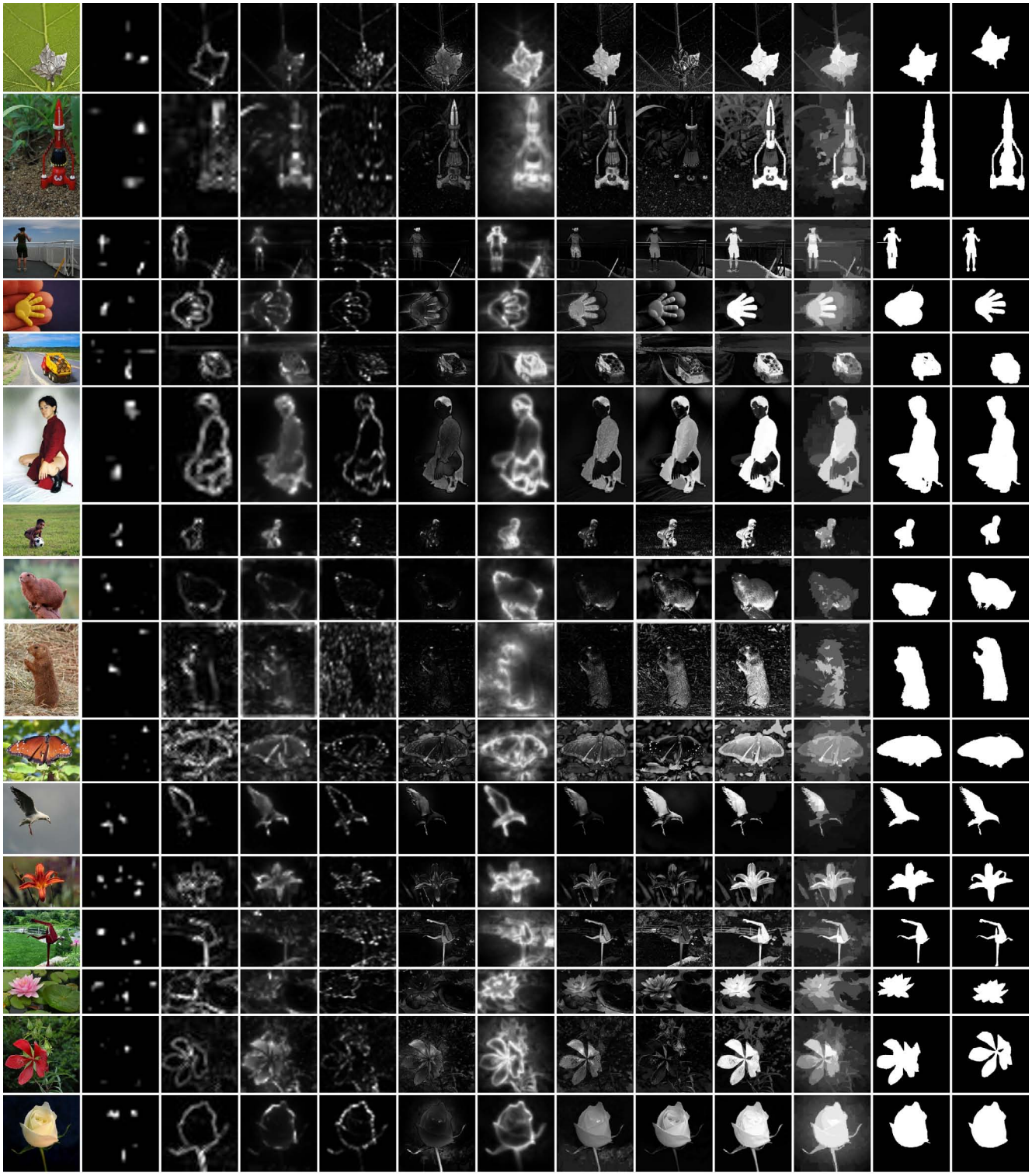

(a) (b) IT[6] (c) MZ[7] (d) GB[4] (e) SR[5] (f) AC[1] (g) CA[3] (h) FT[2] (i) LC[8] (j) HC (k) RC (l) RCC (m) g-tr

Figure 48. Typical saliency maps computed by different state-of-the-art methods (b-i) and by our proposed HC method (j) and RC method (k). Our saliency cut results (l) obtained using RC saliency maps are compared with ground truth (m).

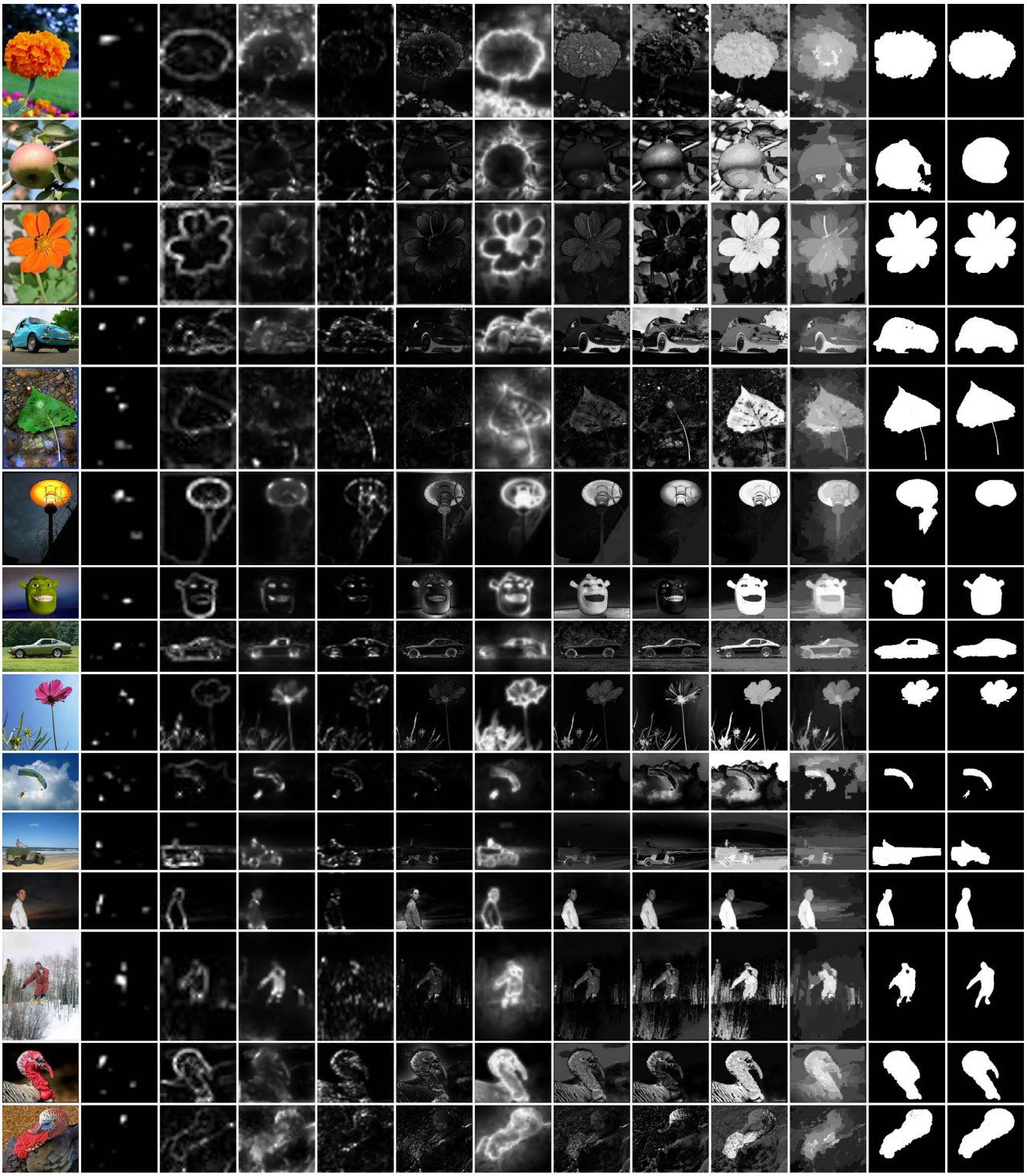

(a) (b) IT[6] (c) MZ[7] (d) GB[4] (e) SR[5] (f) AC[1] (g) CA[3] (h) FT[2] (i) LC[8] (j) HC (k) RC (l) RCC (m) g-tr

Figure 49. Typical saliency maps computed by different state-of-the-art methods (b-i) and by our proposed HC method (j) and RC method (k). Our saliency cut results (l) obtained using RC saliency maps are compared with ground truth (m).

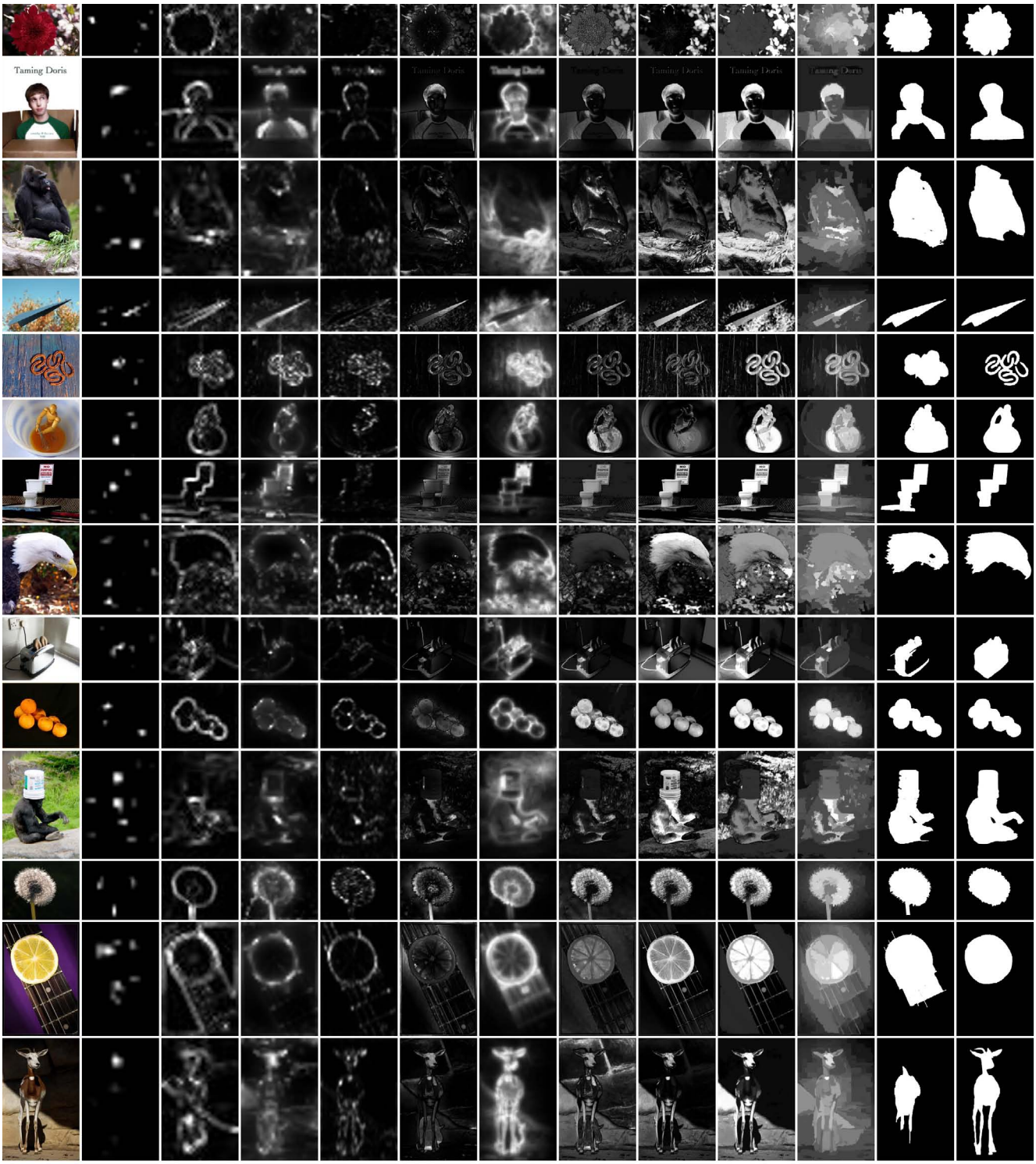

(a) (b) IT[6] (c) MZ[7] (d) GB[4] (e) SR[5] (f) AC[1] (g) CA[3] (h) FT[2] (i) LC[8] (j) HC (k) RC (l) RCC (m) g-tr

Figure 50. Typical saliency maps computed by different state-of-the-art methods (b-i) and by our proposed HC method (j) and RC method (k). Our saliency cut results (l) obtained using RC saliency maps are compared with ground truth (m).

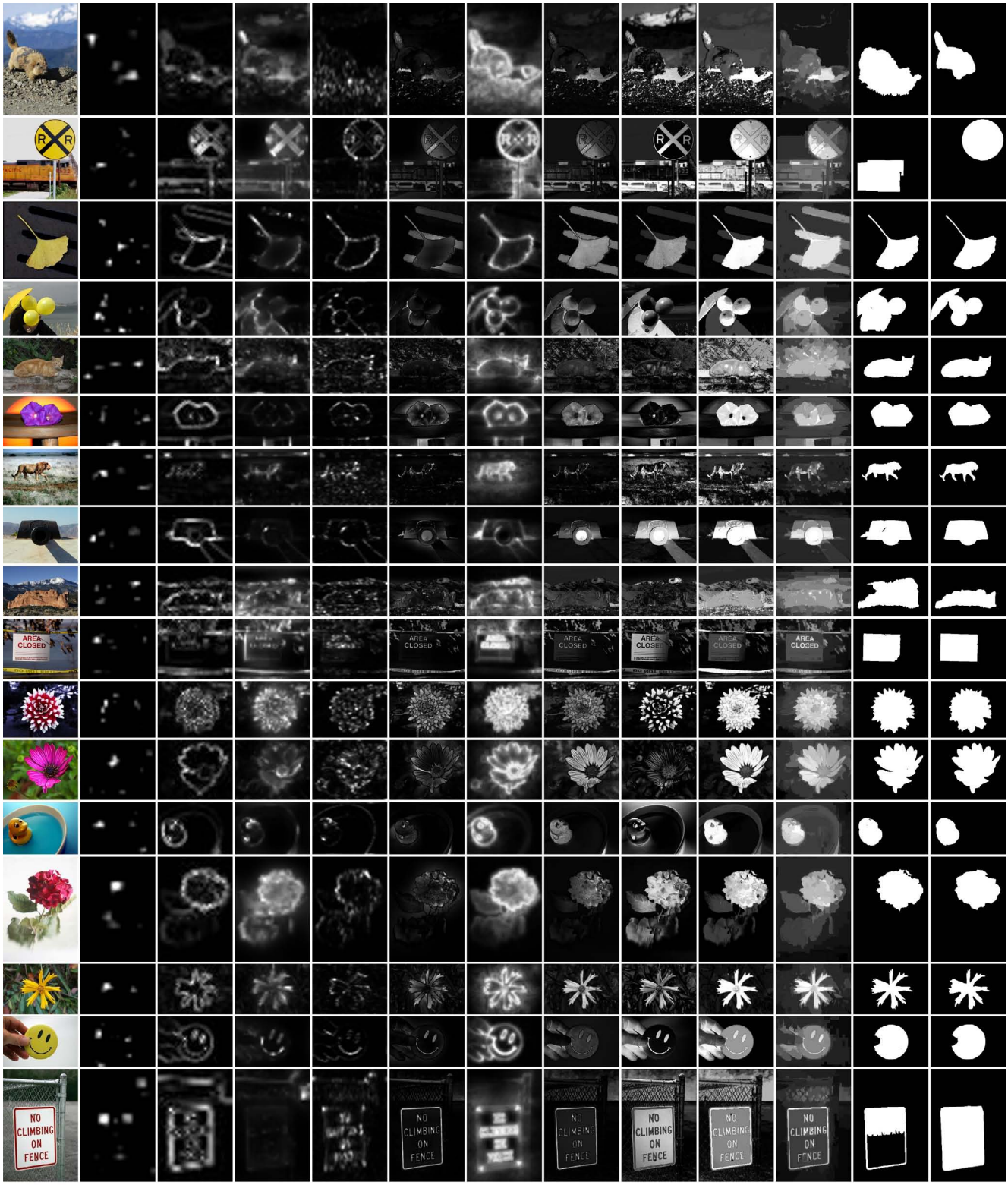

(a) (b) IT[6] (c) MZ[7] (d) GB[4] (e) SR[5] (f) AC[1] (g) CA[3] (h) FT[2] (i) LC[8] (j) HC (k) RC (l) RCC (m) g-tr

Figure 51. Typical saliency maps computed by different state-of-the-art methods (b-i) and by our proposed HC method (j) and RC method (k). Our saliency cut results (l) obtained using RC saliency maps are compared with ground truth (m).

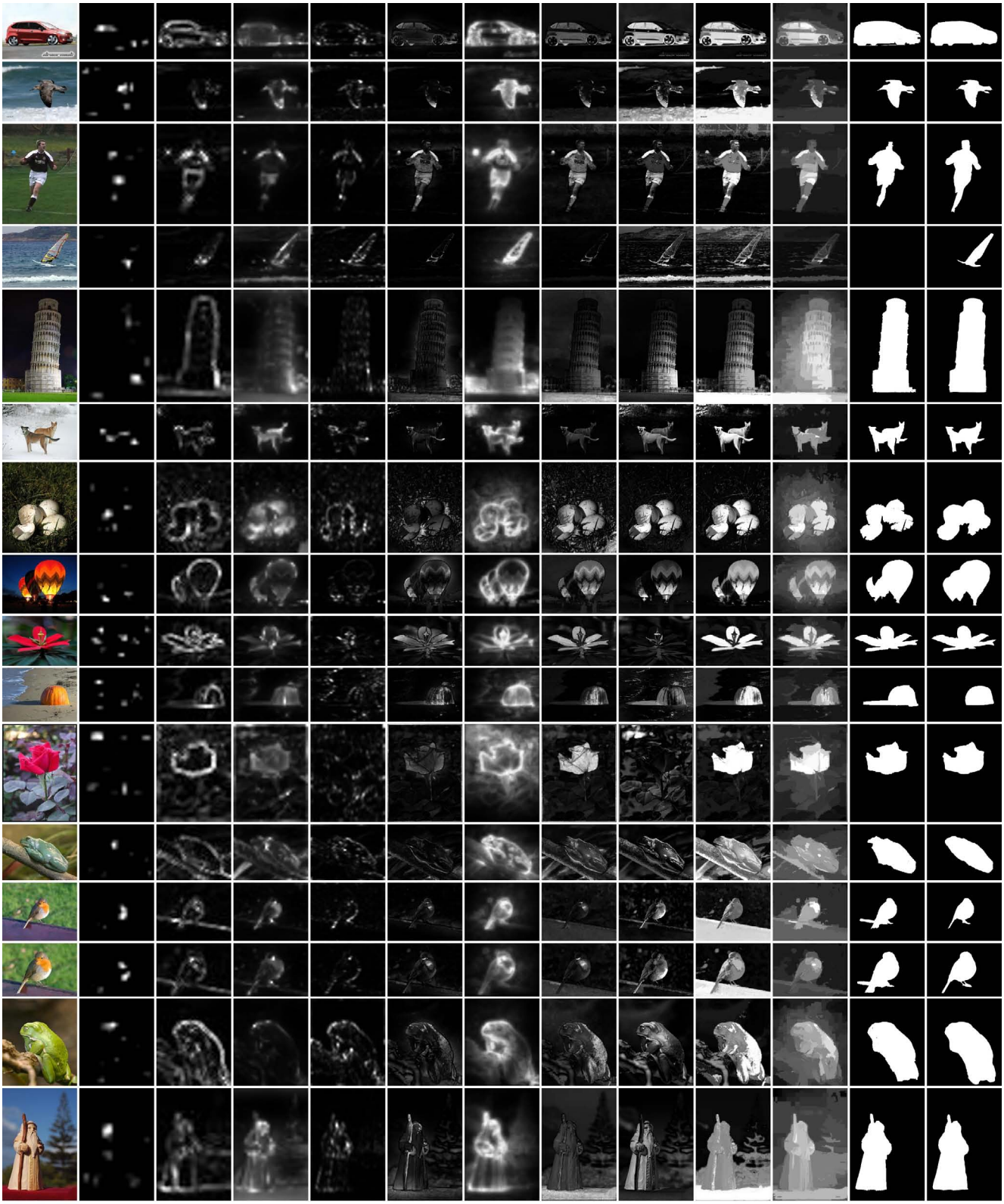

(a) (b) IT[6] (c) MZ[7] (d) GB[4] (e) SR[5] (f) AC[1] (g) CA[3] (h) FT[2] (i) LC[8] (j) HC (k) RC (l) RCC (m) g-tr

Figure 52. Typical saliency maps computed by different state-of-the-art methods (b-i) and by our proposed HC method (j) and RC method (k). Our saliency cut results (l) obtained using RC saliency maps are compared with ground truth (m).

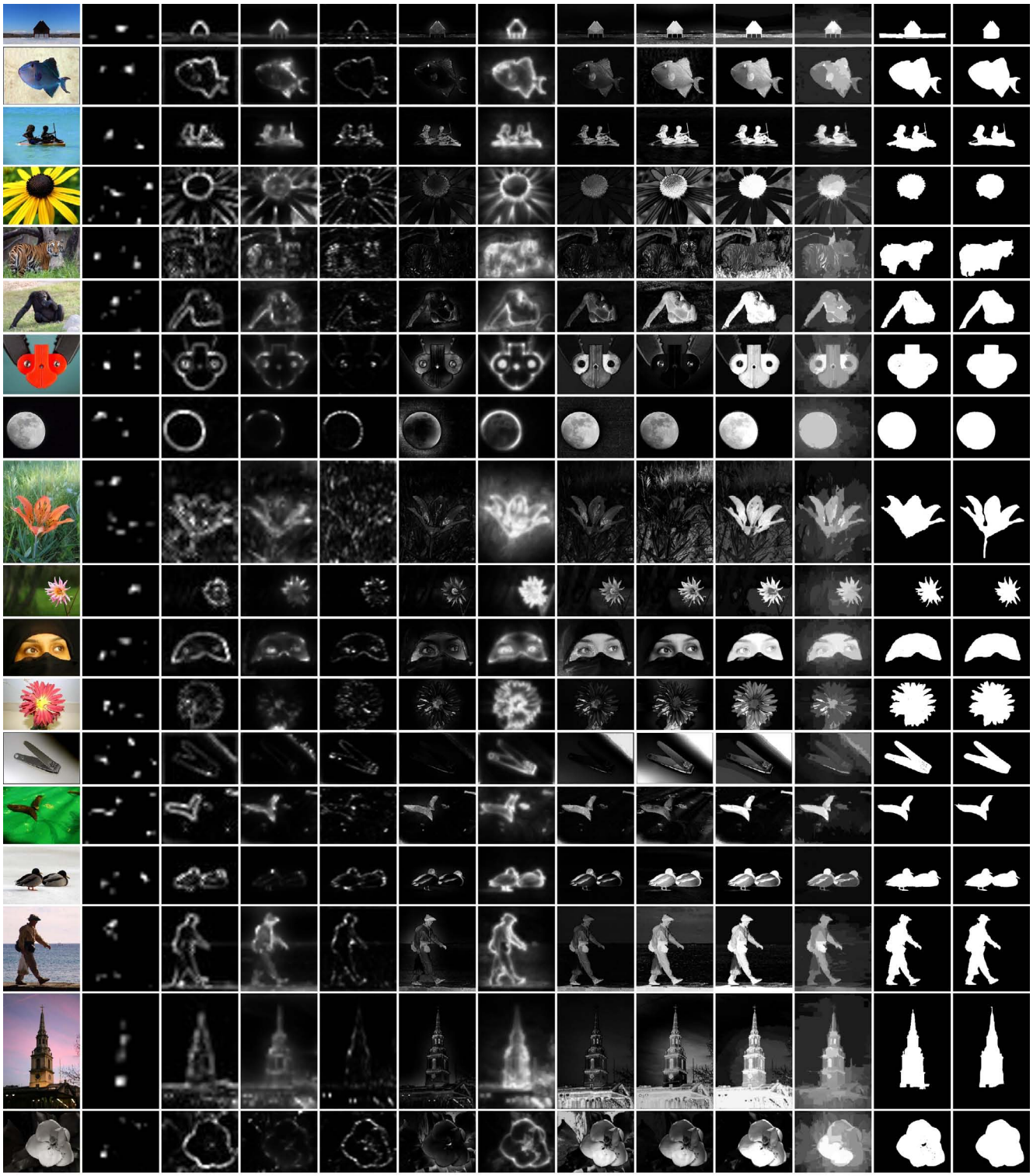

(a) (b) IT[6] (c) MZ[7] (d) GB[4] (e) SR[5] (f) AC[1] (g) CA[3] (h) FT[2] (i) LC[8] (j) HC (k) RC (l) RCC (m) g-tr

Figure 53. Typical saliency maps computed by different state-of-the-art methods (b-i) and by our proposed HC method (j) and RC method (k). Our saliency cut results (l) obtained using RC saliency maps are compared with ground truth (m).

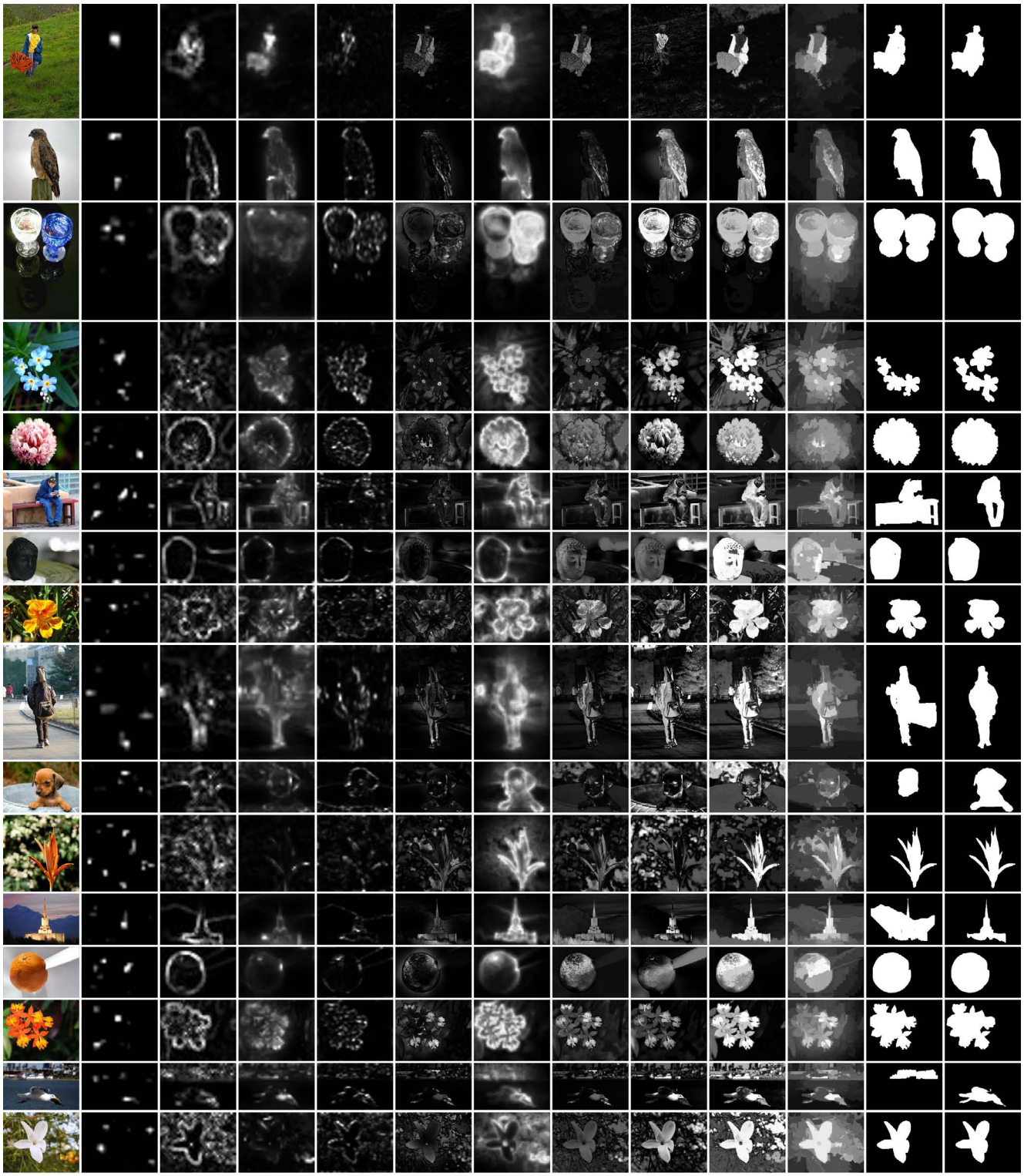

(a) (b) IT[6] (c) MZ[7] (d) GB[4] (e) SR[5] (f) AC[1] (g) CA[3] (h) FT[2] (i) LC[8] (j) HC (k) RC (l) RCC (m) g-tr

Figure 54. Typical saliency maps computed by different state-of-the-art methods (b-i) and by our proposed HC method (j) and RC method (k). Our saliency cut results (l) obtained using RC saliency maps are compared with ground truth (m).

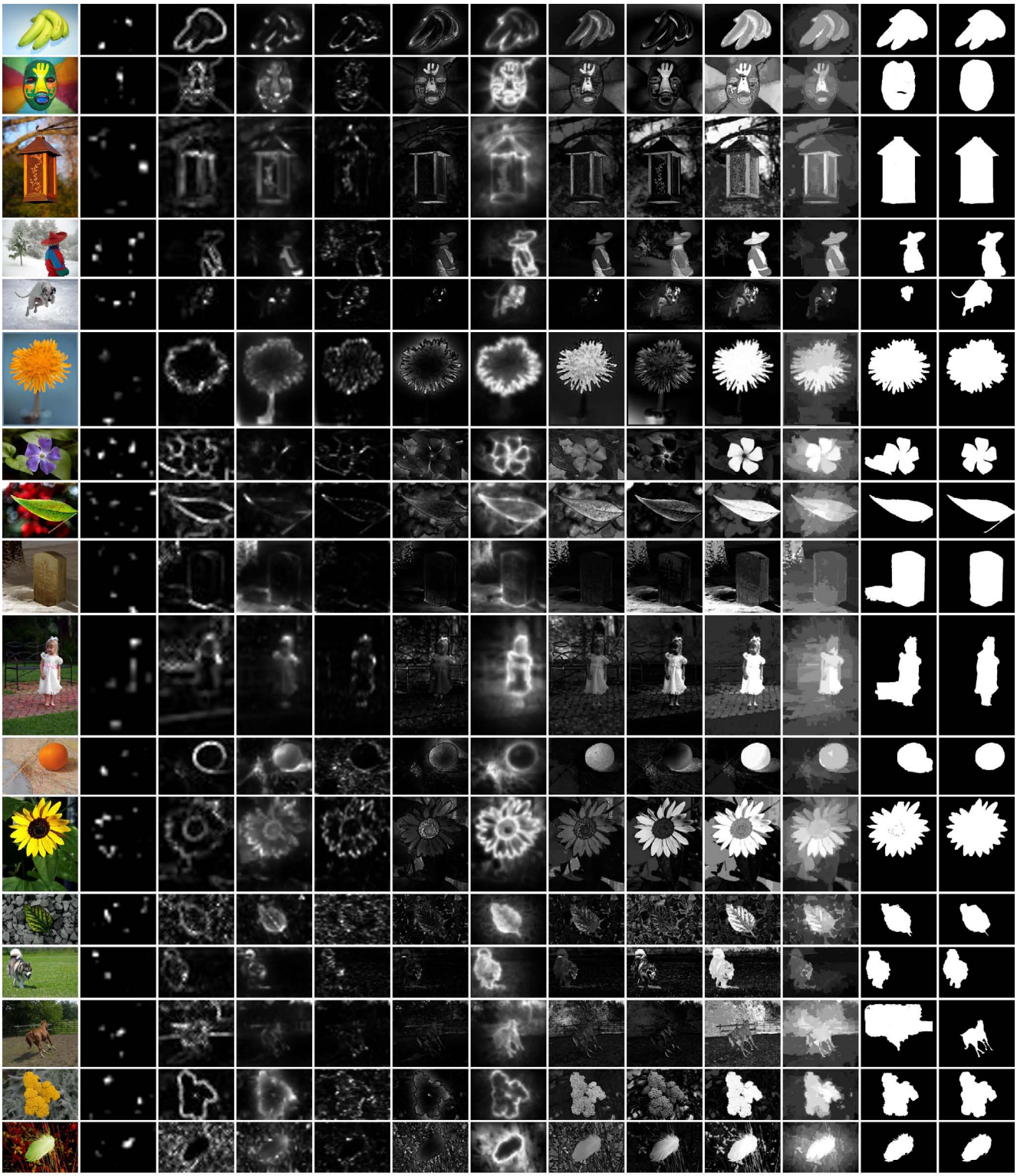

(a) (b) IT[6] (c) MZ[7] (d) GB[4] (e) SR[5] (f) AC[1] (g) CA[3] (h) FT[2] (i) LC[8] (j) HC (k) RC (l) RCC (m) g-tr

Figure 55. Typical saliency maps computed by different state-of-the-art methods (b-i) and by our proposed HC method (j) and RC method (k). Our saliency cut results (l) obtained using RC saliency maps are compared with ground truth (m).

(a) (b) IT[6] (c) MZ[7] (d) GB[4] (e) SR[5] (f) AC[1] (g) CA[3] (h) FT[2] (i) LC[8] (j) HC (k) RC (l) RCC (m) g-tr

Figure 56. Typical saliency maps computed by different state-of-the-art methods (b-i) and by our proposed HC method (j) and RC method (k). Our saliency cut results (l) obtained using RC saliency maps are compared with ground truth (m).

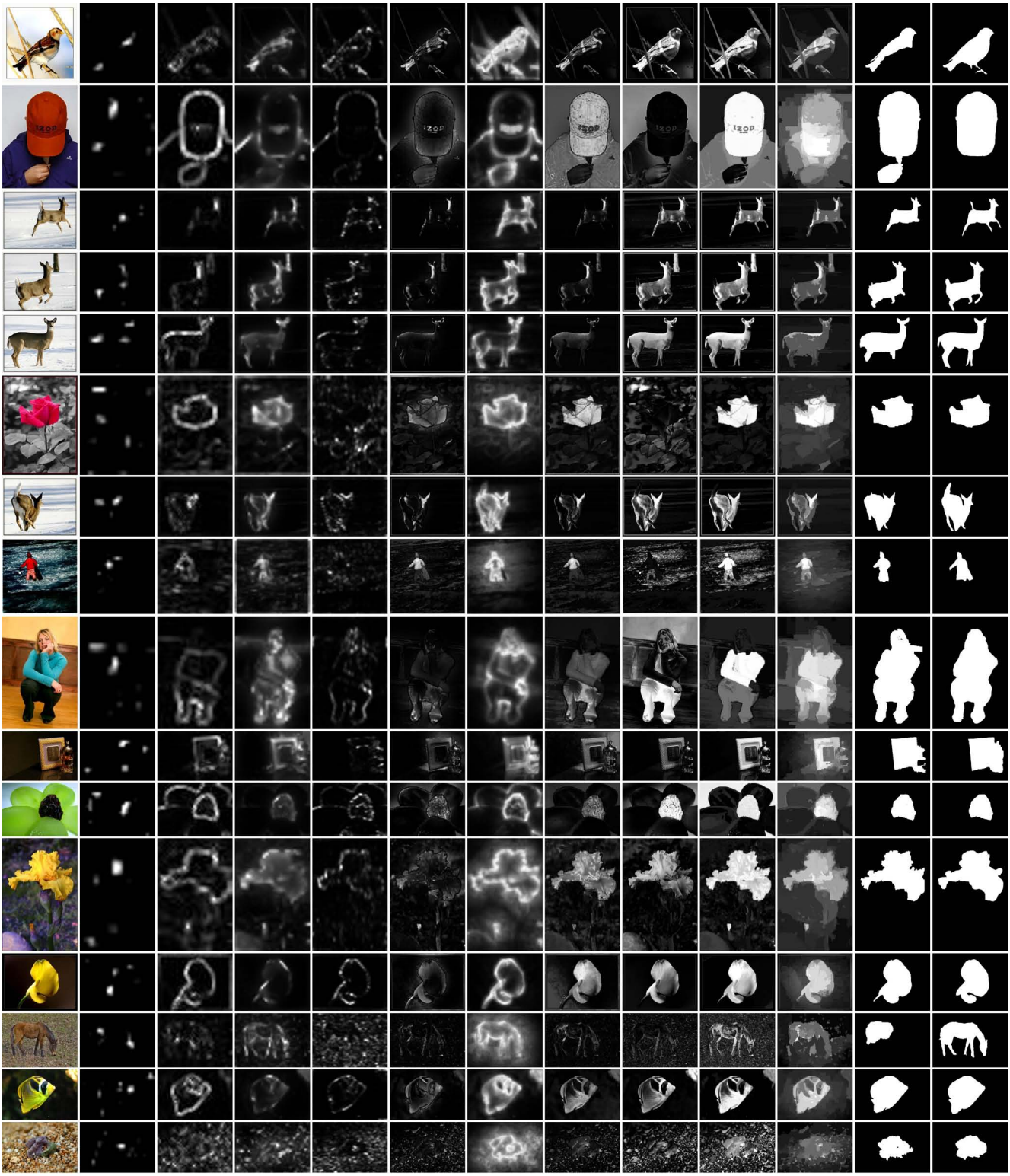

(a) (b) IT[6] (c) MZ[7] (d) GB[4] (e) SR[5] (f) AC[1] (g) CA[3] (h) FT[2] (i) LC[8] (j) HC (k) RC (l) RCC (m) g-tr

Figure 57. Typical saliency maps computed by different state-of-the-art methods (b-i) and by our proposed HC method (j) and RC method (k). Our saliency cut results (l) obtained using RC saliency maps are compared with ground truth (m).

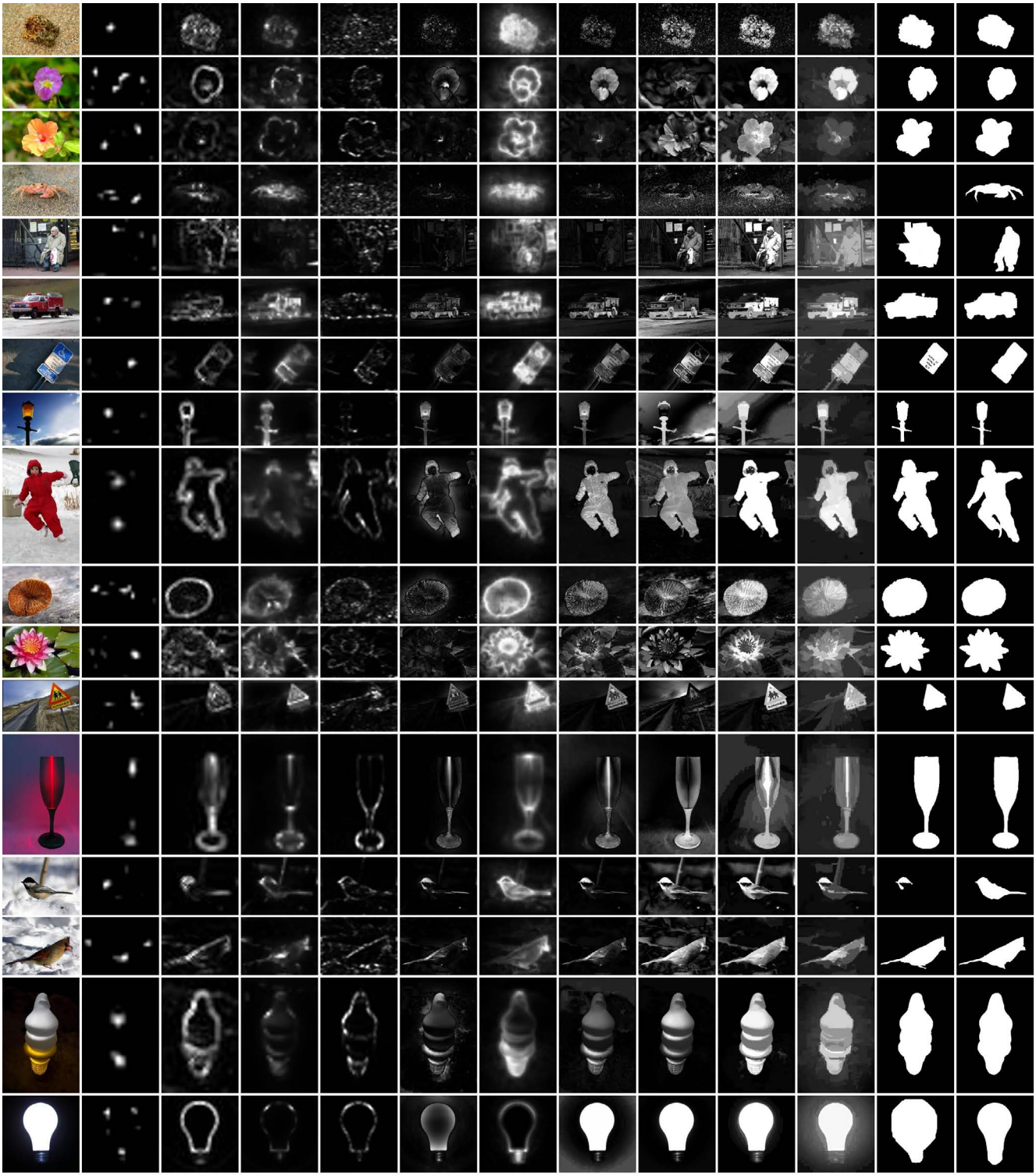

(a) (b) IT[6] (c) MZ[7] (d) GB[4] (e) SR[5] (f) AC[1] (g) CA[3] (h) FT[2] (i) LC[8] (j) HC (k) RC (l) RCC (m) g-tr

Figure 58. Typical saliency maps computed by different state-of-the-art methods (b-i) and by our proposed HC method (j) and RC method (k). Our saliency cut results (l) obtained using RC saliency maps are compared with ground truth (m).

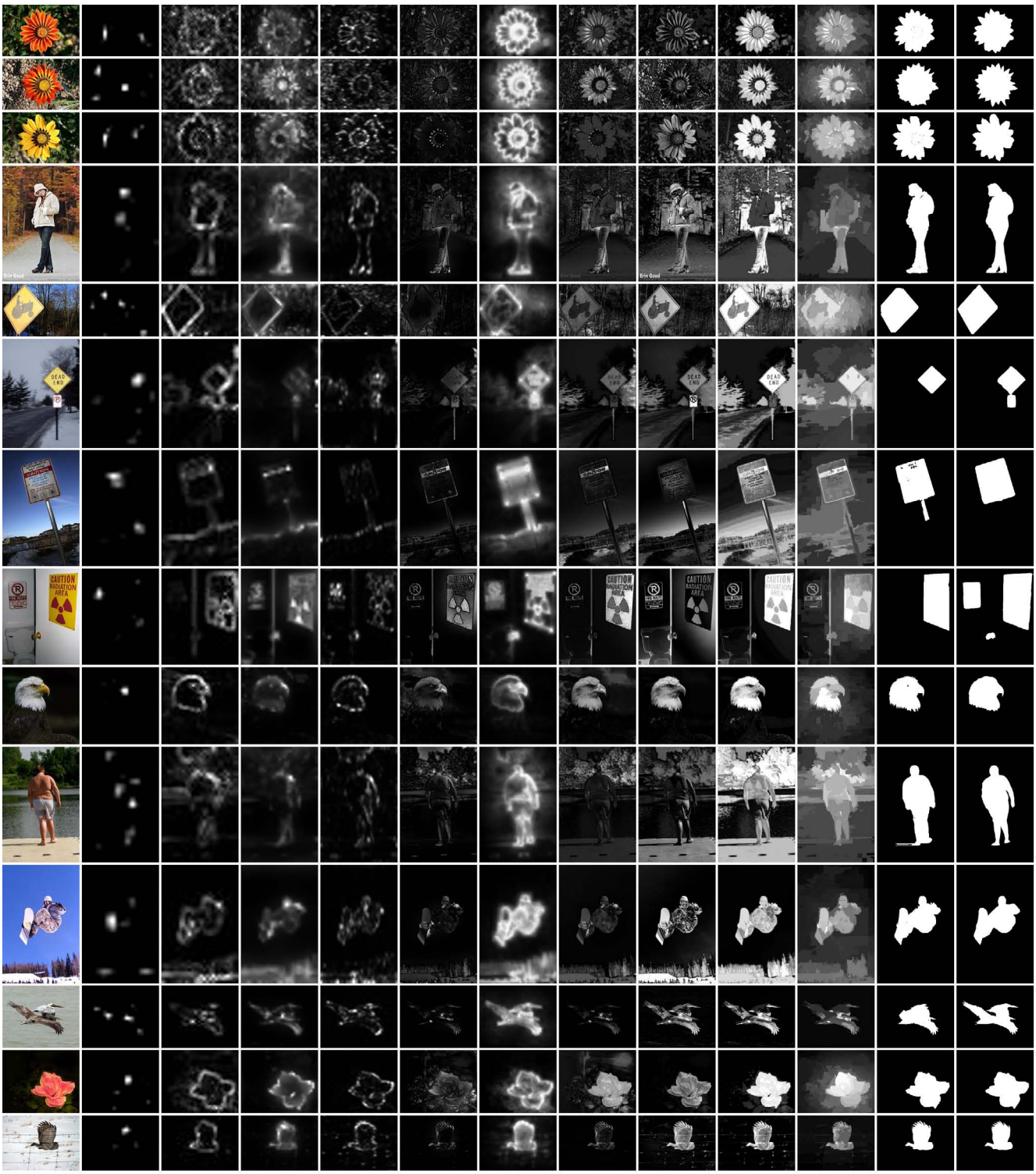

(a) (b) IT[6] (c) MZ[7] (d) GB[4] (e) SR[5] (f) AC[1] (g) CA[3] (h) FT[2] (i) LC[8] (j) HC (k) RC (l) RCC (m) g-tr

Figure 59. Typical saliency maps computed by different state-of-the-art methods (b-i) and by our proposed HC method (j) and RC method (k). Our saliency cut results (l) obtained using RC saliency maps are compared with ground truth (m).

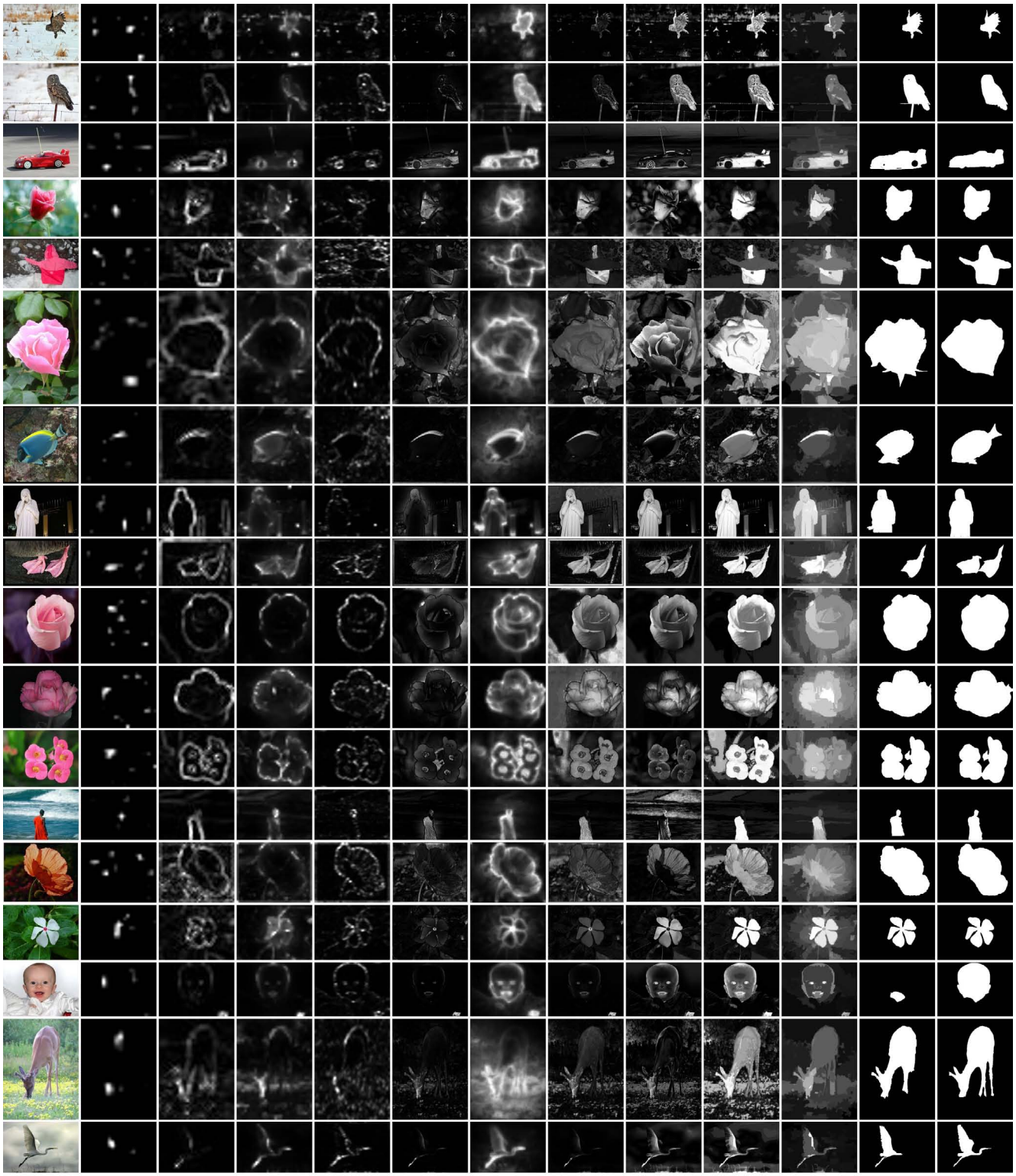

(a) (b) IT[6] (c) MZ[7] (d) GB[4] (e) SR[5] (f) AC[1] (g) CA[3] (h) FT[2] (i) LC[8] (j) HC (k) RC (l) RCC (m) g-tr

Figure 60. Typical saliency maps computed by different state-of-the-art methods (b-i) and by our proposed HC method (j) and RC method (k). Our saliency cut results (l) obtained using RC saliency maps are compared with ground truth (m).

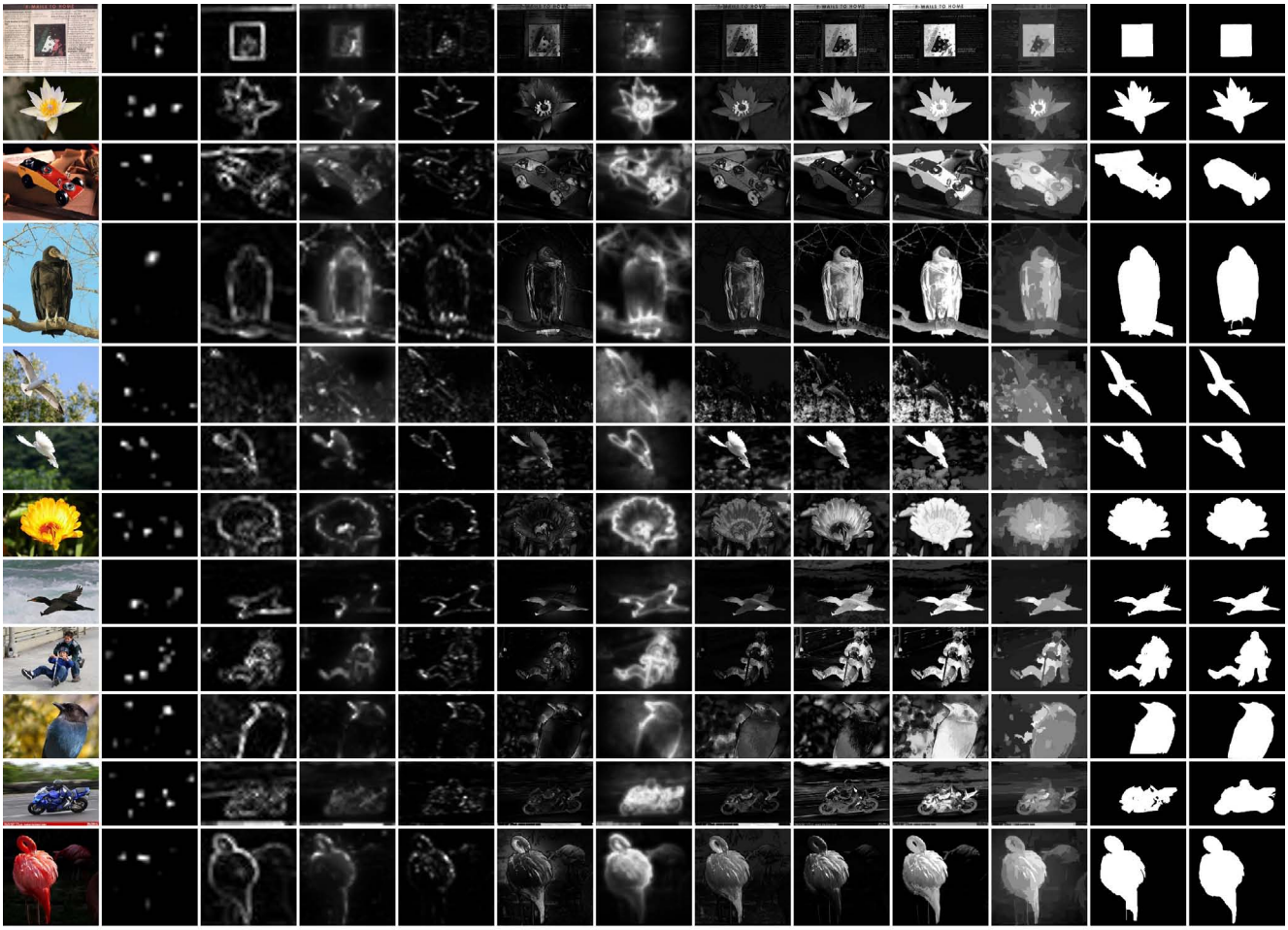

(a) (b) IT[6] (c) MZ[7] (d) GB[4] (e) SR[5] (f) AC[1] (g) CA[3] (h) FT[2] (i) LC[8] (j) HC (k) RC (l) RCC (m) g-tr

Figure 61. Typical saliency maps computed by different state-of-the-art methods (b-i) and by our proposed HC method (j) and RC method (k). Our saliency cut results (l) obtained using RC saliency maps are compared with ground truth (m).